

An Introduction to Mathematical Modelling

Version 2.0

A. C. Fowler

Mathematical Institute, Oxford University

October 14, 2003

Contents

Preface	iii
1 Introduction	1
1.1 Conservation and constitutive laws	3
Exercises	4
2 Non-dimensionalisation and approximation	5
2.1 Non-dimensionalisation	5
2.1.1 The wave equation	6
2.1.2 The heat equation	7
2.2 Scaling	9
2.2.1 The wave equation, again	9
2.3 Simple approximation methods	10
2.4 Perturbation methods	15
2.4.1 Regular perturbation theory	16
2.4.2 Singular perturbation theory: boundary layers	16
2.4.3 Multiple scales and averaging	16
Exercises	16
3 Graphical methods	19
3.1 Curve sketching	19
3.2 Root-finding	30
3.3 Difference equations	35
3.4 Ordinary differential equations	35
3.5 Chemical reactions	36
Exercises	36
4 Stability and oscillations	38
4.1 Linear stability	38
4.2 Nonlinear stability	41
4.3 Phase plane analysis	41
4.4 Relaxation oscillations	42
4.5 Belousov-Zhabotinskii reaction	43
Exercises	43

5	Hysteresis and resonance	46
5.1	Hysteresis	46
5.1.1	Fluid in tubes	46
5.1.2	Combustion	46
5.2	Resonance	50
5.2.1	Forced pendulums	50
	Exercises	55
6	Waves and shocks	56
6.1	Burgers' equation	62
6.2	The Fisher equation	65
6.3	Solitons	67
6.4	Snow melting	68
6.5	Similarity solutions	72
	Exercises	73
7	Nonlinear diffusion	76
7.1	The viscous droplet	78
7.2	Advance and retreat: waiting times	80
7.3	Blow-up	82
	Exercises	87
8	Reaction-diffusion equations	90
8.1	Wave trains	90
8.1.1	λ - ω systems	91
8.1.2	Slowly varying waves	91
8.2	Activator-inhibitor system	94
8.3	Solitary waves in excitable media	94
8.4	Pattern formation	97
	Exercises	100
	References	102

Preface

These notes accompany the o11 course, An introduction to mathematical modelling, and date originally from October 2002. I have given them a version number in order that different web-released versions can be identified. The release number indicates edition.version, thus 1.0 means edition 1, version 0.

Version 2 applies to the year 2003–2004, and subsequent versions will be released whenever any one chapter is updated or revised: which chapter will be indicated here, so that only that updated chapter need be printed.

ACF
October 14, 2003

Chapter 1

Introduction

Mathematical modelling is that abstruse subject which forms the connecting tissue between the problems of the real world which we wish to solve, and the quantitative analysis which we undertake to do so. Almost any problem which requires a quantitative answer, whether it be in industry, medicine, economics, biology or geophysics (for example) involves the formulation of the problem as a *mathematical model*, and it is this formulation, and the techniques which one uses to solve the model, which form the subject of these notes.

There are, perhaps, three kinds of model: statistical, discrete and continuous. We can illustrate their difference with a simple (and topical) example. Suppose fox hunting in England were to be banned. One of the arguments against this is that hunting provides a control on the number of foxes. As with many such assertions, this is one which might be true, or might not. It is a quantitative assertion, and the only way to find out whether it is true is to examine it scientifically. We do this by proposing a model, and examining its validity¹. The statistical method examines the probability that one of two alternative hypotheses is true, by using actual measured data. For example, if hunting were to be banned, one might examine fox population numbers during the five years preceding and following such a ban. As with all models, it is in the interpretation of the results that the skill lies. This is particularly true of statistics, where the aim is to eliminate possibilities, rather than propose constituent mechanisms.

Statistical models have to deal with the issue of predictability. Suppose fox numbers double following a ban; then it would seem likely that there is a connection. But there are other factors which are involved in determining fox populations, and it is always arguable whether one particular factor has a deciding control.

Statistical models are *diagnostic*: they try to interpret process from measured data. Discrete and continuous models are examples of *prognostic* models: they propose a descriptive model of a phenomenon, and then predict what will happen in the future. Such models require validation. This consists initially of matching observation to theory, and often will suggest experiments which can be done to confirm the theory.

A discrete model will propose a difference equation for the variables of interest.

¹This is in fact the scientific method: the models that we propose are no more than hypotheses, and science should never present itself as purveying absolute truth.

In the case of foxes, this might be an estimate for the fox population density u_n at a particular time during the n -th year, and a simple such discrete model is the logistic model with harvesting:

$$u_{n+1} = ru_n \left(1 - \frac{u_n}{K}\right) - hu_n, \quad (1.1)$$

where r is the specific reproductive rate, and the term hu_n represents harvesting (via hunting); the coefficient h represents the effort involved, which one might suppose would be proportional to the number of hunts. This model contains the simple idea that excess populations become limited by competition for resources (the nonlinear term involving K implies decreasing growth rate at larger values of u_n). A discrete model such as (1.1) might be appropriate for fox populations, which have an annual rut, so that the reproductive cycle is repeated annually.

Suppose, for the sake of argument, that (1.1) is a reasonable model. Note that $r > 1$ is a pure number, and so also is h , while K has the same units as u_n . In the absence of hunting, there is a steady population $K(r - 1)/r$, and this is reduced if $h \neq 0$ by a factor $\left[1 - \frac{h}{r - 1}\right]$. So the efficacy of hunting in this model depends on this particular quantity; hunting is effective if $h/(r - 1)$ is significant. This provides a predicted outcome, provided the parameters h and r can be reasonably assessed.

Continuous models are used in the same way, but describe processes using differential equations. It is this kind of model which forms the focus of these notes. The rationale for continuous models is the *continuum hypothesis*, which states that the actual behaviour of a discrete variable, such as a population, can be accurately represented by the evolution of a continuous (and usually differentiable) variable. The basis for this assumption is the ‘fine-grained’ nature of the variable: in a large population, a change by one individual is a small relative change, and can be viewed as being a finite difference approximation to the infinitesimal changes of the calculus.

A continuous version of (1.1) might be the ordinary differential equation

$$\frac{du}{dt} = \rho u \left(1 - \frac{u}{C}\right) - \mu u, \quad (1.2)$$

whose behaviour can be analysed in a similar way to its discrete counterpart.

There are two particular points of view which we can bring to bear on the mathematical models which describe the phenomena which concern us: these are the dynamical systems approach, or equivalently the bifurcation theory approach; and the perturbation theory approach. Each has its place in different contexts, and sometimes they overlap.

The bifurcation theory approach most usually (but not always) is brought to bear on problems which have some kind of complicated time-dependent behaviour. The idea is that we seek to understand the observations through the understanding of a number of simpler problems, which arise successively through bifurcations in the mathematical model, as some critical parameter is changed. A classic example of this approach is in the study of the origin of chaos in the Lorenz equations, or the onset of complicated forms of thermal convection in fluids.

In its simplest form (e.g., in weakly nonlinear stability theory) the perturbative approach is similar in method to the bifurcational one; however, the ethos is rather different. Rather than try and approach the desired solution behaviour through a sequence of simpler behaviours, we try and break down the solution by making approximations, which (with luck) are in fact realistic. In real problems, such approximations are readily available, and part of the art of the applied mathematician is having the facility of being able to judge how to make the right approximations. In these notes, we follow the perturbative approach. It has the disadvantage of being harder, but it is able to get closer to a description of how realistic systems may actually behave.

1.1 Conservation and constitutive laws

The basic building blocks of continuous mathematical models are conservation laws. The continuum assumption adopts the view that the physical medium of concern may be considered continuous, whether it be a porous medium (for example, sand on a beach) or a fluid flow. The continuum hypothesis works whenever the length or time scales of interest are (much) larger than the corresponding microscale. For example, the formation of dunes in a desert (length scale hundreds of metres) can be modelled as a continuous process, since the microscale (sand grain size) is much smaller. Equally, the modelling of large animal populations or of snow avalanches treats the corresponding media as continuous.

Conservation laws arise as mathematical equations which represent the idea that certain quantities are conserved — for example, mass, momentum (via Newton’s law) and energy. More generally, a conservation law refers to an equation which relates the increase or decrease of a quantity to terms representing supply or destruction.

In a continuous medium, the typical form of a conservation law is as follows:

$$\frac{\partial \phi}{\partial t} + \nabla \cdot \mathbf{f} = S. \quad (1.3)$$

In this equation, ϕ is the quantity being ‘conserved’ (expressed as amount per unit volume of medium, i.e. as a density; \mathbf{f} is the ‘flux’, representing transport of ϕ within the medium, and S represents source ($S > 0$) or sink ($S < 0$) terms. Derivation of the point form (1.3) follows from the integral statement

$$\frac{d}{dt} \int_V \phi dV = - \int_{\partial V} \mathbf{f} \cdot \mathbf{n} dS + \int_V S dV, \quad (1.4)$$

after application of the divergence theorem (which requires \mathbf{f} to be continuously differentiable), and by then equating integrands, on the basis that they are continuous and V is arbitrary. Derivation of (1.3) thus requires ϕ and \mathbf{f} to be continuously differentiable, and S to be continuous.

Two basic types of transport are advection (the medium moves at velocity \mathbf{u} , so there is an advective flux $\phi \mathbf{u}$) and diffusion, or other gradient-driven transport (such as chemotaxis). One can thus write

$$\mathbf{f} = \phi \mathbf{u} + \mathbf{J}, \quad (1.5)$$

where \mathbf{J} might represent diffusive transport, for example. The very simplest conservation law is that of conservation of mass, where the conserved quantity is the density ρ , and the mass flux is entirely due to advection:

$$\frac{\partial \rho}{\partial t} + \nabla \cdot (\rho \mathbf{u}) = 0. \quad (1.6)$$

Invariably, conservation laws give more terms than equations. In (1.5), for example, we have one scalar equation for ϕ , but other quantities \mathbf{J} and \mathbf{S} are present as well, and equations for these must be provided. Typically, these take the form of constitutive laws, and are based squarely on experimental measurement. For example, diffusive transport is represented by the assumption

$$\mathbf{J} = -D \nabla \phi, \quad (1.7)$$

where D is a diffusion coefficient. In the heat equation, this is known as Fourier's law, and the heat equation itself takes the familiar form

$$\frac{\partial}{\partial t}(\rho c_p T) + \nabla \cdot [\rho c_p T \mathbf{u}] = \nabla \cdot [k \nabla T] + Q, \quad (1.8)$$

where Q represents any internal heat source or sink.

Exercises

1.1 Consider the discrete population model (1.1):

$$u_{n+1} = r u_n \left(1 - \frac{u_n}{K}\right) - h u_n.$$

By writing $u_n = L w_n$ for some suitable choice of L , show that the model takes the form

$$w_{n+1} = \lambda w_n (1 - w_n),$$

and determine λ . What is the effect of increasing h on the behaviour of the population? What happens if $h > r - 1$?

1.2 Consider the continuous population model (1.2):

$$\frac{du}{dt} = \rho u \left(1 - \frac{u}{C}\right) - \mu u.$$

By writing $u = M w$ for some suitable choice of M , show that the model takes the form

$$\frac{dw}{dt} = \alpha w (1 - w),$$

and determine α . What is the effective of increasing μ on the population? What happens if $\rho < \mu$?

1.3 Starting from an integral conservation law, derive the heat equation in the form (1.8) and the mass conservation equation in the form (1.6).

Chapter 2

Non-dimensionalisation and approximation

Once we have a model, we have to try and solve it. There are two kinds of solutions: exact, analytical solutions, and approximate solutions. Exact solutions are explicit formulae; for example we can exactly solve quadratic equations, and certain differential equations, such as that describing simple harmonic motion. We also consider that solutions such as Taylor series constitute analytic solutions: they can be computed to arbitrary accuracy. The same applies to quadratures, such as the solution of

$$\frac{du}{dt} = f(u), \quad u(0) = u_0, \quad (2.1)$$

which has an implicitly defined solution

$$\int_0^u \frac{d\xi}{f(\xi)} = t. \quad (2.2)$$

Approximate solutions are those where one solves an approximate equation, or an approximating sequence of equations. Approximate methods are best applied when the approximation is based on the size of certain terms. In this chapter we will illustrate the use of such methods, firstly on simple algebraic equations, and then on some differential equations. The whole subject of perturbation theory is extensive, and a thorough discussion is beyond the scope of these notes.

2.1 Non-dimensionalisation

In order to approximate a solution, we need to be able to neglect terms which are small. This raises a concept of fundamental importance, which is that ‘small’ and ‘large’ are adjectives which can only apply quantitatively when a comparison is made between quantities of the same dimension. An equivalent assertion is that we can only make approximations based on the small size of parameters if these parameters are dimensionless. It makes no intrinsic sense to say a quantity is small if it still has dimensions. A speed of 1 cm s^{-1} is small if you are a rocket, but large if you are a

giant African land snail. An ice sheet is thick if you are a human being, but thin if you are a planet. So we always associate large or small quantities with dimensionless numbers, that is, parameters which measure quantities with respect to some reference value. The process of isolating these parameters is called *non-dimensionalisation*.

2.1.1 The wave equation

Putting a mathematical model into non-dimensional form is fundamental. Although technically trivial, there is a certain art to the process of non-dimensionalisation, and the associated concept of scaling, and the only real way to learn how to do it is by example. Let us begin with a simple model, the wave equation, which one learns how to derive in first year applied mathematics courses. We suppose a string, for example a guitar string, is wound between two points a distance l apart. If the tension in the string is T and its density (per unit length) is ρ , then an application of Newton's second law to an infinitesimal segment of the string leads to the equation

$$\rho \frac{\partial^2 y}{\partial t^2} = T \frac{\partial^2 y}{\partial x^2}, \quad y = 0 \quad \text{on} \quad x = 0, l, \quad (2.3)$$

where x is distance along the string, and y is its transverse displacement.

The main assumption that is usually stated in deriving this equation is that the displacement y is small. However, there are at least two other implicit assumptions which are made. One is that gravity is unimportant; the other is that there is no longitudinal displacement.

For a guitar string, these seem to be reasonable assumptions, but why? We expect the effect of gravity to be a deviation of the displacement from the vertical, and this is evidently valid for the guitar string. It is not valid for the hanging chain, or for the wire between telegraph poles. Why? I would say, for the chain, the density is too large; for the telegraph wire, the distance l is too large; while the guitar string is straight because it is tight: T is large. These facts suggest that the 'size' of the gravitational acceleration g may in fact be measured by the dimensionless parameter $\rho g l / T$, which appears to be the only independent dimensionless parameter which can be formed from those in the model if we include gravity.

How can this suspicion be confirmed? From first principles, we derive the wave equation, including gravity, in the form

$$\rho \frac{\partial^2 y}{\partial t^2} = T \frac{\partial^2 y}{\partial x^2} - \rho g, \quad y = 0 \quad \text{on} \quad x = 0, l. \quad (2.4)$$

Next we write the model in dimensionless form. We do this by *non-dimensionalising* the variables so that they are numerically of order one (written $O(1)$). Specifically, we write

$$x = lx^*, \quad y = y_0 y^*, \quad t = (l/c)t^*, \quad (2.5)$$

where

$$c = \sqrt{\frac{T}{\rho}} \quad (2.6)$$

is the wave speed, and y_0 is a measure of the displacement: for example, it could be the maximum initial displacement. The dimensionless model is then obtained in the form

$$\frac{\partial^2 y^*}{\partial t^{*2}} = \frac{\partial^2 y^*}{\partial x^{*2}} - \beta, \quad (2.7)$$

where

$$\beta = \frac{\rho g l^2}{T y_0}, \quad (2.8)$$

with $y^* = O(1)$ initially, and $y^* = 0$ on $x = 0, l$. All of the terms in the equations and in the initial and boundary conditions are dimensionless, and all the coefficients which appear (such as β) are dimensionless.

It is conventional at this dimensionless stage to dispense with the asterisks in writing the variables, and this we now do. The process of choosing particular scales for the variables, or *scaling*, is motivated by the following ideas. Firstly, there is a natural length scale to the problem, l , which is the dimension of the geometric domain on which the problem is to be solved. Further, there is a natural length scale for the displacement, y_0 , which is present in the initial conditions. Next, of the three terms in (2.4), we anticipate (at least for the guitar string) that the gravity term will be ‘small’. It follows that the other two should be the same size, and we choose the time scale so that these two terms ‘balance’, that is their dimensionless scales (here $T y_0^2 / l^2$) are the same. When the model is written in the dimensionless form (2.7), we then have equal dimensionless coefficients multiplying these two terms: here they are both equal to one.

The final, essential idea is that, in general, a dimensionless function $u(x, t)$ which varies by $O(1)$ over an x range of $O(1)$ will have derivatives of $O(1)$. This is true, for example, for $\sin x$, e^{-x} , and x^2 : it is *not* true for the function e^{-10x} , which varies rapidly over a distance of order $x \sim 0.1$ near $x = 0$. With this assumption, the derivative terms $\partial^2 y / \partial t^2$ and $\partial^2 y / \partial x^2$ are $O(1)$, and it follows that the relative size of the gravity term is given by β . Thus gravity is negligible if $\beta \ll 1$, and indeed this means large tension, small density or short length, as we surmised.

2.1.2 The heat equation

Next we consider a form of the heat equation, (1.8). We write it in the form (assuming density ρ and specific heat c_p are constant)

$$\frac{\partial T}{\partial t} + \mathbf{u} \cdot \nabla T = \kappa \nabla^2 T + H, \quad (2.9)$$

where $H = Q / \rho c_p$. We have assumed $\nabla \cdot \mathbf{u} = 0$, which follows from the conservation of mass in the form

$$\frac{\partial \rho}{\partial t} + \nabla \cdot (\rho \mathbf{u}) = 0, \quad (2.10)$$

together with $\rho = \text{constant}$.

Suppose we are to solve (2.9) in a domain D of linear dimension l , on the boundary of which we prescribe

$$T = T_B \quad \text{on} \quad \partial D, \quad (2.11)$$

where T_B is constant. We also have an initial condition

$$T = T_0(\mathbf{x}) \text{ in } D, \quad t = 0, \quad (2.12)$$

and we suppose \mathbf{u} is given, of order U .

We can make the variables dimensionless in the following way:

$$\mathbf{x} = l\mathbf{x}^*, \quad t = [t]t^*, \quad T = T_B + (\Delta T)T^*. \quad (2.13)$$

Again, we do this in order that both dependent and independent variables be of numerical order one, $O(1)$. If we can do this, then we would suppose *a priori* that derivatives such as $\nabla^* T^*$ ($\nabla = l^{-1}\nabla^*$) will also be of numerical $O(1)$, and the size of various terms will be reflected in the dimensionless parameters which occur.

In writing (2.13), it is clear that l is a suitable length scale, as it is the size of D . For example, if D was a sphere we might take l as its radius or diameter. We also suppose that the origin is in D ; if not, we could write $\mathbf{x} = \mathbf{x}_0 + l\mathbf{x}^*$, where $\mathbf{x}_0 \in D$: evidently $\mathbf{x}^* = O(1)$ in D .

A similar motivation underlies the choice of an ‘origin shift’ for T . In the absence of a heat source, the temperature will tend to the uniform state $T \equiv T_B$ as $t \rightarrow \infty$. If $H \neq 0$, the final state will be raised above T_B (if $H > 0$) by an amount dependent on H . We take ΔT to represent this amount, but we do not know what it is in advance — we will choose it by *scaling*. The subtraction of T_B from T before non-dimensionalisation is because the model for T contains only derivatives of T , so that it is really the variation of T about T_B which we wish to scale.

In a similar way, the time scale $[t]$ is not prescribed in advance, and we will choose it also by scaling, in due course.

With the substitutions in (2.13), the heat equation (2.9) can be written in the form

$$\left(\frac{l^2}{\kappa[t]} \right) \frac{\partial T^*}{\partial t^*} + \left(\frac{Ul}{\kappa} \right) \mathbf{u}^* \cdot \nabla^* T^* = \nabla^{*2} T^* + \left(\frac{Hl^2}{\kappa \Delta T} \right), \quad (2.14)$$

where we have written $\mathbf{u} = U\mathbf{u}^*$, so that $\mathbf{u}^* = O(1)$. This equation is dimensionless, and the bracketed parameters are dimensionless. They are somewhat arbitrary, since $[t]$ and ΔT have not yet been chosen: we now do so by scaling.

The solution of the equation can depend only on the dimensionless parameters. It is thus convenient to *choose* $[t]$ and ΔT so that two of these are set to some convenient value. There is no unique way to do this.

The temperature scale ΔT appears only in the source term. Since it is this which determines the temperature rise, it is natural to *choose*

$$\Delta T = \frac{Hl^2}{\kappa}. \quad (2.15)$$

It is also customary to choose the time scale so that the two terms of the advective derivative on the left of (2.14) are the same size, and this gives the convective time scale

$$[t] = \frac{l}{U}. \quad (2.16)$$

Finally, we remove the asterisks. When this is done, the dimensionless equation takes the form

$$Pe \left[\frac{\partial T}{\partial t} + \mathbf{u} \cdot \nabla T \right] = \nabla^2 T + 1, \quad (2.17)$$

where the Péclet number is

$$Pe = \frac{Ul}{\kappa}, \quad (2.18)$$

and the solution of the model depends only on this parameter (as well as the initial condition). The boundary condition is

$$T = 0 \quad \text{on} \quad \partial D, \quad (2.19)$$

and the initial condition is

$$T = \theta(\mathbf{x}) \quad \text{at} \quad t = 0, \quad (2.20)$$

where

$$\theta(\mathbf{x}) = \frac{T_0(l\mathbf{x}) - T_B}{\Delta T}. \quad (2.21)$$

2.2 Scaling

A well-scaled problem generally refers to a model in which the dimensionless parameters are $O(1)$ or less. Evidently, this can be ensured simply by dividing through by the largest parameter in any equation. More importantly, if parameters are numerically small, then (as we discuss below) approximate solutions can be obtained by neglecting them. The problem is well-scaled if the resulting approximation makes sense. For example, (2.17) is well-scaled for any value of Pe . However, the problem $\varepsilon T_t = \varepsilon \nabla^2 T + 1$, with $\varepsilon \ll 1$, is not well scaled. One makes a problem well-scaled in this situation by *rescaling* the variables, and we now consider the wave equation (2.7) again in this light.

2.2.1 The wave equation, again

In the statement of the wave equation with gravity, there are in fact two dimensionless parameters:

$$B = \frac{\rho g l}{T}, \quad \varepsilon = \frac{y_0}{l}. \quad (2.22)$$

The parameter ε is a measure of the amplitude of the motion, and it is on the basis that $\varepsilon \ll 1$ that we derive the linear wave equation in the first place. The parameter $\beta = B/\varepsilon$, so the assumption of negligible gravity is equivalent to the assumption that $B \ll \varepsilon \ll 1$.

If $B \sim \varepsilon$, then $\beta = O(1)$. The problem is sensibly scaled, but gravity is no longer negligible. There is a steady state $y = \frac{1}{2}\beta x(l - x)$ (the hanging chain), and, because the equation is linear, the string simply oscillates about this steady state.

Now suppose that $\beta \gg 1$. The model is now not correctly scaled (because the limit $\beta \rightarrow \infty$ gives no sensible approximation). In fact the model suggests that a

steady state will have $y \sim \beta$, and that the string will oscillate about this steady state with a similar amplitude. In order to obtain a sensibly scaled problem, we simply have to *rescale* the displacement by writing $y = \beta Y$, and the discussion can proceed as before, except that the initial condition has $Y \ll 1$.

It seems that all is now well; we have discussed the cases $\beta \ll 1$, $\beta = O(1)$, and $\beta \gg 1$. However, there is more concern when β becomes as large as $O(1/\varepsilon)$. In this case, the model suggests oscillations about a steady state of order $\beta \sim 1/\varepsilon$, and dimensionally of order l . Because of this, the basis of the original derivation is suspect, and the model must be re-derived: in fact this can be done (see question 2.1), so that the model equation (2.7) remains valid. However, the initial value scale y_0 is *not* now an appropriate scale for y ; the appropriate (dimensional) scale is $y \sim l$, and this *a posteriori* adjustment is the rescaling alluded to above. In dimensionless terms, we rescale the model by writing $y = (l/y_0)Y = Y/\varepsilon$, and we find

$$\frac{\partial^2 Y}{\partial t^2} = \frac{\partial^2 Y}{\partial x^2} - B, \quad (2.23)$$

and this version of the model is appropriate if $B = O(1)$. If $B \gg 1$, a further rescaling simply takes $Y \sim B$.

2.3 Simple approximation methods

Suppose we wish to solve the equation

$$x^3 - \varepsilon x - 1 = 0, \quad (2.24)$$

where ε is relatively small: for example if $\varepsilon = 0.1$. Formulae do in fact exist for writing solutions of cubic (and also quartic) equations, but they are fairly unpleasant and are rarely used. A much better way is to use an approximation method, based on the idea that the *parameter* ε in equation (2.24) is small.

Graphically, it is clear (see figure 2.1) that when ε is small, (2.24) will have a unique, positive real root, and in fact it will be close to $x = 1$ (since $1 + \varepsilon x \approx 1$). (In passing, note that there will be exactly one root for $\varepsilon < \varepsilon_c$, where ε_c is the value corresponding to tangency of the line with the curve; at this value $x^3 = 1 + \varepsilon x$ and $3x^2 = \varepsilon$, so that $\varepsilon_c = 3/2^{2/3} \approx 1.89$.)

A simple iterative method to solve (2.24) is

$$x_{n+1} = (1 + \varepsilon x_n)^{1/3}. \quad (2.25)$$

If we choose $\varepsilon = 0.1$ and $x_0 = 1$, then successively

$$\begin{aligned} x_1 &= 1.0322801, \\ x_2 &= 1.0332889, \\ x_3 &= 1.0333204, \\ x_4 &= 1.0333214, \end{aligned} \quad (2.26)$$

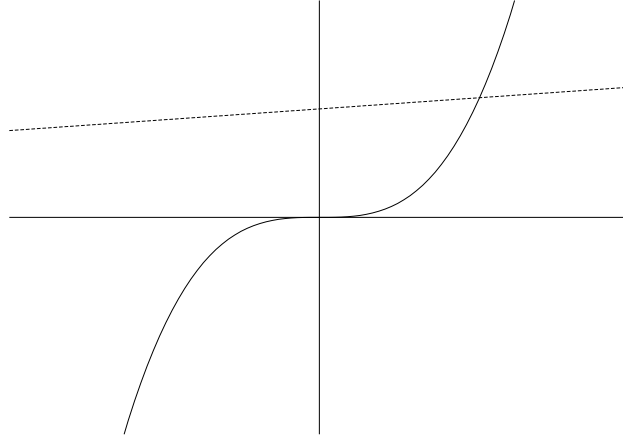


Figure 2.1: The graphs of x^3 and $1 + \varepsilon x$, with $\varepsilon = 0.1$.

and this last value is the root. It is of course trivial to compute the positive root for a range of ε , but it would be convenient to have an *analytic* (as opposed to numerical) approximation. We construct this by using a *perturbation method*.

We can use the binomial expansion to write (2.24) in the form

$$x = (1 + \varepsilon x)^{1/3} = 1 + \frac{1}{3}\varepsilon x - \frac{1}{9}\varepsilon^2 x^2 + \frac{5}{81}\varepsilon^3 x^3 \dots \quad (2.27)$$

Since $\varepsilon \ll 1$, we see that $x \approx 1 + O(\varepsilon)$: that is, terms of *order* ε , i.e. of size about ε . A better estimation is then

$$x \approx 1 + \frac{1}{3}\varepsilon x \approx 1 + \frac{1}{3}\varepsilon, \quad (2.28)$$

and we can see that this relatively crude approximation is in fact accurate to four decimal places when $\varepsilon = 0.1$! Repeating this idea, we would have

$$\begin{aligned} x &\approx 1 + \frac{1}{3}\varepsilon x - \frac{1}{9}\varepsilon^2 x^2 \\ &\approx 1 + \frac{1}{3}\varepsilon(1 + \frac{1}{3}\varepsilon) - \frac{1}{9}\varepsilon^2(1 + \dots)^2 \approx 1 + \frac{1}{3}\varepsilon \end{aligned} \quad (2.29)$$

(there is no $O(\varepsilon^2)$ term), but a more methodical procedure is to anticipate (by inspection) that the root can be written in the form of a series

$$x = x_0 + \varepsilon x_1 + \varepsilon^2 x_2 + \dots; \quad (2.30)$$

we substitute this into (2.24), expand in powers of ε , and *equate coefficients of powers of* ε : a little thought indicates why this procedure is necessary. For (2.24), we thus have

$$(x_0 + \varepsilon x_1 + \varepsilon^2 x_2 + \dots)^3 - \varepsilon(x_0 + \varepsilon x_1 + \dots) - 1 = 0, \quad (2.31)$$

whence

$$\begin{aligned} (x_0^3 - 1) &+ \varepsilon(3x_0^2 x_1 - x_0) + \varepsilon^2(3x_0^2 x_2 + 3x_0 x_1^2 - x_1) \\ &+ \varepsilon^3(3x_0^2 x_3 + 3x_0 x_1 x_2 + x_1^3 - x_2) + \dots = 0, \end{aligned} \quad (2.32)$$

so that, sequentially,

$$\begin{aligned}
x_0^3 - 1 &= 0, \\
3x_0^2x_1 - x_0 &= 0, \\
3x_0^2x_2 + 3x_0x_1^2 - x_1 &= 0, \\
3x_0^2x_3 + 3x_0x_1x_2 + x_1^3 - x_2 &= 0, \\
&\dots,
\end{aligned} \tag{2.33}$$

from which we obtain

$$x_0 = 1, \quad x_1 = \frac{1}{3}, \quad x_2 = 0, \quad x_3 = -\frac{1}{81}, \tag{2.34}$$

and hence the root is

$$x \approx 1 + \frac{1}{3}\varepsilon - \frac{1}{81}\varepsilon^3 + O(\varepsilon^4). \tag{2.35}$$

With $\varepsilon = 0.1$, we have $x \approx 1.033321$: practically, the exact result. Even, for $\varepsilon = 1$, the approximate result is 1.321, while the exact root is 1.3247.

Singular approximations

The approximation above is called a *regular* approximation, because the limit when $\varepsilon = 0$ gives an approximation to the root. Now consider the cubic

$$\varepsilon x^3 - x - 1 = 0, \quad \varepsilon \ll 1. \tag{2.36}$$

Graphically (figure 2.2), there are clearly three real roots. One of these is near -1 and can be recovered by a regular approximation. The others are at large values of $|x|$, and are determined by *balancing* εx^3 with x ; that is, $\varepsilon x^3 \sim x$ when $x \sim \varepsilon^{-1/2}$, so we first write

$$x = \varepsilon^{-1/2}X, \tag{2.37}$$

and then

$$X^3 - X - \varepsilon^{1/2} = 0, \tag{2.38}$$

with approximate roots $X \approx 0, \pm 1$. The root $X \approx 0$ corresponds to $x \approx -1$ and is determined by the regular approximation for x . The larger roots are determined by a regular approximation of (2.38), as a power series in $\varepsilon^{1/2}$. Thus

$$X = X_0 + \varepsilon^{1/2}X_1 + \varepsilon X_2 + \dots, \tag{2.39}$$

and substituting this into (2.38) and equating powers of $\varepsilon^{1/2}$, leads to the approximate solutions (written in terms of x)

$$x \approx \pm \frac{1}{\sqrt{\varepsilon}} + \frac{1}{2} \mp \frac{3}{8}\sqrt{\varepsilon} + \frac{7}{32}\varepsilon + \dots \tag{2.40}$$

The upper sign gives the positive root, the lower the negative root. For example if $\varepsilon = 0.1$, the approximate positive root from (2.40) is 3.565567, while the exact root is

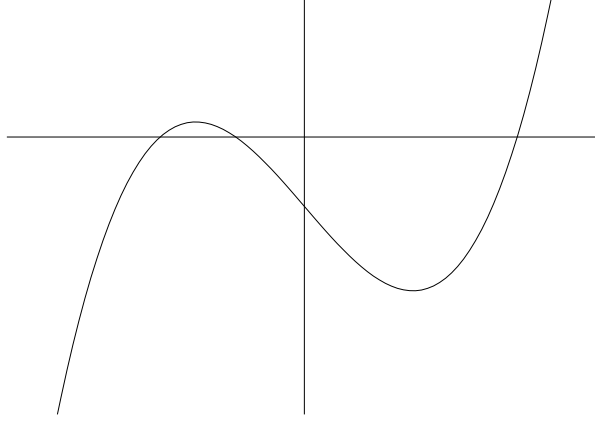


Figure 2.2: The graph of $\varepsilon x^3 - x - 1$, for $\varepsilon = 0.1$.

3.5770894. For $\varepsilon = 1$, the approximate root is 1.1468753, while as we have seen, the exact root is 1.3247. This is less good, but can be improved by taking further terms in the series (2.40). We see that approximation methods can provide a very useful way of solving algebraic equations.

Now suppose we wish to solve

$$\tan x = \tanh x. \quad (2.41)$$

Each function is odd, so $x = 0$ is a solution, and graphically (figure 2.3) it is clear that there is a sequence of positive roots x_1^*, x_2^*, \dots (and thus also negative roots $-x_1^*, -x_2^*, \dots$), and that as $n \rightarrow \infty$,

$$x_n^* \approx (n + \tfrac{1}{4})\pi. \quad (2.42)$$

Suppose we put

$$x_n^* = (n + \tfrac{1}{4})\pi + \theta; \quad (2.43)$$

then

$$\begin{aligned} \sin x_n^* &= \frac{(-1)^n}{\sqrt{2}}(\cos \theta + \sin \theta), \\ \cos x_n^* &= \frac{(-1)^n}{\sqrt{2}}(\cos \theta - \sin \theta), \end{aligned} \quad (2.44)$$

so (2.41) is

$$\tan x_n^* = \frac{\cos \theta + \sin \theta}{\cos \theta - \sin \theta} = \frac{1 - e^{-2x_n^*}}{1 + e^{-2x_n^*}}. \quad (2.45)$$

We expect $\theta \ll 1$, and also $x_n^* \gg 1$, and thus, since

$$\begin{aligned} \cos \theta &\approx 1 - \tfrac{1}{2}\theta^2, \\ \sin \theta &\approx \theta, \end{aligned} \quad (2.46)$$

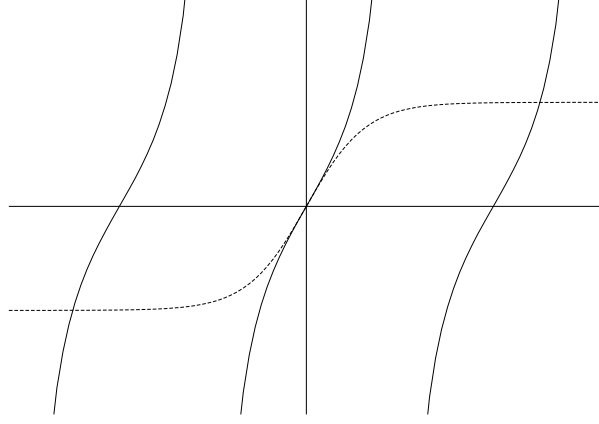


Figure 2.3: The graphs of $\tan x$ and $\tanh x$.

we have, with use of the binomial expansion for $(1 + y)^{-1}$,

$$\begin{aligned}
 \frac{1 - \frac{1}{2}\theta^2 \dots + \theta \dots}{1 - \frac{1}{2}\theta^2 \dots - \theta \dots} &= (1 - e^{-2x_n^*})(1 - e^{-2x_n^*} + \dots) \\
 \Rightarrow (1 + \theta - \frac{1}{2}\theta^2 \dots)(1 + \{\theta + \frac{1}{2}\theta^2 + \dots\} + \{\theta^2 + \dots\} \dots) &= 1 - 2e^{-2x_n^*} \dots \\
 \Rightarrow 1 + 2\theta + 2\theta^2 + \dots = 1 - 2e^{-(2n+\frac{1}{2})\pi-2\theta} \dots \\
 \Rightarrow \theta + \theta^2 + \dots = -e^{-(2n+\frac{1}{2})\pi}(1 - 2\theta \dots), & \quad (2.47)
 \end{aligned}$$

so that, finally,

$$\theta \approx -e^{-(2n+\frac{1}{2})\pi}, \quad (2.48)$$

and

$$x_n^* \approx (n + \frac{1}{4})\pi - e^{-(2n+\frac{1}{2})\pi}. \quad (2.49)$$

Numerical approximation

Iterative numerical methods are discussed further in the next chapter. A general iterative method to find a root of $f(x) = 0$ is to define a sequence $x = x_0, x_1, \dots$, satisfying $x_{n+1} = g(x_n)$, where the function g is chosen so that $x = g(x)$ if $f(x) = 0$: for example, $g(x) = f(x) + x$. A simple iterative method to solve

$$L(x) = R(x) \quad (2.50)$$

is as follows: define

$$L(x_{r+1}) = R(x_r), \quad (2.51)$$

i.e. $x_{r+1} = L^{-1} \circ R(x_r)$. The sequence will converge if $|(L^{-1} \circ R)'| < 1$ at a root, and using the chain rule (via $f = L^{-1} \circ R$ if $L[f(x)] = R(x)$, so $L'f' = R'$, and at a root

$f(x) = x$, $f' = R'/L'$) we find that this is $|L'| > |R'|$. Consulting figure 2.3, we see that the iteration

$$x_{r+1} = \tan^{-1}[\tanh x_r] + n\pi \quad (2.52)$$

will converge to x_n^* (since \tan^{-1} is defined to be less than $\pi/2$ on a calculator).

The lowest root ($n = 1$) is approximated by

$$x_1^* \approx \frac{5}{4}\pi - e^{-5\pi/2} = 3.9266026 \quad (2.53)$$

compared with the exact value 3.9266024. Here an approximation based on the limit $n \rightarrow \infty$ is accurate even when $n = 1$.

2.4 Perturbation methods

Let us consider (2.17) with (2.19) and (2.20), and suppose that $\theta_0 \leq O(1)$. If $Pe \ll 1$, we obtain an approximation by putting $Pe = 0$: $\nabla^2 T + 1 \approx 0$. Evidently, we cannot satisfy the initial condition, and this suggests that we rescale t : put $t = Pe\tau$, so that (approximately)

$$\frac{\partial T}{\partial \tau} = \nabla^2 T + 1; \quad (2.54)$$

now we can satisfy the initial condition (at $\tau = 0$) too. Often one abbreviates the rescaling by simply saying, ‘rescale $t \sim Pe$, so that $T_t \approx \nabla^2 T + 1$ ’.

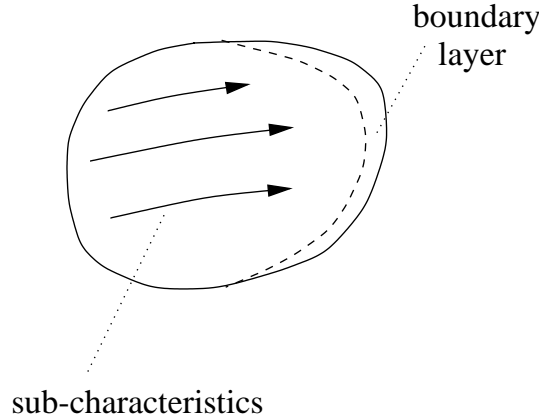


Figure 2.4: Sub-characteristics and boundary layer for the equation (2.17). The sub-characteristics are the flow lines $d\mathbf{x}/dt = \mathbf{u}$, and the boundary layer (of thickness $O(1/Pe)$) is on the part of the boundary where the flow lines terminate.

On the other hand, if $Pe \gg 1$, then $T_t + \mathbf{u} \cdot \nabla T \approx 0$, and we can satisfy the initial condition but not the boundary condition on all of ∂D , since the approximating equation is hyperbolic (its characteristics are called ‘sub-characteristics’). To remedy this, one has to rescale \mathbf{x} near the part of the boundary where the boundary condition

is not satisfied. This gives a spatially thin region, called (evidently) a boundary layer, of thickness $1/Pe$ (see figure 2.4).

The other possibility is if $\theta \gg 1$, say $\theta \sim \theta_0 \gg 1$. We discuss only the case $Pe \gg 1$ (see also exercise 1.2). Since $T \sim \theta_0$ initially, we need to rescale T , say $T = \theta_0 \tilde{T}$. then $Pe[\tilde{T}_t + \mathbf{u} \cdot \nabla \tilde{T}] = \nabla^2 \tilde{T} + \theta_0^{-1}$, and with $\tilde{T} = O(1)$, we have $\tilde{T}_t + \mathbf{u} \cdot \nabla \tilde{T} \approx 0$ for $Pe \gg 1$. The initial function is simply advected along the flow lines (sub-characteristics), and the boundary condition $\tilde{T} = 0$ is advected across D . In a time of $O(1)$, the initial condition is ‘washed out’ of the domain. Following this, we revert to T , thus $T_t + \mathbf{u} \cdot \nabla T = Pe^{-1}(\nabla^2 T + 1)$. Evidently T will remain ≈ 0 in most of D , with a boundary layer near the boundary as shown in figure 2.4. If n is the coordinate normal to ∂D in this layer, then $\mathbf{u} \cdot \nabla T \sim u_n \partial T / \partial n \sim Pe T$, $Pe^{-1} \nabla^2 T \sim Pe^{-1} \partial^2 T / \partial n^2 \sim Pe T$, and in the steady state, these must balance the source term Pe^{-1} : thus in fact, the final state has the rescaled $T \sim Pe^{-2}$, and this applies also for $\theta_0 \leq O(1)$.

These ideas of perturbation methods are very powerful, but a full exposition is beyond the scope of these notes. Nevertheless, they will relentlessly inform our discussion. While it is possible to use formal perturbation expansions, it is sufficient in many cases to give more heuristic forms of argument, and this will typically be the style we choose.

2.4.1 Regular perturbation theory

$$u'' - u = \varepsilon u^2, \quad u(0) = 0, \quad u(1) = 1, \quad (2.55)$$

where $\varepsilon \ll 1$.

2.4.2 Singular perturbation theory: boundary layers

$$\varepsilon u'' - u = u^2, \quad u(0) = 0, \quad u(1) = 1, \quad (2.56)$$

where $\varepsilon \ll 1$.

2.4.3 Multiple scales and averaging

$$u'' + u = \varepsilon u^2, \quad u(0) = u'(0) = 0, \quad (2.57)$$

where $\varepsilon \ll 1$.

Exercises

- 2.1 Derive the wave equation describing oscillations of a string of length l from first principles, when gravity is included, assuming displacements are small and of order y_0 . Show how to non-dimensionalise the equation to obtain the form

$$\frac{\partial^2 y}{\partial t^2} = \frac{\partial^2 y}{\partial x^2} - \beta,$$

and define β .

Now suppose that $y_0 \sim l$. Suppose that in the unstretched state where the displacement $y = 0$, the density ρ_0 is constant. By careful consideration of the application of Newton's second law to an infinitesimal segment of length ds (stretched from its original length dx), show that the (dimensional) wave equation can be derived in the form

$$\rho_0 \frac{\partial^2 y}{\partial t^2} = T_0 \frac{\partial^2 y}{\partial x^2} - \rho_0 g,$$

assuming only that displacements are purely vertical, where T_0 is the horizontal component of the tension exerted at the fixed end points at $x = 0$, $x = l$.

Non-dimensionalise the model in this case and describe the form of the resulting oscillation.

2.2 Explain why the iterative method

$$x_{n+1} = (1 + \varepsilon x_n)^{1/3}$$

used to solve (2.24) will converge to its solution. Does this depend on the value of ε ?

2.3 (i) Find approximations to the solution of

$$\varepsilon x^3 - x - 1 = 0, \quad \varepsilon \ll 1,$$

which is close to $x = -1$. Compare with the numerical solution when $\varepsilon = 0.1$; $\varepsilon = 0.01$.

(ii) Use perturbation methods to find approximate roots to the equation

$$xe^{-x} = \varepsilon, \quad 0 < \varepsilon \ll 1.$$

(Use graphical methods to find the location of the roots. For the larger root, take logs and note that if $x \gg 1$, then $x \gg \ln x$.)

2.4 Suppose

$$Pe \left[\frac{\partial T}{\partial t} + \mathbf{u} \cdot \nabla T \right] = \nabla^2 T + 1 \quad \text{in } D,$$

with

$$\begin{aligned} T &= 0 \quad \text{on } \partial D, \\ T &= \theta_0 \Theta(\mathbf{x}) \quad \text{in } D \quad \text{at } t = 0, \end{aligned}$$

and $\Theta = O(1)$, $\theta_0 \gg 1$, $Pe \ll 1$. Discuss appropriate scales for the various phases of the solution.

2.5 A population of size N is subject to immigration at rate I , and mutual pair destruction at a rate kN^2 , so that $\dot{N} = I - kN^2$. By appropriate scaling of the variables, show that the model can be written in the form $\dot{x} = 1 - x^2$.

2.6 Each of the equations

$$z^5 - \varepsilon z - 1 = 0,$$

$$\varepsilon z^5 - z - 1 = 0,$$

has five (possibly complex) roots. Find approximations to these if $\varepsilon \ll 1$. Can you refine the approximations?

Chapter 3

Graphical methods

A component of the bag of tricks of the applied mathematician is the facility of gaining a qualitative understanding of solutions to equations without actually solving them. The simplest version of this skill lies in the ability to draw graphs of functions without exact information. Just as calculators have led to the demise of basic arithmetic skills, so the use of graphical programs has led to an inability to follow this most basic of geometric skills. This is a facility which should not be lost.

3.1 Curve sketching

The simplest curves to sketch are polynomials. The function $y = x^2$ has the well-known *paraboloidal* shape shown in figure 1. How do we know this? Well, $y = x^2$ is positive, and clearly $y \rightarrow \infty$ as $x \rightarrow \pm\infty$. Furthermore, $y' = 2x$, and this is negative (so y decreases) for $x < 0$, and positive (so y increases) for $x > 0$. Particularly, y has a minimum at $x = 0$. These few simple facts are sufficient to provide the sketch in figure 3.1.

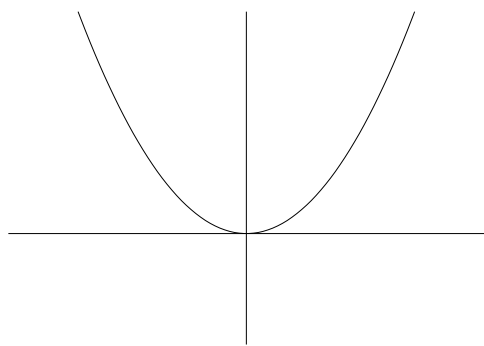


Figure 3.1: $y = x^2$

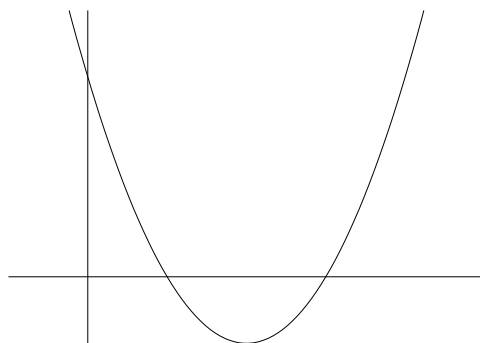


Figure 3.2: $y = (x - 1)(x - 3)$

More generally, other quadratics have a similar shape; the polynomial $y = ax^2 + bx + c$ can be written

$$y = a\left(x + \frac{b}{2a}\right)^2 - \frac{1}{4a}(b^2 - 4ac), \quad (3.1)$$

and we see that the graph of y can be obtained from that in figure 3.1 by translation to a new origin $(-b/2a, -(b^2 - 4ac)/4a)$, and magnification of the x -axis by a factor of \sqrt{a} ; see figure 3.2. This assumes $a > 0$: if $a < 0$, the parabola is upside down, as may be seen by considering the graph of $-y$ versus x .

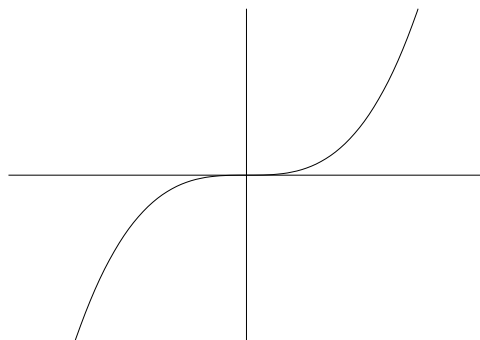


Figure 3.3: $y = x^3$

Cubic polynomials have an extra twist. If we consider $y = x^3$, then $y \rightarrow \pm\infty$, also $y' = 3x^2 > 0$, so y is monotonically increasing, though $y' = 0$ at $x = 0$ — the origin is an inflection point. The graph is shown in figure 3.3. For more general cubics, the general shape is monotonic as in figure 3.3, or non-monotonic as in figure 3.4, with two turning points. Apart from the fact that cubics generally have three roots, this can be most easily seen by realising that, since y' is a quadratic, there are generally two zeroes of y' , so that y has two turning points. This tells us the general shape

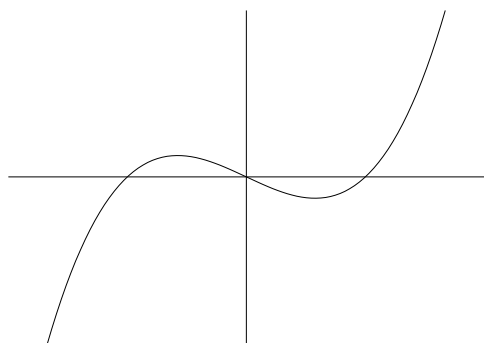


Figure 3.4: $y = x^3 - x$

of cubics, and in fact by extension we see that n -th order polynomials will generally have $n - 1$ turning points (though just as for the cubic, some may be absent). Most generally, n -th order polynomials have n zeroes; again, some may be absent.

Exponentials and logarithms

The exponential function e^x can be defined in various ways. For example, it is the solution of the differential equation

$$y' = y, \quad y(0) = 1, \quad (3.2)$$

and it has the Taylor series expansion

$$y = 1 + x + \frac{x^2}{2!} + \cdots + \frac{x^n}{n!} + \dots \quad (3.3)$$

It is clear from the definition in (3.3) that for positive x , y is positive (and thus increasing, since $y' = y > 0$), and in fact y grows faster than any polynomial, since $y > x^n/n!$ for all n . The graph of e^x is thus convex upwards, as shown in figure 3.5. For $x < 0$, the above reasoning is not useful in (3.3). However, since $e^x = e^{-M} \times e^{x+M}$, we see that the graph is *self-similar*, since e^{x+M} simply represents a shift of the origin to $x = -M$, and the premultiplicative factor e^{-M} is simply a scaling of the y -axis. By such reasoning, we see that e^x is positive and convexly increasing for all x .

The function $y = \ln x$ is the natural logarithm of x , and can be graphed using the fact that if $y = \ln x$, then (by definition) $x = e^y$: we obtain figure 3.6 by inverting and rotating figure 3.5. Note that $\ln x$ is not defined for $x < 0$. Nor does it have a series representation akin to (3.3); this is in fact evident because as $x \rightarrow 0$, $y \rightarrow -\infty$. Also $\ln x$ grows more slowly than any power of x as $x \rightarrow \infty$ (for the same reason that e^x grows faster than any power of x). In fact $(\ln x)' = 1/x$, so that the slope of $\ln x$ tends to zero, although $\ln x \rightarrow \infty$.

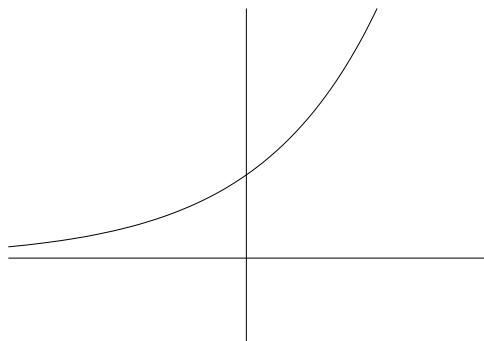


Figure 3.5: $y = e^x$

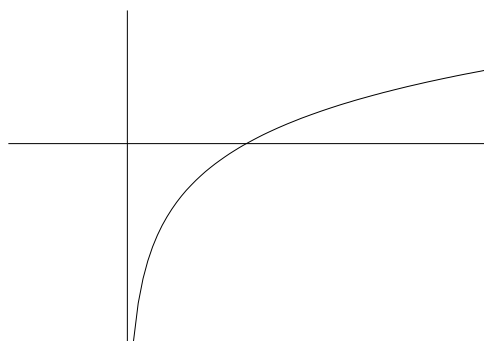


Figure 3.6: $y = \ln x$

When we wish to write statements such as ‘ $\ln x$ is much smaller than x when x is large’, we use the notation $\ln x \ll x$, or $x \gg \ln x$ (for $x \gg 1$). In this vein, we have

$$\begin{aligned} e^x &\gg x^n \text{ as } x \rightarrow \infty, \text{ for any } n, \\ \ln x &\ll x^\alpha \text{ as } x \rightarrow \infty, \text{ for any } \alpha > 0, \end{aligned} \tag{3.4}$$

and other more exotic examples, such as

$$1 \ll \ln \ln x \ll \ln x \text{ as } x \rightarrow \infty. \tag{3.5}$$

Often one wants to approximate functions $f(x)$ when x is large or small, and these notions of relative size can be very useful, but beware: although e^x is certainly large when x is ($e^x \approx 2.2 \times 10^4$ when $x = 10$), a function like $\ln \ln x$ is appallingly slow to increase ($\ln \ln x \approx 3$ if $x = 10^{10}$).

Inverses

The graph of the hyperbola $y = 1/x$ is shown in figure 3.7. It is simply obtained through reciprocation, or inversion, of the graph of $y = x$: x is monotone decreasing,

so $1/x$ is decreasing; $1/x < 0$ if $x < 0$, and > 0 if $x > 0$ (we write $1/x \lesseqgtr 0$ if $x \lesseqgtr 0$); $1/x \rightarrow 0$ as $x \rightarrow \pm\infty$; $1/x \rightarrow \pm\infty$ as $x \rightarrow 0\pm$ (i. e., as x tends to zero from above or below).

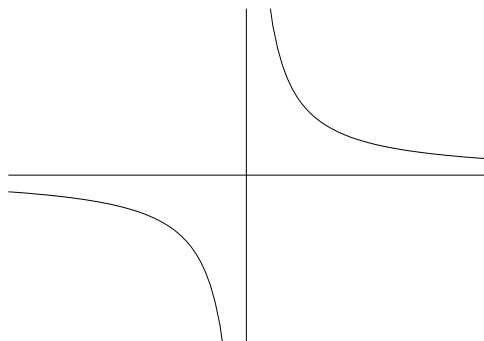


Figure 3.7: $y = 1/x$

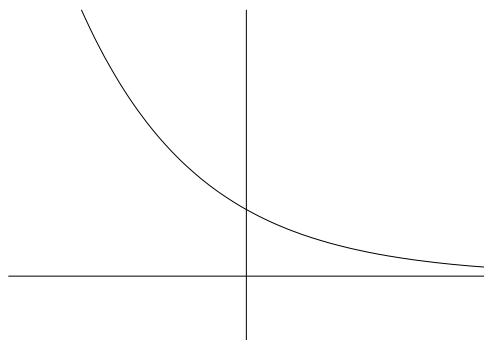


Figure 3.8: $y = e^{-x}$

More generally, inversion can be applied to other graphs via a kind of ‘nonlinear reflection’ about the line $y = 1$. For example, the graph of e^{-x} is shown in figure 3.8. It is the inversion of e^x (or: it is the reflection of e^x about the y -axis). Figure 3.9 shows a slightly more complicated example, the graph of $y = 1/(x^3 - x)$. The cubic denominator has roots at ± 1 and 0 , so that $y \rightarrow \pm\infty$ at these points, and $y \rightarrow 0$ as $x \rightarrow \pm\infty$.

Combinations

Figure 3.10 shows the graph of $y = xe^{-x}$ for $x > 0$. For $x \rightarrow 0$, $y \approx x$, since $y = x(1 - x + \frac{x^2}{2!} \dots)$, while as $x \rightarrow \infty$, $y \rightarrow 0$ (since $x \ll e^x$, i.e. $xe^{-x} \ll 1$). In fact, since x is an increasing function and e^{-x} is decreasing, it is clear that y must

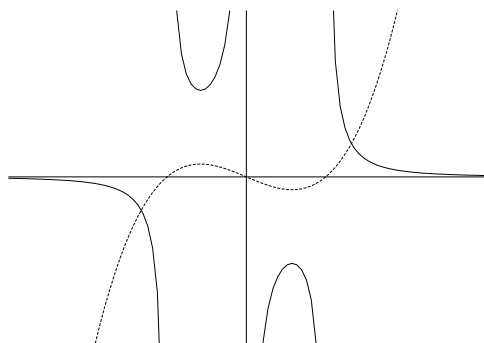


Figure 3.9: The cubic $x^3 - x$ and its inverse $y = (x^3 - x)^{-1}$

have a single maximum, and this is confirmed by simple differentiation. The graphs of $x^n e^{-x}$, $x > 0$, $n > 1$, are similar, but with a flat minimum at $x = 0$. Alternatively, one can graph $x e^{-x}$ by visual multiplication of x and e^{-x} .

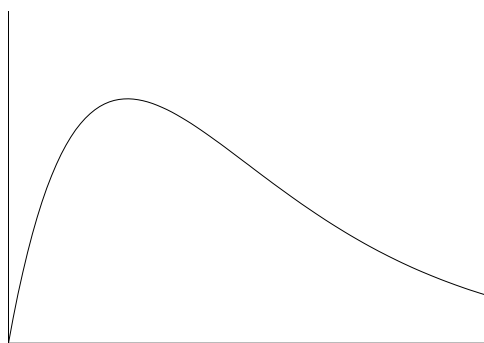


Figure 3.10: $y = x e^{-x}$

The graph of $\tanh x$ is shown in figure 3.11, and can be realised in several ways. For example,

$$\tanh x = 1 - \frac{2}{1 + e^{2x}}; \quad (3.6)$$

since e^{2x} is an increasing function, so also is $\tanh x$, and since $e^x \rightarrow \infty$ (0) as $x \rightarrow \infty$ ($-\infty$), we have $\tanh x \rightarrow \pm 1$ as $x \rightarrow \pm \infty$. In fact, $\tanh x$ is an *odd* function ($y(-x) = -y(x)$; an *even* function is one for which $y(-x) = y(x)$), so that its graph displays a rotational (by π) symmetry about the origin. In particular, $\tanh 0 = 0$; further, for small x , we have

$$\tanh x \approx 1 - \frac{2}{1 + (1 + 2x \dots)} \approx x + \dots, \quad (3.7)$$

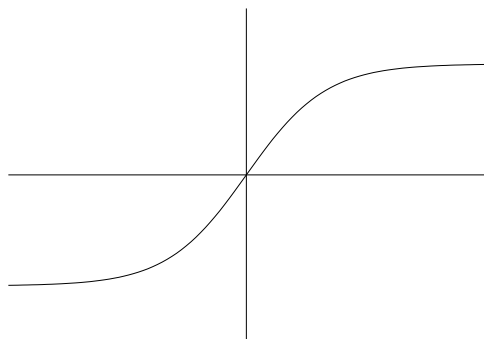


Figure 3.11: $y = \tanh x$

so that its slope is one at the origin.

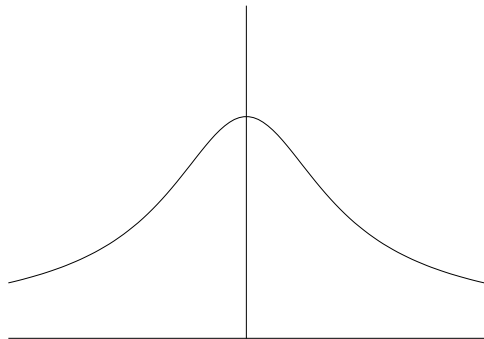


Figure 3.12: $y = x^{-1} \tanh x$

Further combinations with other algebraic functions are easily sketched. For example, figure 3.12 shows the graph of $y = \frac{\tanh x}{x}$. Clearly, y is even (since $\tanh x$ and x are both odd), $y \rightarrow 0$ as $x \rightarrow \infty$, and $y(0) = 1$.

Implicitly defined functions

If $y(x)$ is defined by

$$y^3 - y = x, \quad (3.8)$$

we can easily draw the graph of $y(x)$ simply by swapping the axes on figure 3.4. Note that such *implicitly defined* functions are no longer necessarily *single-valued* (a better known example is that of the inverse trigonometric function $y = \sin^{-1} x$).

A more complicated example is afforded by $y(x)$ defined by

$$x - y = K(x + y)^3, \quad (3.9)$$

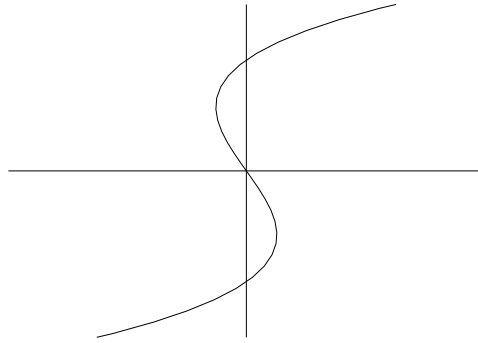


Figure 3.13: $y^3 - y = x$

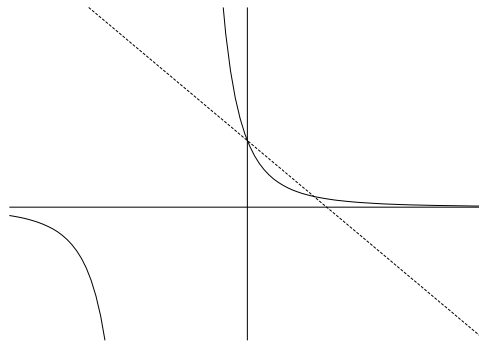


Figure 3.14: The graphs of $1 - u$ and $1/(1 + u)^3$.

where for example $K > 0$. The easiest way to sketch this is to realise that $(x - y)/\sqrt{2}$ and $(x + y)/\sqrt{2}$ represent orthogonal coordinates in a set of axes inclined at $\pi/4$ to the (x, y) axes. But we can also deduce the shape of the graph by more elementary considerations. First put $y = xu$, so that u satisfies

$$\frac{1 - u}{1 + u^3} = Kx^2; \quad (3.10)$$

we find the graph of u , and then that of y by multiplication with x . Figure 3.14 shows the graphs of $1 - u$ and $1/(1 + u)^3$ as functions of u ; multiplication of these yields $(1 - u)/(1 + u)^3$ in figure 3.15. With $K > 0$, x is then defined as either square root (but only where $(1 - u)/(1 + u)^3 > 0$):

$$x = \pm \left[\frac{1 - u}{K(1 + u)^3} \right]^{1/2}, \quad (3.11)$$

shown also in figure 3.15. Note the infinite slope of $x(u)$ at $u = 1$, due to the fact that $x \sim \pm(1 - u)^{1/2}$ there. (The symbol “ \sim ” is less precise than “ \approx ”; we say $f \sim g$

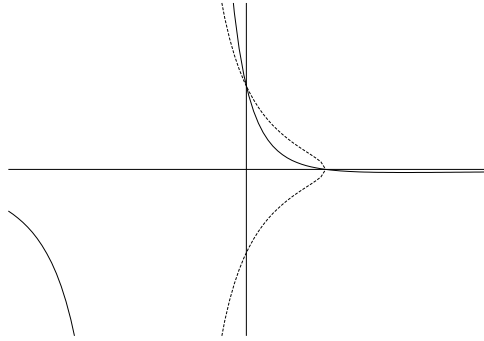


Figure 3.15: The graphs of $(1 - u)/(1 + u)^3$ and $\pm \left[\frac{1 - u}{K(1 + u)^3} \right]^{1/2}$ ($K = 1$).

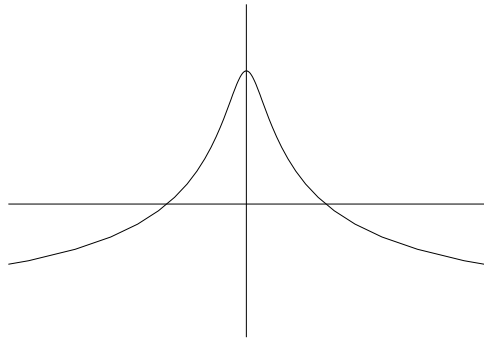


Figure 3.16: $u(x)$ given by $x = \pm \left[\frac{1 - u}{K(1 + u)^3} \right]^{1/2}$ ($K = 1$).

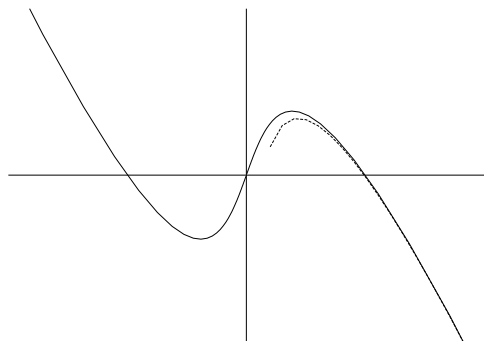


Figure 3.17: $y = xu(x)$; also shown on the right is the approximation in (3.13).

as $x \rightarrow x_0$ if f/g tends to a finite limit; thus $x^2 + 1 \sim 1$ as $x \rightarrow 0$, $x^2 + 1 \sim x^2$ as $x \rightarrow \infty$, and so on.) Inversion of u now yields figure 3.16, having the same shape as $\frac{2 \tanh x}{x} - 1$, or $\frac{2}{1+x^2} - 1$. Multiplication by x finally yields figure 3.17. The function $y(x)$ is defined (for $K > 0$) as a single-valued odd function of x . We see that $y \rightarrow \mp\infty$ as $x \rightarrow \pm\infty$. Since $x \ll x^3$ and $y \ll y^3$, we infer that in these limits, $x - y \ll K(x + y)^3$ (which is impossible since they are equal) unless $x \sim -y$. Note the correct use of the asymptotic equivalence notation “ \sim ” here; we cannot correctly say $x \rightarrow -y$ as neither tends to a finite limit: nor can we say $x + y \rightarrow 0$, which is not true (in fact $x + y \rightarrow \pm\infty$). We can use the *asymptotic* relation $x \sim -y$ as $x \rightarrow \pm\infty$, to refine the approximation for large x . If $y \approx -x$, then we have from (3.9)

$$y + x = \left[\frac{2x - (y + x)}{K} \right]^{1/3}, \quad (3.12)$$

and this forms the basis of a regular perturbative method to approximate y , as discussed in chapter 2. Here we simply give the result, which is also shown in figure 3.17 (and we see that the approximation at large positive x is quite accurate for $x > 2/3\sqrt{3K}$, roughly (where $y' = 0$)):

$$y \approx -x + \left(\frac{2x}{K} \right)^{1/3} - \frac{1}{3K^2} \left(\frac{2x}{K} \right)^{-1/3} + O\left(\frac{1}{x} \right). \quad (3.13)$$

The notation $O(1/x)$ means terms of the same size as $1/x$ (as, here, $x \rightarrow \infty$). It is an alternative to the ‘ \sim ’ notation: we say $f = O(g)$ if $f \sim g$ (as $x \rightarrow x_0$).

The final example we use is an algebraic equation which arises in combustion theory: it has to do with striking a match! Let the function $T(\mu)$ be defined by

$$\frac{T}{\mu} = \exp \left[\frac{T}{1 + \varepsilon T} \right], \quad (3.14)$$

where ε is a positive parameter (i.e., we take it to be fixed as we vary μ). In applications ε is usually small ($\varepsilon \ll 1$), and it is convenient (though not necessary) to suppose this is the case. Equality in (3.14) can only occur for $T > 0$, and we therefore limit our attention to positive T . The logistic function $T/(1 + \varepsilon T)$ is monotone increasing with T and *saturates* (i.e., tends to a positive limit) as $T \rightarrow \infty$. Since the exponential function is also increasing, $\exp[T/(1 + \varepsilon T)]$ increases and also saturates: it is a *sigmoidal* curve with an inflection point, which is most easily seen when $\varepsilon \ll 1$, for then $\exp[T/(1 + \varepsilon T)] \approx e^T$ for $T = O(1)$ (numerically, ‘about’ one), but the function must turn round when T is large (specifically, when $T = O(1/\varepsilon)$).

When μ is small, it is clear (see figure 3.18) that there is one value of T satisfying (3.14), and $T \rightarrow 0$ as $\mu \rightarrow 0$; similarly for large T , there is one intersection, and $T \rightarrow \infty$ as $\mu \rightarrow \infty$. In fact $T \approx \mu$, $\mu \ll 1$, while $T \approx \mu e^{1/\varepsilon}$, $\mu \gg 1$. But for intermediate values of μ , these two branches (‘cold’ and ‘hot’) are joined by an intermediate ‘warm’ branch, so that, as shown in figure 3.19, three different values are possible.

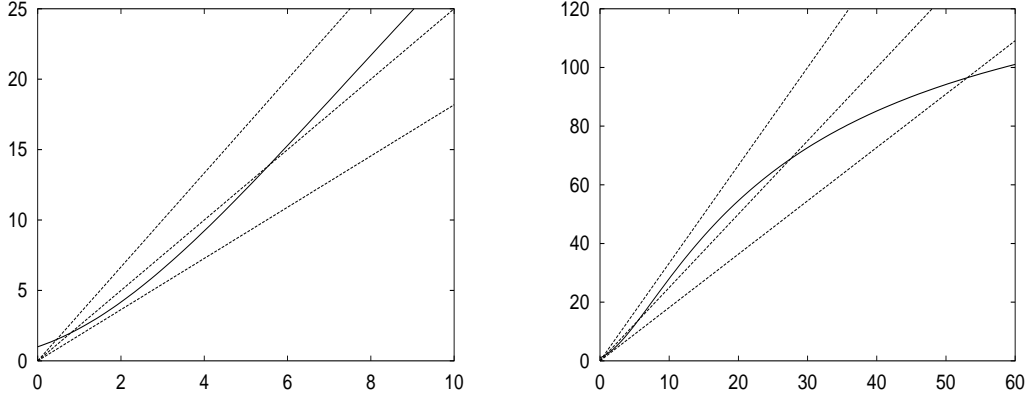


Figure 3.18: Two views of the graphs of T/μ (for $\mu = 0.3, 0.4$ and 0.55) and $\exp\left[\frac{T}{1+\varepsilon T}\right]$ (with $\varepsilon = 0.2$), indicating the possibility of one, two or three intersections; note the disparity in T and μ scales in the two figures.

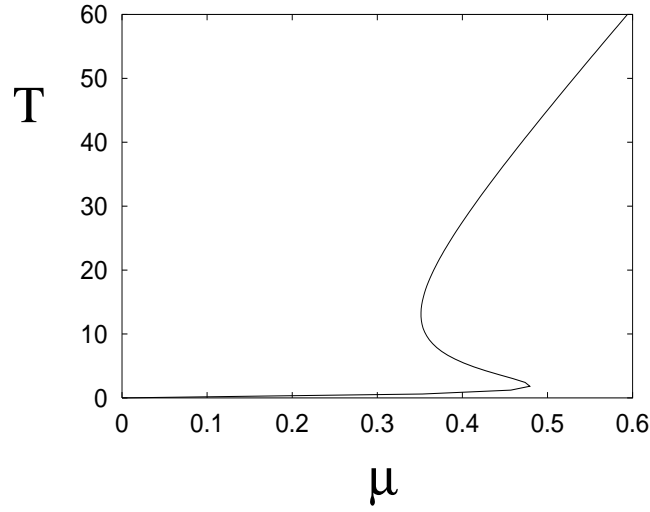


Figure 3.19: T versus μ given by equation (3.14), with $\varepsilon = 0.2$.

3.2 Root-finding

Suppose we want to solve the algebraic (as opposed to differential, or integral) equation

$$f(x) = 0. \quad (3.15)$$

In general, exact analytic techniques are not available, and the problem must be solved by an approximate method, and often this means using numerical methods. A general class of numerical technique to solve (3.15) is by the use of *iterative methods*, and we begin by reviewing some of these. In general, one defines a sequence $x_0, x_1, \dots, x_n, \dots$, where usually x_n is determined in terms of x_{n-1} , and the methods differ in the choice of iterative procedure.

Interval bisection

Interval bisection is slow (thus bad) but guaranteed to work. We assume only that f is continuous, and that two initial values x_-, x_+ are known, for which (say) $f(x_-) < 0$, $f(x_+) > 0$. We then define the bisection value $w = (x_+ + x_-)/2$, and calculate $f(w)$. We then reassign x_{\pm} as follows:

$$\begin{aligned} x_+ &= w & \text{if } f(w) > 0, \\ x_- &= w & \text{if } f(w) < 0. \end{aligned} \quad (3.16)$$

The iterative step defines two sequences x_- and x_+ (or $x_-^{(n)}$ and $x_+^{(n)}$), with the property that $x_+ - x_- \rightarrow 0$ and $f(x_+) > 0$, $f(x_-) < 0$. The root x^* where $f(x^*) = 0$ is thus sandwiched between the upper and lower estimates.

The error goes down by at least a factor of 2 each iteration, so that the error ε_n after n iterations is

$$\varepsilon_n = \frac{\varepsilon_0}{2^n}; \quad (3.17)$$

in particular, the number of steps N_ε which is required to calculate the root with an error of ε is

$$N_\varepsilon \approx \frac{\ln(1/\varepsilon)}{\ln 2}. \quad (3.18)$$

Interval bisection is plodding but effective; however, it is no use in more than two variables (imagine trying to find a zero of $f(x, y) = x^2 + y^2 - \frac{1}{4}$, with f evaluated at the four points of the unit square $(0, 0), (1, 0), (0, 1), (1, 1)$).

Secant method

If f is relatively smooth, then the arc between two successive points $(x_{n-1}, f(x_{n-1}))$ and $(x_n, f(x_n))$ provides a better and more rapid approximation, see figure 3.20. The iterative method is defined by

$$\begin{aligned} x_{n+1} &= x_n - \frac{f_n(x_n - x_{n-1})}{f_n - f_{n-1}} \\ &= \frac{x_{n-1}f_n - x_nf_{n-1}}{f_n - f_{n-1}}, \end{aligned} \quad (3.19)$$

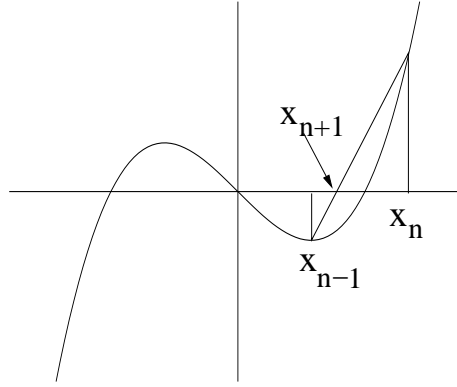


Figure 3.20: Secant method

and is clearly better than interval bisection, and particularly if the function is *smooth*, i. e., continuously differentiable, $f \in C^1$. A disadvantage is that two previous iterates are used, and in fact since we expect x_n to be closer to the root than x_{n-1} , one might hope that a better version of this method might exist.

Newton's method

The better method is the Newton-Raphson iterative method. Unlike the secant method, it requires f to be differentiable, but it does not need two preceeding iterates. It is defined (see figure 3.21) by

$$x_n = x_{n-1} - \frac{f(x_{n-1})}{f'(x_{n-1})}. \quad (3.20)$$

Suppose that $f(x^*) = 0$, and that the error at the n -th step is ε_n , so $x_n = x^* + \varepsilon_n$, thus

$$\varepsilon_n = \varepsilon_{n-1} - \frac{f(x^* + \varepsilon_{n-1})}{f'(x^* + \varepsilon_{n-1})}. \quad (3.21)$$

We have (via Taylor series)

$$f'(x^* + \varepsilon) \approx f'(x^*) + \varepsilon f''(x^*), \quad (3.22)$$

and

$$f(x^* + \varepsilon) \approx \varepsilon f'(x^*) + \frac{\varepsilon^2}{2} f''(x^*). \quad (3.23)$$

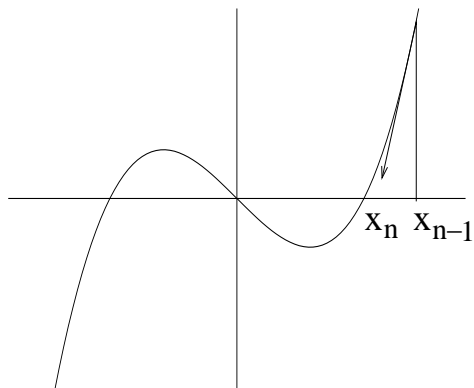


Figure 3.21: Newton's method

If we substitute (3.22) and (3.23) into (3.21), we find

$$\begin{aligned}
 \varepsilon_n &\approx \varepsilon_{n-1} - \frac{\varepsilon_{n-1}[f'(x^*) + \frac{\varepsilon_{n-1}}{2}f''(x^*)]}{f'(x^*) + \varepsilon_{n-1}f''(x^*)} \\
 &= \varepsilon_{n-1} \left[1 - \left\{ 1 + \frac{\varepsilon_{n-1}f''(x^*)}{2f'(x^*)} \right\} \left\{ 1 + \frac{\varepsilon_{n-1}f''(x^*)}{f'(x^*)} \right\}^{-1} \right] \\
 &\approx \frac{f''(x^*)}{2f'(x^*)} \varepsilon_{n-1}^2
 \end{aligned} \tag{3.24}$$

(assuming, of course, that f can be differentiated twice). Writing $c = f''(x^*)/2f'(x^*)$, the solution of this is (by induction)

$$\varepsilon_n = \frac{1}{c} \{c\varepsilon_0\}^{2^n}, \tag{3.25}$$

and the convergence is *super-exponential*. The number of steps required to reduce the error to a tolerance ε is given by

$$N_\varepsilon \approx \frac{\ln \ln(1/\varepsilon)}{\ln 2}. \tag{3.26}$$

Newton iteration is therefore *much* faster than interval bisection.

Convergence

Equation (3.24) indicates that (as is obvious) Newton iteration will be bad if $f'(x^*) \approx 0$. More generally, large excursions occur if $f'(x_{n-1}) \approx 0$; this raises the issue not only of when Newton iteration will work, but also as to what solution it will converge to. For example, consider Newton iteration for the solution of

$$f(x) = x^3 - x = 0. \tag{3.27}$$

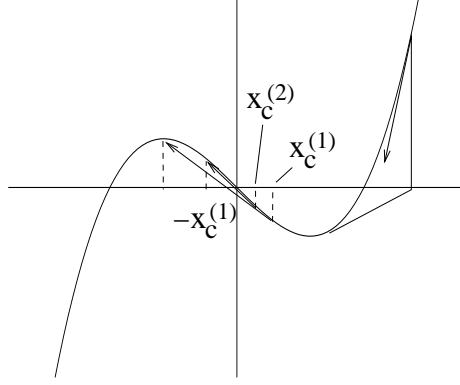


Figure 3.22: The critical values x_c^i .

There are three roots: 0, 1 and -1 , and the graph has two turning points at $\pm 1/\sqrt{3}$. It is pretty clear (see figure 3.22) that if $x_0 > 1/\sqrt{3}$, then $x_2 \rightarrow 1$ as $n \rightarrow \infty$ (similarly if $x_0 < -1/\sqrt{3}$, $x_n \rightarrow -1$). Also if x_0 is sufficiently close to zero, it is clear that $x_n \rightarrow 0$. The values $\pm 1/\sqrt{3}$ are critical, for if x_0 is *just* less than $1/\sqrt{3}$, then $x_1 < -1/\sqrt{3}$, and $x_n \rightarrow -1$. This will be the case for x_0 in a range $x_c^{(1)} < x_0 < 1/\sqrt{3} = x_c^{(0)}$, where $x_c^{(1)}$ is the pre-image under iteration of $-1/\sqrt{3}$. If we denote the Newton iteration method as

$$x_n = G(x_{n-1}) \quad (3.28)$$

(for (3.27), $G(x) = 2x^3/(3x^2 - 1)$), then $x_c^{(1)}$ (> 0) is defined (evidently uniquely) as that value such that

$$G(x_c^{(1)}) = -x_c^{(0)}. \quad (3.29)$$

So far we thus have the following:

$$\begin{aligned} x_0 &> x_c^{(0)}, & x_n &\rightarrow 1; \\ x_c^{(1)} &< x_0 < x_c^{(0)}, & x_n &\rightarrow -1. \end{aligned} \quad (3.30)$$

Now if x_0 is *just* less than $x_c^{(1)}$, then x_1 will be *just* larger than $-1/\sqrt{3} = -x_c^{(0)}$, so that $x_2 > 1/\sqrt{3}$, and $x_n \rightarrow +1$. Again there will be a range where this occurs, bounded by the value $x_c^{(2)}$ such that

$$G(x_c^{(2)}) = -x_c^{(1)}. \quad (3.31)$$

Thus for

$$x_c^{(2)} < x_0 < x_c^{(1)}, \quad x_n \rightarrow +1. \quad (3.32)$$

Evidently one can carry on in this way, and this suggests the existence of a denumerable set of intervals $(x_c^{(m)}, x_c^{(m+1)})$ on which $x_n \rightarrow (-1)^m$ as $n \rightarrow \infty$, where the end-points are defined by the iterative scheme

$$G(x_c^{(m)}) = -x_c^{(m-1)}, \quad (3.33)$$

with $x_c^{(0)} = 1/\sqrt{3}$. Figure 3.22 suggests that the values $x_c^{(m)}$ converge to a limit, say x_c , defined by $G(x_c) = -x_c$, so that $x_c = 1/\sqrt{5}$, and that $x_n \rightarrow 0$ for all $|x_0| < x_c$. At each value $x_0 = x_c^{(m)}$, Newton's method fails using exact arithmetic, although practical numerical calculations will always allow convergence to either 1 or -1 .

Other iterative methods

There are plenty of ways to define iterative methods to solve $f(x) = 0$. For example, we can write the equation in the form $x = G(x) \equiv x + f(x)$, and then define a sequence

$$x_{n+1} = G(x_n); \quad (3.34)$$

or if $x = h(y)$, then an iterative method for y could be

$$y_{n+1} = h^{-1}[G\{h(y_n)\}] \quad (3.35)$$

(where h^{-1} denotes the inverse function of h ; that is $y = h^{-1}(x)$ if (and only if) $x = h(y)$.) Such methods are not generally very fast, but lack the requirement (sometimes non-trivial) of differentiability, and have the advantage over interval bisection of explicitness; however, they do not always converge.

Suppose (3.34) has a root x^* , and the (small) error at the n -th step is ε_n ; then

$$\varepsilon_{n+1} \approx G'(x^*)\varepsilon_n, \quad (3.36)$$

and thus

$$\varepsilon_n \approx [G'(x^*)]^n \varepsilon_0. \quad (3.37)$$

Normally the error is like that of interval bisection; it is only super-exponential if $G'(x^*) = 0$ (because then, in fact, $\varepsilon_{n+1} \approx [G''(x^*)/2]\varepsilon_n^2$: Newton iteration satisfies this criterion precisely). Equation (3.37) implies that $\varepsilon_n \rightarrow 0$, or $x_n \rightarrow x^*$, if $|G'(x^*)| < 1$, and this is the criterion for convergence of the iteration scheme.

As an illustration, we reconsider equation (3.14),

$$T = \mu \exp \left[\frac{T}{1 + \varepsilon T} \right]. \quad (3.38)$$

For intermediate values of μ , this can have three equilibria, and a stable method to calculate the lowest and highest of these two is

$$T_{n+1} = \mu \exp \left[\frac{T_n}{1 + \varepsilon T_n} \right]. \quad (3.39)$$

It is clear from figure 3.23 that this iterative scheme does converge as indicated. If, on the other hand, we want to calculate the middle root, another strategy is necessary. Most simply, we can iterate the inverse function, thus $T_{n+1} = G^{-1}(T_n)$, or for (3.38), this is

$$T_{n+1} = \frac{\ln(T_n/\mu)}{1 - \varepsilon \ln(T_n/\mu)}. \quad (3.40)$$

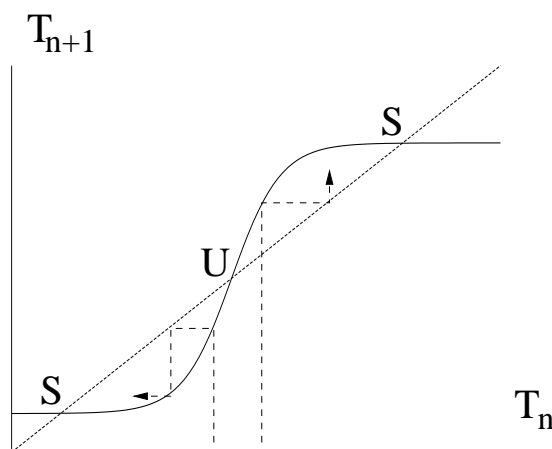


Figure 3.23: Convergence where the slope is less than one.

3.3 Difference equations

3.4 Ordinary differential equations

Graphical methods have their uses also in differential equations. In chapter 4, we will consider graphical methods for two-dimensional ordinary differential equation systems (phase plane analysis). Here we briefly discuss the simplest ordinary differential equation (or ODE): the first order autonomous equation

$$\dot{x} = f(x), \quad (3.41)$$

where the notation \dot{x} indicates the first derivative, and the use of an overdot is normally associated with the use of time t as the independent variable, i. e., $\dot{x} = dx/dt$.

The solution of (3.41) can be written as the *quadrature*

$$t = t_0 + \int_{x_0}^x \frac{d\xi}{f(\xi)}, \quad (3.42)$$

and, depending on the function f , this may be inverted to find x explicitly. So, for example, the solution of $\dot{x} = 1 - x^2$ is $x = \tanh(t + c)$ (if $|x(t_0)| < 1$).

Going on with this latter example, we see that $x \rightarrow 1$ as $t \rightarrow \infty$ (and $x \rightarrow -1$ as $t \rightarrow -\infty$, and in practice, this may be all we want to know. If a population is subject to constant immigration and removal by mutual pair destruction, so that $\dot{x} = 1 - x^2$, then after a transient (a period of time dependence), the population will equilibrate stably to $x = 1$. But to ascertain this, all we need to know is the shape of the curve $f(x) = 1 - x^2$. Simply by finding the zeros of $1 - x^2$ and the slope of the graph there, we can immediately infer that for all initial values $x(0) > -1$, $x \rightarrow 1$ as $t \rightarrow \infty$, while if $x(0) < -1$, then $x \rightarrow -\infty$ as $t \rightarrow -\infty$: see figure 3.24. And this can be done for *any* function $f(x)$ in the equation $\dot{x} = f(x)$.

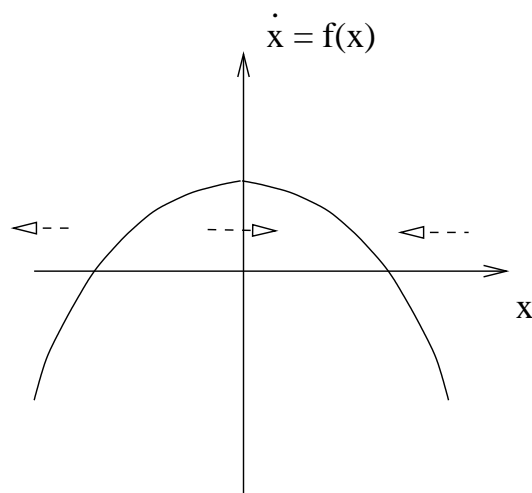


Figure 3.24: The evolution of the solutions of $\dot{x} = f(x)$ depends only on the sign of x .

This simple example carries an important message. Approximate or qualitative methods may be just as useful, or more useful, than the ability to obtain exact results. An extension of this insight suggests that it may often be the case that approximate analytic insights can provide more information than precise, computational results.

3.5 Chemical reactions

Exercises

- 3.1 (a) Sketch the function $y = x^3 e^{-x}$, $x > 0$.
 (b) Sketch $y = x \ln x$, $x > 0$. (Note $\ln x \ll \frac{1}{x}$ when $x \ll 1$; why?)
 (c) If $y = x^x$, $x > 0$, and $y(0) = 1$, sketch $y(x)$.
 (d) Sketch y defined by $y = x + (x + y)^3$.
 (e) Sketch y defined by $\tan x = \tanh y$.
 (f) Sketch $T(\mu)$ defined by $T = \mu \exp\left(\frac{T}{1 + \varepsilon T}\right)$, where $\varepsilon > 0$, for $\mu > 0$.
- 3.2 (a) Newton's method to solve $x^3 - x = 0$ yields the difference equation

$$x_{n+1} = G(x_n),$$

where

$$G(x) = \frac{2x^3}{3x^2 - 1}.$$

Sketch $G(x)$, and explain why convergence to the solution $x = 1$ (for example) is very rapid. Solve the equation

$$G(x_c) = -x_c, \quad x_c > 0,$$

and test (numerically) the conjecture that for $|x_0| < x_c$, Newton iterates x_n tend to the solution $x = 0$, but that for $x_c < x_0 < 1/\sqrt{3}$, there is a sequence of intervals in which alternatively $x_n \rightarrow +1$ or -1 .

(b) Consider the equation

$$xe^{-x} = a,$$

where $0 < a < e^{-1}$, a is constant.

- (i) Devise iterative methods which you can guarantee will converge to the lower root; to the higher root.
- (ii) By consideration of Newton's method applied to this equation, estimate the range of initial values x_0 which will converge to the lower root; to the higher root.
- (iii) Test your results numerically, e.g., with $a = 0.1$.

3.3 The differential equation

$$\dot{x} = a - xe^{-x}, \quad x > 0, \quad a > 0,$$

may have 0, 1 or 2 steady states. Determine how these depend on a , and describe how solutions behave for $a > e^{-1}$ and $a < e^{-1}$, depending on the value of $x(0)$.

Chapter 4

Stability and oscillations

If we move from first order systems to second order systems of the form

$$\begin{aligned}\dot{x} &= f(x, y), \\ \dot{y} &= g(x, y),\end{aligned}\tag{4.1}$$

more interesting phenomena can occur. There is indeed a hierarchy of complexity which one ascends as the order of the equation increases. As we saw in the preceding chapter, first order equations have steady state solutions which are alternately stable and unstable, and the instability is direct, in the sense that loss of stability as a parameter changes leads to a transient migration towards another fixed point.

In second order systems, a different kind of instability can occur. As well as the direct instability, or exchange of stability, between different fixed points, oscillatory instability can occur, and the consequence of such instabilities is that permanent oscillatory (periodic) solutions can occur: in two dimensions there is dynamic behaviour.¹

4.1 Linear stability

We illustrate the technique of linear stability analysis for (4.1). The analysis applies (and is easy) in two dimensions, but evidently the method applies in n dimensions, although the classification of behaviour takes its essence from the two-dimensional example.

A steady state of (4.1) is a constant pair (x_0, y_0) which satisfies the equations, i. e., $f(x_0, y_0) = g(x_0, y_0) = 0$. For small perturbations about this state, we write

$$x = x_0 + X, \quad y = y_0 + Y,\tag{4.2}$$

and linearise the system (4.1) to obtain the approximate equations

$$\begin{pmatrix} \dot{X} \\ \dot{Y} \end{pmatrix} = \begin{pmatrix} f_x & f_y \\ g_x & g_y \end{pmatrix} \begin{pmatrix} X \\ Y \end{pmatrix},\tag{4.3}$$

¹When one proceeds to third or higher order systems, more exotic behaviour can occur: period-doubling, quasi-periodic oscillations, and chaos, for example.

where the partial derivatives are evaluated at (x_0, y_0) . The matrix

$$M = \begin{pmatrix} f_x & f_y \\ g_x & g_y \end{pmatrix} \quad (4.4)$$

is sometimes called the community matrix (particularly in applications in population biology), and its trace and determinant will be denoted

$$T = \text{tr } M, \quad D = \det M. \quad (4.5)$$

Because M is a constant matrix, solutions of (4.3) are of the form

$$\begin{pmatrix} X \\ Y \end{pmatrix} = \mathbf{u} e^{\lambda t}, \quad (4.6)$$

where \mathbf{u} is an eigenvector of M and λ is the corresponding eigenvalue; thus λ is a root of the quadratic equation

$$\lambda^2 - T\lambda + D = 0. \quad (4.7)$$

Classification of the different kinds of behaviour follows from the different combinations of pairs of values of λ . For $D > T^2/4$, the roots are complex, and the consequent phase portrait is a spiral; unstable if $T > 0$, and stable if $T < 0$. Examples are shown in figure 4.1.

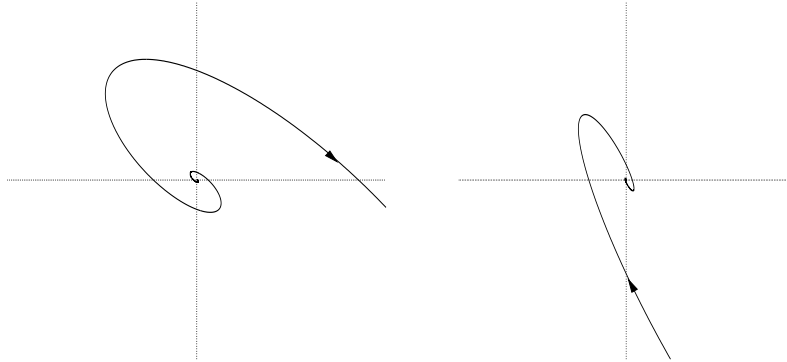


Figure 4.1: Unstable (left) and stable (right) spirals solving (4.3) with $M = \begin{pmatrix} 1 & 1 \\ -1 & -0.4 \end{pmatrix}$ (left) and $M = \begin{pmatrix} 1 & 1 \\ -3 & -2 \end{pmatrix}$ (right).

If $0 < D < T^2/4$, the fixed point is a node, with two real eigenvalues of M having the same sign. The node is unstable if $T > 0$ and stable if $T < 0$. An example is shown in figure 4.2.

Finally, a saddle point is shown in figure 4.3. This occurs if $D < 0$. The eigenvalues are real and opposite in sign. There is one stable direction and one unstable, and the fixed point is thus unstable. Putting these results together, we see that stability occurs if and only if $D > 0$ and $T < 0$, and the classification of fixed points as spiral, node or saddle can be represented in (D, T) space as shown in figure 4.4.

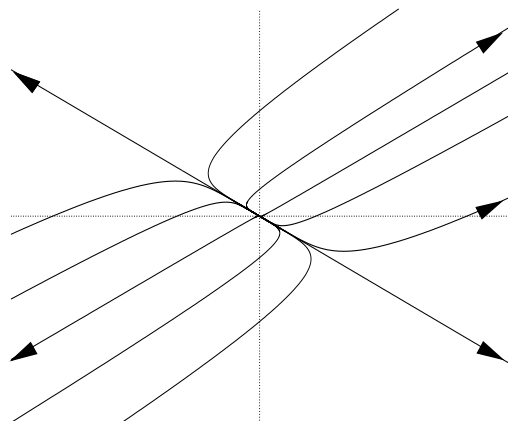


Figure 4.2: Unstable node with $M = \begin{pmatrix} 1 & 1 \\ 0.5 & 1 \end{pmatrix}$.

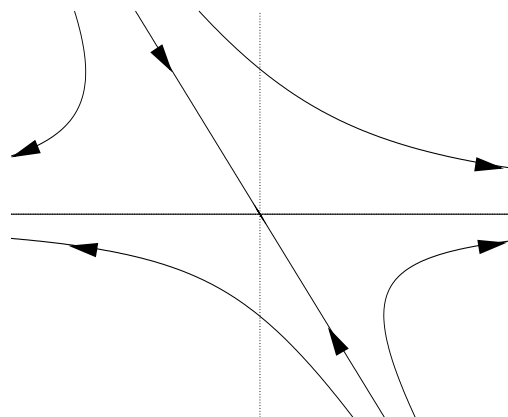


Figure 4.3: Saddle point: $M = \begin{pmatrix} 1 & 1 \\ 0 & -1 \end{pmatrix}$.

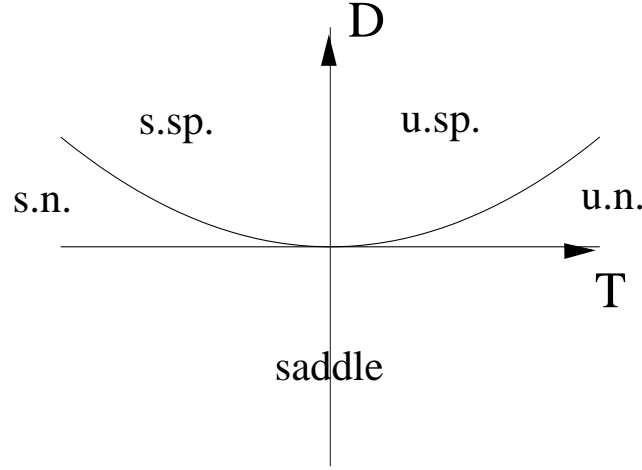


Figure 4.4: T - D parameter space indicating location of stable and unstable spirals and nodes, and saddles.

4.2 Nonlinear stability

4.3 Phase plane analysis

To go beyond linear stability analysis and complete the phase portrait of solution trajectories is the subject of phase plane analysis, and the most interesting feature of the phase plane is that periodic oscillations can occur. An illuminating example is illustrated in figure 4.5, and is typified by (but is not restricted to) the equations

$$\begin{aligned}\dot{x} &= g(x) - y, \\ \dot{y} &= y - h(x),\end{aligned}\tag{4.8}$$

where the functions g and h are as shown in the figure: g is unimodal (e.g., like $g = xe^{-x}$) and h is monotonic decreasing (e.g., like $h = 1/(x - c)$). The graphs of $g(x)$ and $h(x)$ (and more generally, the curves where $\dot{x} = 0$ and $\dot{y} = 0$) are called the nullclines of x and y , and it is simple to see that where they intersect, there is a steady state solution, and also that in the four regions separated by the nullclines, the trajectories wind round the fixed point in an anti-clockwise manner.

The next issue is whether the fixed point is unstable. If we denote it as (x^*, y^*) , write $x = x^* + X$, $y = y^* + Y$, and linearise for small X and Y , then

$$\begin{pmatrix} \dot{X} \\ \dot{Y} \end{pmatrix} \approx \begin{pmatrix} g' & -1 \\ -h' & 1 \end{pmatrix} \begin{pmatrix} X \\ Y \end{pmatrix},\tag{4.9}$$

where the derivatives are evaluated at the fixed point. The stability of this two by two system with community matrix $A = \begin{pmatrix} g' & -1 \\ -h' & 1 \end{pmatrix}$ is governed by the trace and

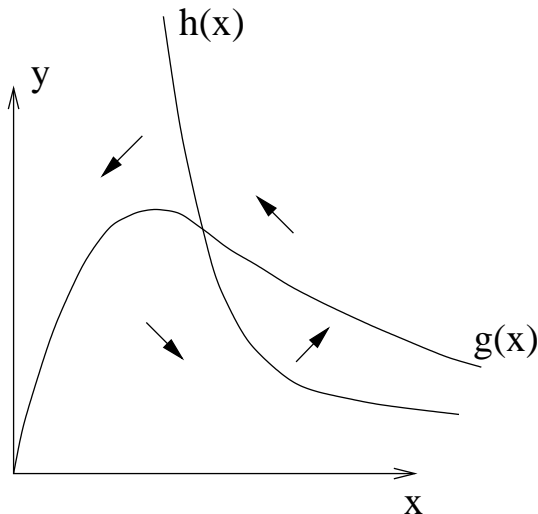


Figure 4.5: Nullclines for (4.8).

determinant of A , as indicated in figure 4.4. In the present case, $\text{tr } A = g' + 1$, $\det A = g' - h'$, so that for the situation shown in figure 4.5, where $h' < g' < 0$, $\det A > 0$, and the fixed point is an unstable spiral (or node) if $g' > -1$. When $g' = -1$, there is a Hopf bifurcation, and if the system has bounded trajectories (as is normal for a model of a physical process) then one expects a stable periodic solution to exist. Figure 4.6 illustrates an example.

4.4 Relaxation oscillations

It is a general precept of the applied mathematician that there are three kinds of numbers: small, large, and of order one. And the chances of a number being $O(1)$ are not great. Thus for systems of the form (4.1), it is often the case in practice that the time scales for each equation are different, so that in suitable dimensionless units, a second order system might take the form

$$\begin{aligned}\varepsilon \dot{x} &= y - g(x), \\ \dot{y} &= h(x) - y,\end{aligned}\tag{4.10}$$

where the parameter ε is small. The system (4.10) is essentially the same as (4.8) with time reversed, but now suppose that the nullclines are as shown in figure 4.7, i.e. g has a cubic shape. Trajectories now rotate clockwise, and linearisation about the fixed point yields a community matrix A with $\text{tr } A = -(g'/\varepsilon) - 1$, $\det A = (g' - h')/\varepsilon$, thus with $g' > h'$, the fixed point is a spiral or node, and with $\varepsilon \ll 1$, $\text{tr } A \approx -g'/\varepsilon > 0$, so it is unstable. Thus we expect a limit cycle, and because $\varepsilon \ll 1$, this takes the form of a *relaxation oscillation* in which the trajectory jumps rapidly backwards and forwards between branches of the x nullcline. For $\varepsilon \ll 1$, x rapidly jumps to its

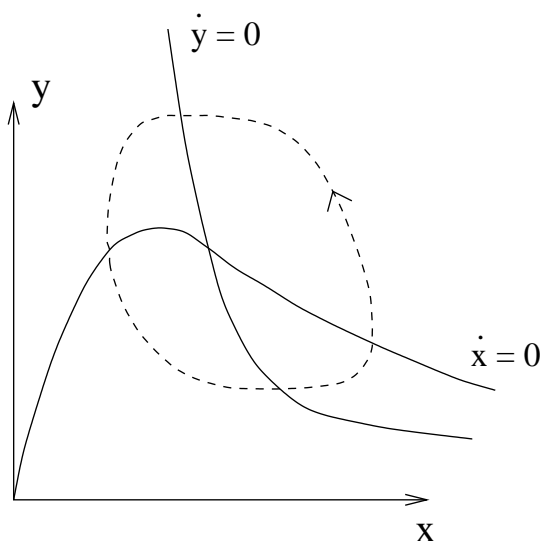


Figure 4.6: Typical form of limit cycle for a system with nullclines as in figure 4.5.

quasi-equilibrium $y \approx g(x)$, and then y migrates slowly ($\dot{x} \approx [h(x) - g(x)]/g'(x)$) until $g' = 0$ and x jumps rapidly to the other branch of g . Figure 4.8 shows the time series of the resulting oscillation. The motion is called ‘relaxational’ because the fast variable x ‘relaxes’ rapidly to a quasi-stationary state after each transient excursion.

4.5 Belousov-Zhabotinskii reaction

Exercises

4.1 u and v satisfy the ordinary differential equations

$$\begin{aligned}\dot{u} &= k_1 - k_2 u + k_3 u^2 v, \\ \dot{v} &= k_4 - k_3 u^2 v,\end{aligned}$$

where $k_i > 0$. By suitably scaling the equations, show that these can be written in the dimensionless form

$$\begin{aligned}\dot{u} &= a - u + u^2 v, \\ \dot{v} &= b - u^2 v,\end{aligned}$$

where a and b should be defined. Show that if u, v are initially positive, they remain so. Draw the nullclines in the positive quadrant, show that there is a unique steady state and examine its stability. Are periodic solutions likely to exist?

4.2 The relaxational form of the van der Pol oscillator is

$$\varepsilon \ddot{x} + (x^2 - 1)\dot{x} + x = 0, \quad \varepsilon \ll 1.$$

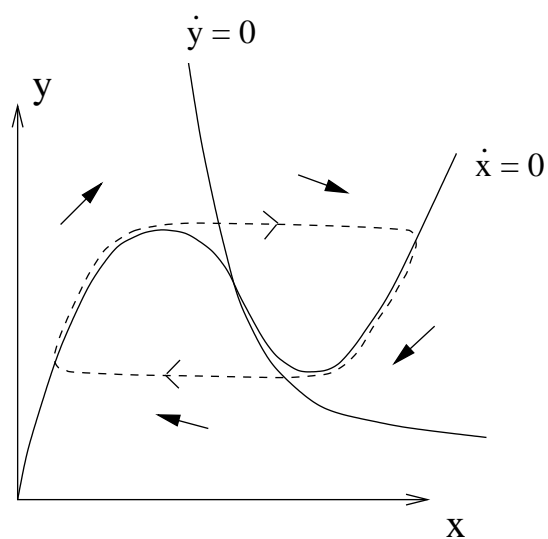


Figure 4.7: Typical form of relaxation oscillation in phase plane for (4.10).

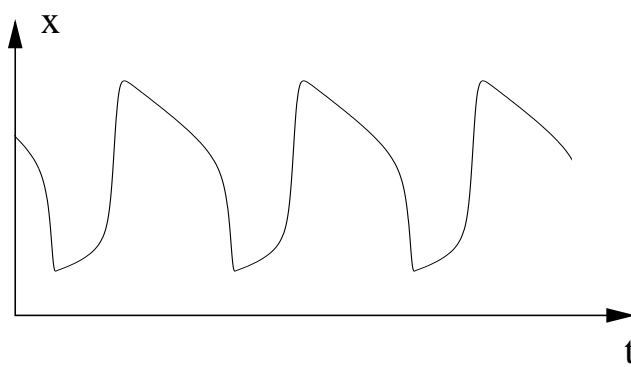


Figure 4.8: Time series for x corresponding to figure 4.7.

A suitable phase plane is spanned by (x, y) , where $y = \varepsilon \dot{x} + \frac{1}{3}x^3 - x$. Describe the motion in this phase plane, and find, approximately, the period of the relaxation oscillation. What happens if $\varepsilon < 0$?

- 4.3 The Belousov-Zhabotinskii chemical reaction can be approximately described by the two component pair of ordinary differential equations

$$\varepsilon \dot{X} = X(1 - X) - \left(\frac{X - \delta}{X + \delta} \right) Z,$$

$$\dot{Z} = \gamma X - Z,$$

where ε and δ are very small, and γ is $O(1)$. Show that relaxation oscillations will occur for γ within a certain range (γ_-, γ_+) , and give approximations for the values of γ_{\pm} .

Chapter 5

Hysteresis and resonance

5.1 Hysteresis

5.1.1 Fluid in tubes

[taryn's stuff]

5.1.2 Combustion

Lighting a match is an everyday experience, but an understanding of why it occurs is less obvious. As the match is lit, a reaction starts to occur, which is exothermic, i. e., it releases heat. The amount of heat released is proportional to the rate of reaction, and this itself increases with temperature (coal burns when hot, but not at room temperature). The heat released is given by the Arrhenius expression $A \exp(-E/RT)$, where E is the activation, R is the gas constant, T is the absolute temperature, and we take A as constant (it actually depends on reactant concentration). A simple model for the match temperature is then

$$c \frac{dT}{dt} = -k(T - T_0) + A \exp(-E/RT), \quad (5.1)$$

where ε is a suitable specific heat capacity, k is a cooling rate coefficient, and T_0 is ambient (e. g., room) temperature. The terms on the right represent the source term due to the reactive heat release, and a Newtonian cooling term (cooling rate proportional to temperature excess over the surroundings).

We can solve (5.1) as a quadrature, but it is much simpler to look at the problem graphically. Bearing in mind that T is absolute temperature, the source and sink terms typically have the form shown in figure 5.1, and we can see that there are three equilibria, and the lowest and highest ones are stable. Of course, one could have only the low equilibrium (for example, if k is large or T_0 is low) or the high equilibrium (if k is small or T_0 is high). The low equilibrium corresponds to the quiescent state — the match in the matchbox; the high one is the match alight. If we vary T_0 , then the equilibrium excess temperature Δ ($= T - T_0$) varies as shown in figure 5.2: the upper and lower branches are stable.

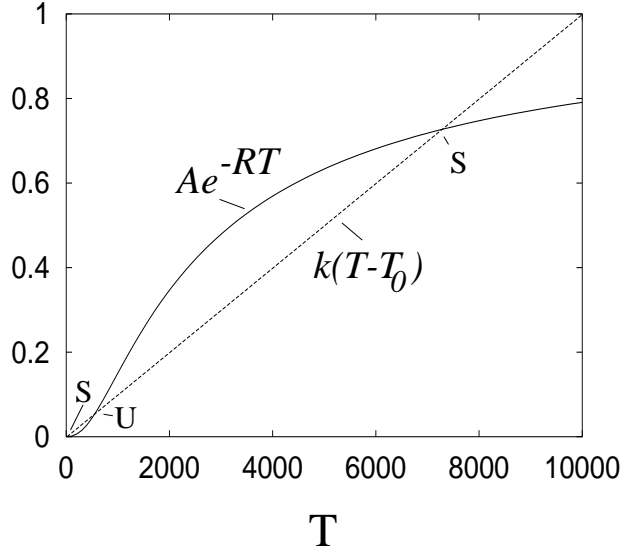


Figure 5.1: Plots of the functions $A \exp[-E/R(T + T_m)]$ and $k(T - T_0)$ using values $T_m = 273$ (so T is measured in centigrade), with values $A = 1$, $E = 20,000$, $R = 8.3$, $k = 10^{-4}$, $T_0 = 15^\circ \text{C}$.

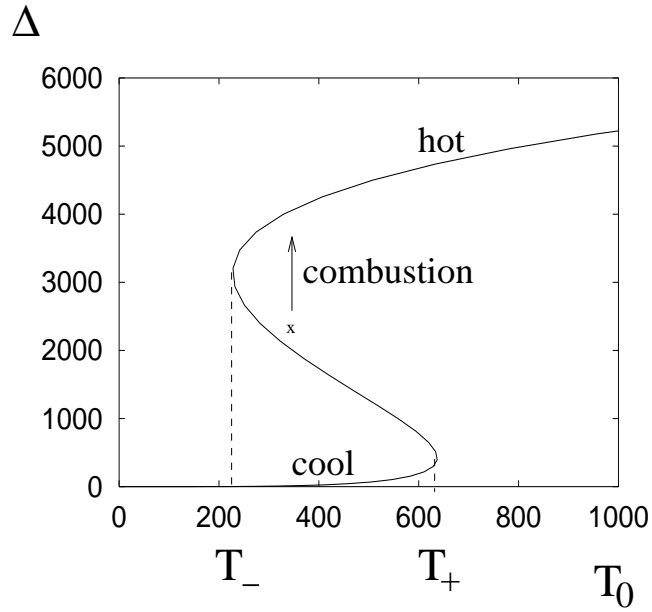


Figure 5.2: Equilibrium curve for Δ_0 as a function of T_0 , parameters as for figure 5.1, but $E = 35,000$. An initial condition above the unstable middle branch leads to combustion.

We can model lighting a match as a local perturbation to Δ ; the heat of friction in striking a match raises the temperature excess from near zero to a value above the unstable equilibrium on the middle branch, and Δ then migrates to the stable upper branch, where the reaction (like that of a coal fire) is self-perpetuating. Figure 5.2 also explains why it is difficult to light a wet match, but a match will spontaneously light if held at some distance above a lighted candle.

Figure 5.2 exhibits a form of hysteresis, meaning non-reversibility. Suppose we place a (very large, so it will not burn out) match in an oven, and we slowly raise the ambient temperature from a very low value to a very high value, and then lower it once again. Because the variation is slow, the excess temperature will follow the equilibrium curve in figure 5.2. At the value T_+ , Δ suddenly jumps (spontaneous combustion) to the hot branch, and remains on this if T_0 is increased further. Now if T_0 is decreased, Δ remains on the hot branch until $T_0 = T_-$, below which it suddenly drops to the cool branch again (extinction).¹ The path traced out in the $(T_0, \Delta T)$ plane is not reversible (it is not an arc but a closed curve).

The reason the multiple equilibria exist (at least for matches) is that for many reactions, E/R is very large and also A is very large. This just says that it is possible that $Ae^{-E/RT}$ is very small near T_0 but jumps rapidly at higher T to a large asymptote. To be more specific, we non-dimensionalise (5.1) by putting

$$T = T_0 + (\Delta T)\theta, \quad t = [t]t^*, \quad (5.2)$$

and in fact we choose the cooling time scale $[t] = c/k$. Then we have, dropping the asterisk, and after some simplification,

$$\dot{\theta} = -\theta + \frac{A}{k\Delta T} \exp\left(-\frac{E}{RT_0}\right) \exp\left[\frac{E\Delta T}{RT_0^2} \frac{\theta}{1 + \varepsilon\theta}\right], \quad (5.3)$$

where $\varepsilon = \Delta T/T_0$. The temperature rise scale ΔT has to be chosen, and there are two natural choices: to set the exponent coefficient $E\Delta T/RT_0^2$ to one, or the pre-multiplicative constant to one. In one way, the latter seems the better choice: it seems to balance the source with the sink. But because E/R is large, we might then find $E\Delta T/RT_0^2$ to be large, which would ruin the intention. So we choose (but it does not really matter)

$$\Delta T = \frac{RT_0^2}{E}, \quad (5.4)$$

so that

$$\dot{\theta} = -\theta + \lambda \exp\left[\frac{\theta}{1 + \varepsilon\theta}\right], \quad (5.5)$$

where

$$\lambda = \frac{EA}{kRT_0^2} \exp\left(-\frac{E}{RT_0}\right), \quad \varepsilon = \frac{RT_0}{E}. \quad (5.6)$$

¹We can understand why T follows the equilibrium curve as follows. We can write (5.1) in terms of suitable dimensionless variables as $\dot{\Delta} = T_0 - g(\Delta)$, where $g(\Delta)$ is a cubic-like curve similar to the function $T_0(\Delta)$ depicted in figure 5.2. if T_0 is slowly varying, then $T_0 = T_0(\varepsilon t)$ where $\varepsilon \ll 1$, and putting $\tau = \varepsilon t$, we have $\varepsilon d\Delta/d\tau = T_0(\tau) - g(\Delta)$; thus on the slow time scale τ , Δ will tend rapidly to a (quasi-equilibrium) zero of the right hand side.

If typical values are $T_0 = 300$ K, $E/R = 10,000$ K, we see that $\varepsilon \ll 1$, and also, since

$$\lambda = \frac{\lambda_0}{\varepsilon^2} \exp\left(-\frac{1}{\varepsilon}\right), \quad \lambda_0 = \frac{A}{kE}, \quad (5.7)$$

λ is extremely sensitive to ε and thus T_0 .

So long as $\theta = O(1)$, or at least $\theta \ll 1/\varepsilon$ (i.e. $T - T_0 \ll T_0$), we can neglect the $\varepsilon\theta$ term, so that

$$\dot{\theta} \approx -\theta + \lambda e^\theta. \quad (5.8)$$

This gives the lower part of the S -shaped curve in figure 5.2, and the equilibria are given by $\theta e^{-\theta} = \lambda$, and these coalesce and disappear if $\lambda > e^{-1}$. This corresponds to the value of $T_0 = T_+$ in figure 5.2, and implies

$$\frac{E}{RT_+} \approx 1 + \ln \lambda_0 + 2 \ln\left(\frac{E}{RT_+}\right). \quad (5.9)$$

There are two roots to this, but only one has $E/RT_+ \gg 1$. Further, since $x \gg 2 \ln x$ if $x \gg 1$, we have, approximately,

$$T_+ \approx \frac{E}{R[1 + \ln \lambda_0 + 2 \ln\{1 + \ln \lambda_0\}]}. \quad (5.10)$$

If $E/R \gg T_0$, then the fact that one can light matches at room temperature suggests that λ_0 is large, and specifically $\ln \lambda_0 \sim E/RT_0$. (Note that this does not imply $\lambda = O(1)$.)

Carrying on in this vein, let us suppose that we define a temperature T_q by

$$\lambda_0 = \exp\left[\frac{E}{RT_q}\right], \quad (5.11)$$

and we suppose $T_q \sim T_0$. It follows that $T_+ \approx T_q$, or more precisely,

$$T_+ \approx \frac{T_q}{1 + \varepsilon_q \{1 + 2 \ln(1 + \varepsilon_q^{-1})\}}, \quad (5.12)$$

where $\varepsilon_q = RT_q/E$. The stable cool branch and unstable middle branch are then the roots of

$$\theta e^{-\theta} \approx \lambda = \frac{1}{\varepsilon^2} \exp\left[-\frac{1}{\varepsilon} \left(1 - \frac{T_0}{T_q}\right)\right], \quad (5.13)$$

and in general $\lambda \ll 1$ (if $T_0 < T_q$), so that we find the stable cool branch (when $\theta \ll 1$)

$$\theta \approx \lambda \approx \left(\frac{E}{RT_0}\right)^2 \exp\left[\frac{E}{R} \left(\frac{1}{T_+} - \frac{1}{T_0}\right)\right], \quad (5.14)$$

and the unstable middle branch (where $\theta \gg 1$),

$$\theta \approx \frac{1}{\varepsilon} \left(1 - \frac{T_0}{T_q}\right) \approx \frac{E}{R} \left(\frac{1}{T_0} - \frac{1}{T_+}\right). \quad (5.15)$$

Evidently θ becomes $O(1/\varepsilon)$ on the middle branch, and to allow for this, we put

$$\theta = \Theta/\varepsilon, \quad (5.16)$$

and (5.5) becomes

$$\dot{\theta} = -\Theta + \frac{1}{\varepsilon} \exp \left[\frac{1}{\varepsilon} \left\{ \frac{\Theta}{1 + \Theta} - \left(1 - \frac{T_0}{T_q} \right) \right\} \right]. \quad (5.17)$$

Equating the right hand side to zero gives the approximate equilibria

$$\theta \approx \frac{T_+ - T_0 + \varepsilon T_+ \ln \left(\frac{T_+ - T_0}{T_0} \right)}{T_0 - \varepsilon T_+ \ln \left(\frac{T_+ - T_0}{T_0} \right)} \quad (5.18)$$

and Θ tends to infinity as $T_0 \rightarrow 0$. The hot branch is recovered for even higher values of Θ , so that $\Theta \gg 1$, in which case equilibria of (5.16) are given by

$$\Theta \approx \frac{1}{\varepsilon} \exp \left[\frac{T_0}{\varepsilon T_q} \right], \quad (5.19)$$

and increase again with T_0 .

The critical value of T is that on the unstable middle branch, as this gives the necessary temperature which must be generated in order for combustion to occur. From (5.17) (ignoring terms in ε), this can be written dimensionally in the simple approximate form

$$T \approx T_+, \quad (5.20)$$

where T_+ is the critical temperature at the nose of the curve in figure 5.2. The fact that T is approximately constant on the unstable branch is due to the steepness of the exponential curve in figure 5.1, which is in turn due to the large value of E/R . In terms of the parameters of the problem, the critical (ignition) temperature is

$$T_+ \approx \frac{E}{R \ln \left(\frac{A}{kE} \right)}. \quad (5.21)$$

Hysteresis and multiplicity of solutions is a theme which will recur again and again in this book.

5.2 Resonance

5.2.1 Forced pendulums

Swinging a pendulum is an everyday experience, and one which one learns about in a first year mechanics course. If one holds a pendulum, and waves one's hand backand forth, one has a forced pendulum, and an interesting phenomenon occurs. At low forcing frequencies, the pendulum oscillates in phase with the oscillating point of support. At high forcing frequencies, it oscillates out of phase with the support.

Moreover, this change in phase appears to occur abruptly, at a particular value of the forcing frequency. At the same time, there is also a sudden rise in amplitude of the motion, although it is less easy to see this in a casual experiment. These observations are associated with the phenomenon of resonance, jumping in a springboard, or in the surging of telegraph wires in the wind. One illustrates the phenomenon of resonance mathematically by solving the equation of a forced (linear) oscillator, and we can find the same phenomenon in the forced pendulum.

To be specific, we will take as a model equation

$$\ddot{u} + \beta\dot{u} + \Omega_0^2 \sin u = \varepsilon \sin \omega t. \quad (5.22)$$

This represents the motion of a damped, non-linear pendulum, with a forcing on the right hand side which mimics (it is not a precise model) the pendulum with an oscillating support. We suppose that the model is dimensionless, and that ε is small, so that the response amplitude of u will be also. We also suppose that the damping term β is small.

The simplest approximation of (5.22) neglects β altogether, and linearises $\sin u$, so that

$$\ddot{u} + \Omega_0^2 u \approx \varepsilon \sin \omega t, \quad (5.23)$$

to which the forced solution is

$$u = A \sin \omega t, \quad (5.24)$$

where the response amplitude A is given by

$$A = \frac{\varepsilon}{\Omega_0^2 - \omega^2}. \quad (5.25)$$

Plotting $|A|$ versus ω gives the familiar resonant response diagram of figure 5.3, in which the amplitude tends to infinity as $\omega \rightarrow \Omega_0$. (If one actually solves (5.23) at $\omega = \Omega_0$, one obtains a solution whose amplitude grows linearly in time.)

The two effects we have neglected, damping and non-linearity, have two separate effects on this diagram. If we include only damping, so that

$$\ddot{u} + \beta\dot{u} + \Omega_0^2 u = \varepsilon \operatorname{Im} e^{i\omega t}, \quad (5.26)$$

then the forced solution is again

$$u = \operatorname{Im} [A e^{i\omega t}], \quad (5.27)$$

where now

$$A = \frac{\varepsilon}{\Omega_0^2 + i\beta\omega - \omega^2}, \quad (5.28)$$

and the presence of the damping term causes a phase shift, and caps the response amplitude, as shown in figure 5.4, since

$$|A| = \frac{\varepsilon}{[(\Omega_0^2 - \omega^2)^2 + \beta^2\omega^2]^{1/2}}; \quad (5.29)$$

the peak amplitude at resonance is $|A| = \varepsilon/\beta\omega$.

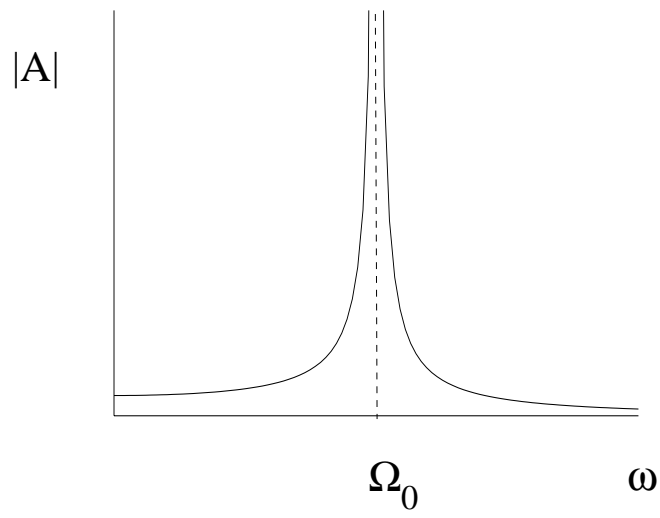


Figure 5.3: Resonant amplitude response.

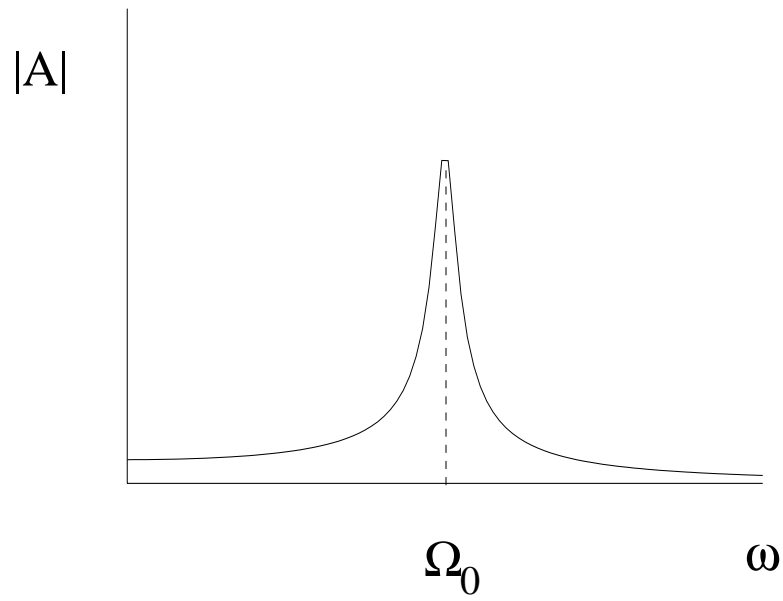


Figure 5.4: Resonant amplitude response with damping.

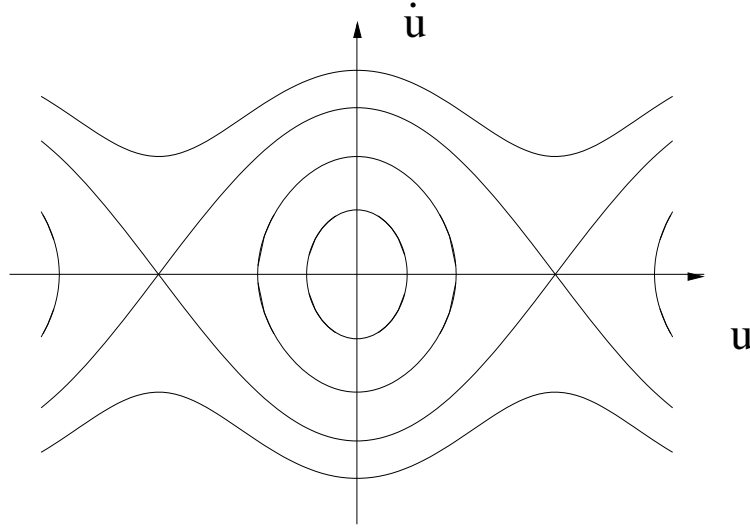


Figure 5.5: Phase plane for the simple pendulum.

The other effect is nonlinearity, which is less easy to deal with. In fact, one can use perturbation methods to assess its effect in a formal manner, but our present purpose is more rough and ready. Our idea is this: resonance occurs when the forcing frequency ω equals the frequency of the underlying oscillator. The difference with a nonlinear pendulum is that this frequency (call it Ω) now depends on the amplitude of the oscillation A , $\Omega = \Omega(A)$.

To be specific, we again put $\beta = 0$, and consider simply the unforced pendulum:

$$\ddot{u} + \Omega_0^2 \sin u = 0. \quad (5.30)$$

A first (energy) integral is

$$\frac{1}{2}\dot{u}^2 + \Omega_0^2(1 - \cos u) = E, \quad (5.31)$$

where E is constant (and depends on amplitude, with $E(A)$ increasing with A). The phase plane is shown in figure 5.5 and is symmetric about both u and \dot{u} axes. Thus a quadrature of (5.30) implies the period P is given by

$$P = \frac{2\sqrt{2}}{\Omega_0} \int_0^A \frac{du}{[\cos u - \cos A]^{1/2}}, \quad (5.32)$$

where we have used the fact that the amplitude A is given by

$$E = \Omega_0^2(1 - \cos A). \quad (5.33)$$

Substituting this in to (5.32), we find the frequency $\Omega = 2\pi/P$ in the form

$$\Omega(A) = \frac{\pi\Omega_0}{\sqrt{2} \int_0^A \frac{du}{[\cos u - \cos A]^{1/2}}}. \quad (5.34)$$

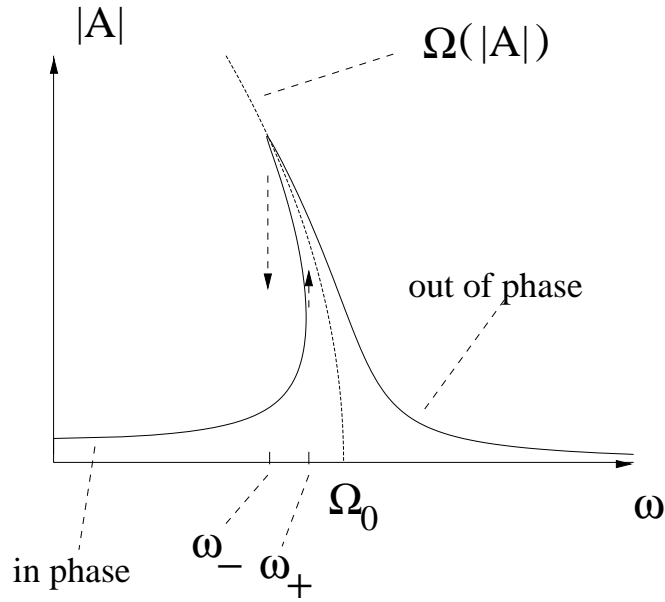


Figure 5.6: Nonlinearity bends the resonant response curve, producing hysteresis.

Ω is a monotonically decreasing function of A in $(0, \pi)$, with $\Omega(0) = \Omega_0$ and $\Omega(\pi) = 0$, and this is represented as the dotted curve in figure 5.6.

Without actually now solving the forced damped, nonlinear equation, we can guess intelligently what happens. For small amplitude oscillations, $|A|$ starts to increase as ω approaches Ω_0 ; but as $|A|$ increases, the natural frequency Ω decreases, and as it is the approach of ω to the natural frequency which is the instrument of resonance, so the amplitude response curve bends round, as shown in figure 5.6, to try and approach the dotted $\Omega(A)$ curve. Finally, the effect of damping can be expected to be as in the linear case, to put a cap on the two asymptotes to $\Omega(A)$. Thus, we infer the response diagram shown in figure 5.6, and this is in fact correct. Moreover, (5.25) suggests $A \lesseqgtr 0$ for $\omega \lesseqgtr \Omega_0$, i.e., the solution is in phase with the forcing for $\omega > \Omega_0$, and out of phase for $\omega < \Omega_0$. Extending this to the nonlinear case, we infer that at low frequencies, the response is in phase, but that it is out of phase at high frequencies.

The response also involves hysteresis (if damping is small enough). If ω is increased gradually, then at a value $\omega_+ < \Omega_0$, there is a sudden jump to an out of phase oscillation with higher amplitude. Equivalently as ω is reduced for this high frequency response, there is a sudden jump down in amplitude to an in phase oscillation at a value $\omega_- < \omega_+$. This response diagram explains what one sees in the simple experiment and illustrates the important effects of nonlinearity.

Exercises

- 5.1 Find a scaling of the combustion equation (5.1) so that it can be written in the form

$$\dot{\theta} = \theta_0 - g(\theta),$$

where $\theta_0 = RT_0/E$ and $g = \theta - \alpha e^{-1/\theta}$. Give the definition of α . Hence show that the steady state θ is a multiple-valued function of θ_0 if $\alpha > \frac{1}{4}e^2$.

- 5.2 Find approximations to the smaller and larger positive roots of $x^2 e^{-x} = \varepsilon$, where ε is small and positive.

Hence find the approximate range (θ_-, θ_+) of θ_0 in question 5.2.1 for which there are three steady solutions.

- 5.3 Suppose that θ satisfies $\dot{\theta} = \theta_0 - g(\theta)$, where $g(\theta)$ is as in question 5.2.1 and $\alpha > \frac{1}{4}e^2$, and θ_0 varies slowly according to

$$\dot{\theta}_0 = \varepsilon(\theta^* - \theta),$$

where $\varepsilon \ll 1$. Show that there are three possible outcomes, depending on the value of θ^* , and describe them.

- 5.4 A forced pendulum is modelled by the (dimensional) equation

$$l\ddot{\theta} + k\dot{\theta} + g \sin \theta = \alpha \sin \lambda t.$$

By non-dimensionalising the equation, show how to obtain (5.22), and identify the parameters $\varepsilon, \beta, \Omega_0$ and ω .

- 5.5 It is asserted after (5.34) that $\Omega(A)$ is a decreasing function of A for $0 < A < \pi$, or equivalently, that the function

$$p(A) = \frac{1}{\sqrt{2}} \int_0^A \frac{du}{[\cos u - \cos A]^{1/2}}$$

is increasing. Show that this is true by writing p in the form

$$p = \int_0^1 \left(\frac{\theta}{\sin \theta} \right)^{1/2} \left(\frac{\phi}{\sin \phi} \right)^{1/2} \frac{dw}{(1-w^2)^{1/2}}$$

for some functions $\theta(w, A)$ and $\phi(w, A)$, and using the fact that $\theta/\sin \theta$ is an increasing function of θ in $(0, \pi)$.

[Hint: $\cos u - \cos A = 2 \sin \left(\frac{A-u}{2} \right) \sin \left(\frac{A+u}{2} \right)$.]

Chapter 6

Waves and shocks

Any introductory course on partial differential equations will provide the classification of second order partial differential equations into the three categories: elliptic, parabolic, hyperbolic; and one also finds the three simple representatives of these: Laplace's equation $\nabla^2 u = 0$, governing steady state temperature distribution (for example); the heat equation $u_t = \nabla^2 u$, which describes diffusion of heat (or solute); and the wave equation $u_{tt} = \nabla^2 u$, which describes the oscillations of a string or of a drum. These equations are of fundamental importance, as they describe diffusion or wave propagation in many other physical processes, but they are also linear equations; however the way in which they behave carries across to nonlinear equations, but of course nonlinear equations have other behaviours as well.

In the linear wave equation (in one dimension, describing waves on strings) $u_{tt} = c^2 u_{xx}$, the general solution is $u = f(x+ct) + g(x-ct)$, and represents the superposition of two travelling waves of speed c . In more than one space dimension, the equivalent model is $u_{tt} = c^2 \nabla^2 u$, and the solutions are functions of $(\mathbf{k} \cdot \mathbf{x} \pm \omega t)$, where ω is frequency and \mathbf{k} is wave vector; the wave speed is then $c = \omega/|\mathbf{k}|$.

Even simpler to discuss is the first order wave equation

$$u_t + cu_x = 0, \quad (6.1)$$

which is trivially solved by characteristics to give

$$u = f(x - ct), \quad (6.2)$$

representing a wave of speed c . The idea of finding characteristics generalises to systems of the form

$$A\mathbf{u}_t + B\mathbf{u}_x = \mathbf{0}, \quad (6.3)$$

where $\mathbf{u} \in \mathbf{R}^n$ and A and B are constant $n \times n$ matrices. We can solve this system as follows. The eigenvalue problem

$$\lambda A\mathbf{w} = B\mathbf{w} \quad (6.4)$$

will in general have n solution pairs (\mathbf{w}, λ) , where each value of λ is one of the roots of the n -th order polynomial

$$\det(\lambda A - B) = 0. \quad (6.5)$$

Suppose the n values of λ , λ_i , are distinct (which is the general case); then the corresponding \mathbf{w}_i are independent, and the matrix P formed by the eigenvectors as columns (i.e., $P = (\mathbf{w}_1, \dots, \mathbf{w}_n)$) satisfies $BP = APD$, where D is the diagonal matrix $\text{diag}(\lambda_1, \dots, \lambda_n)$. P is invertible, and if we write $\mathbf{v} = P^{-1}\mathbf{u}$, then $AP\mathbf{v}_t + BP\mathbf{v}_x = 0$, whence $\mathbf{v}_t + D\mathbf{v}_x = 0$, and the general solution is

$$\mathbf{u} = P \left[\sum_i f_i(x - \lambda_i t) \right], \quad (6.6)$$

representing the superposition of n travelling waves with speeds λ_i . This procedure works providing A is invertible, and also if all the λ_i are real, in which case we say the system is hyperbolic.

More precisely, we can use the above prescription to solve the nonlinear equation

$$A\mathbf{u}_t + B\mathbf{u}_x = c(x, t, \mathbf{u}), \quad (6.7)$$

where we allow A and B to depend on x and t also. The diagonalisation procedure works exactly as before, leading to

$$A \frac{\partial}{\partial t}(P\mathbf{v}) + B \frac{\partial}{\partial x}(P\mathbf{v}) = c[x, t, P\mathbf{v}]; \quad (6.8)$$

now, however, λ , \mathbf{w} and therefore also P will depend on x and t . Thus we find

$$\mathbf{v}_t + D\mathbf{v}_x = P^{-1}A^{-1}\mathbf{c} - [P^{-1}P_t + DP^{-1}P_x]\mathbf{v}, \quad (6.9)$$

and the components of \mathbf{v} can be solved as a set of coupled ordinary differential equations along the characteristics $dx/dt = \lambda_i$.

If A and B depend also on \mathbf{u} , the procedure is less clear for systems. However, the method of characteristics always works in one dimension, so we now return our attention to this case. Consider as an example the nonlinear evolution equation

$$u_t + uu_x = 0, \quad (6.10)$$

to be solved on the whole real axis. The method of characteristics leads to the implicitly defined general solution

$$u = f(x - ut), \quad (6.11)$$

which is analogous to (6.2), and represents a wave whose *speed depends on its amplitude*. Thus higher orders of u propagate more rapidly, and this leads to the wave steepening depicted in figure 6.1.

In fact, it can be seen that eventually u becomes multi-valued, and this signifies a break down of the solution. The usual way in which this multi-valuedness is avoided is to allow the formation of a *shock*, which is a point of discontinuity of u . the characteristic solution applies in front of and behind the shock, and the characteristics intersect at the shock, whose propagation forwards is described by an appropriate *jump condition*: see figure 6.2.

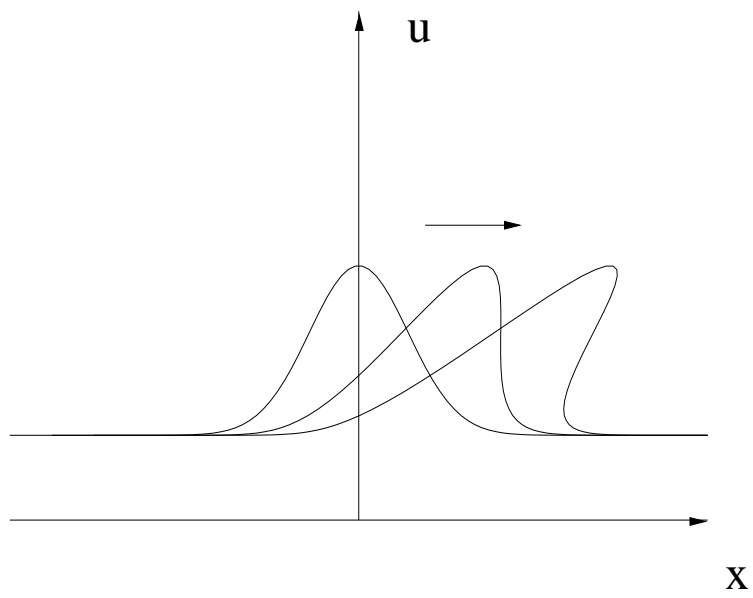


Figure 6.1: Nonlinearity causes wave steepening.

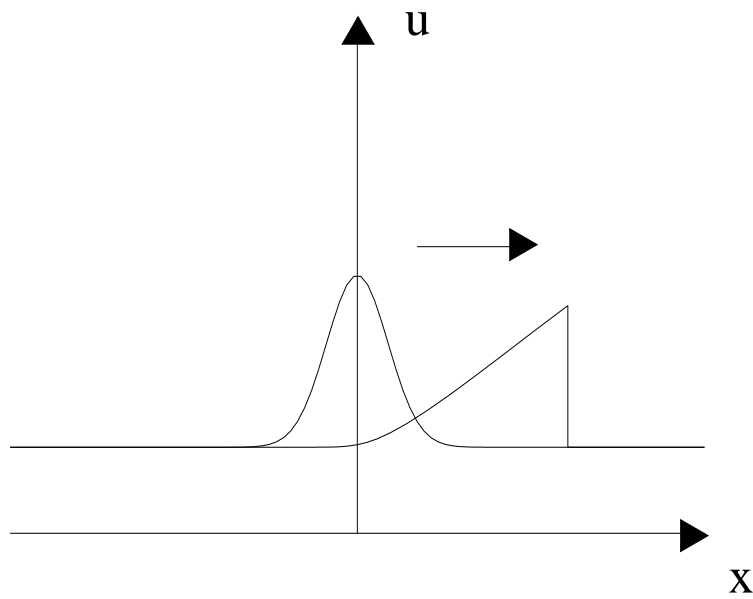


Figure 6.2: Intersection of characteristics leads to shock formation.

This seemingly arbitrary escape route is motivated by the fact that evolution equations such as (6.10) are generally derived from a conservation law, here of the form

$$\frac{\partial}{\partial t} \int_A^B u \, dx = -[\tfrac{1}{2}u^2]_A^B, \quad (6.12)$$

where the square-bracketed term represents the jump in $\tfrac{1}{2}u^2$ between A and B . The deduction of the point form (6.10) from (6.12) required the additional assumption that u was continuously differentiable; however, it is possible to satisfy (6.12) at a point of discontinuity of u . Suppose u is discontinuous at $x = x_S(t)$, and denote the jump in a quantity q across the shock is $[q]_{-}^{+} = q(x_{S+}, t) - q(x_{S-}, t)$. Then by letting $B \rightarrow x_{S+}$, $A \rightarrow x_{S-}$, we find that (6.12) implies the jump condition

$$\dot{x}_S = \frac{[\tfrac{1}{2}u^2]_{-}^{+}}{[u]_{-}^{+}} = \tfrac{1}{2}(u_{+} + u_{-}). \quad (6.13)$$

An example

We illustrate how to solve a problem of this type by considering the initial value

$$u = u_0(x) = \frac{1}{1+x^2} \quad \text{at } t = 0. \quad (6.14)$$

The implicitly defined solution is then

$$u = \frac{1}{1+(x-ut)^2}, \quad (6.15)$$

or, in characteristic form,

$$u = u_0(\xi) = \frac{1}{1+\xi^2}, \quad x = \xi + ut. \quad (6.16)$$

This defines a single-valued function so long as u_x is finite. Differentiating (6.16) leads to

$$u_x = \frac{u'_0(\xi)}{1+tu'_0(\xi)}, \quad (6.17)$$

and this shows that $u_x \rightarrow -\infty$ as $t \rightarrow t_c = \min_{\xi: u'_0 < 0} [-\frac{1}{u'_0(\xi)}]$. Since $-u'_0 = 2\xi/(1+\xi^2)^2$, we find the relevant value of ξ is $1/\sqrt{3}$, and thus $t_c = 8/3\sqrt{3}$ and the corresponding value of x is $x_c = \sqrt{3}$. Thus (6.15) applies while $t < t_c = 8/3\sqrt{3}$, and thereafter the solution also applies in $x < x_S(t)$ and $x > x_S(t)$, where

$$\dot{x}_S = \tfrac{1}{2}[u(x_{S+}) + u(x_{S-})], \quad (6.18)$$

with

$$x_S = \sqrt{3} \quad \text{at } t = \frac{8}{3\sqrt{3}}. \quad (6.19)$$

As indicated in figure 6.3, the characteristics intersect at the shock, and it is geometrically clear from figure 6.1, for example, that u_{+} and u_{-} are the largest and smallest

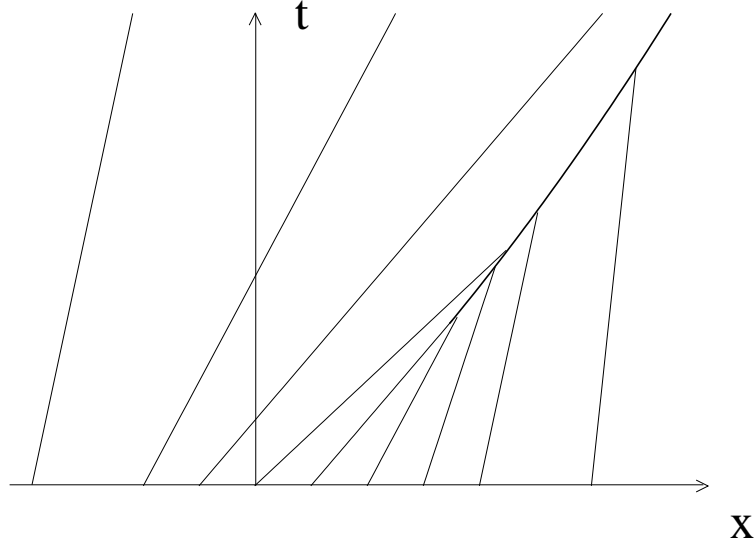


Figure 6.3: Characteristic diagram indicating shock formation.

roots of the cubic (6.15). An explicit solution for x_s is not readily available, but it is of interest to establish the long term behaviour, and for this we need approximations to the roots of (6.14) when $t \gg 1$.

We write the cubic in the form

$$u = \frac{x}{t} \pm \frac{1}{t} \left(\frac{1-u}{u} \right)^{1/2}. \quad (6.20)$$

We know that $u \leq 1$, and we expect the largest root, at least, to tend to infinity as $t \rightarrow \infty$. In that case $u \approx x/t$ if $u = O(1)$, and the next corrective term gives

$$u \approx \frac{x}{t} \pm \frac{1}{t} \left(\frac{t-x}{x} \right)^{1/2}. \quad (6.21)$$

This evidently gives the upper two roots for $x < t$ (since they coalesce at $u = 1$ when $x = t$). For large x , the other root must have $u \ll 1$, and in fact

$$u \approx \frac{1}{x^2}, \quad (6.22)$$

in order that (6.20) not imply (6.21). Alternatively, (6.22) follows from consideration of (6.15) in the form

$$t^2 u^3 - 2xtu^2 + (x^2 + 1)u - 1 = 0, \quad (6.23)$$

providing $x \gg t^{1/3}$.

(6.22) gives the right hand nose of the (rightmost) curve in figure 6.1. The left nose can be determined from the observation that the approximation that $u \approx x/t$

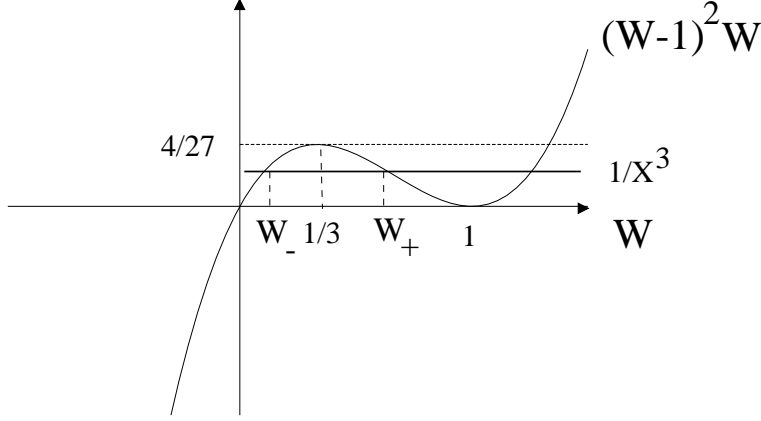


Figure 6.4: Determination of $W(X)$.

breaks down (from (6.21)) when $x \sim t^{1/3}$, which is also where (6.22) becomes invalid. This suggests writing

$$u = \frac{x}{t} W(X), \quad X = \frac{x}{t^{1/3}}, \quad (6.24)$$

and then $W(X)$ is given approximately, for large t , by

$$W(W-1)^2 = \frac{1}{X^3}, \quad (6.25)$$

and for $X = O(1)$ there are three roots providing $X > 3/2^{2/3}$; at $X = 3/2^{2/3}$, the two lower roots coalesce at $W = \frac{1}{3}$: this is the left nose of the curve.

As X becomes large, the upper two roots approach $W = 1$, i.e. $u \approx x/t$, while the lower approaches zero, specifically $W \approx 1/X^3$, i.e. $u \approx 1/x^2$: see figure 6.4. Thus these roots match to the approximations when $x \sim t$. As X becomes small, the remaining root is given by $W \approx 1/X$, i.e. $u \approx 1/t^{2/3}$, and (6.23) shows that this is the correct approximation as long as $|x| \ll t^{1/3}$. The situation is shown in figure 6.5).

In order to determine the shock location x_S , we make the ansatz that $t^{1/3} \ll x_S \ll t$, i.e., that the shock is far from both noses. In that case

$$u_+ \approx \frac{1}{x_S^2}, \quad u_- \approx \frac{x_S}{t}, \quad (6.26)$$

and at leading order we have

$$\dot{x}_S \approx \frac{x_S}{2t}, \quad (6.27)$$

whence

$$x_S \approx at^{1/2}, \quad (6.28)$$

confirming our assumption that $t^{1/3} \ll x_S \ll t$.

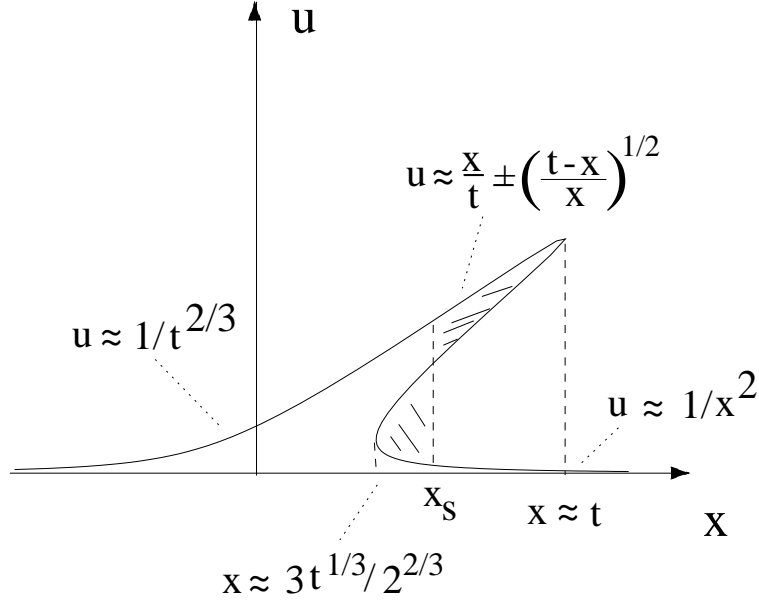


Figure 6.5: Large time solution of the characteristic solution.

To determine the coefficient a , we may use the equal area rule, which follows from conservation of mass, and implies that the two shaded areas in figure 6.5 are equal. We use (6.24) for the left hand area, and (6.21) for the right hand area. then

$$\int_{3t^{1/3}/2^{2/3}}^{at^{1/2}} \frac{x}{t} [w_+(X) - w_-(X)] dx \approx \int_{at^{1/2}}^t \frac{2}{t} \left(\frac{t-x}{x} \right)^{1/2} dx, \quad (6.29)$$

where W_+ and W_- are the middle and lowest roots of (6.25), as shown in figure 6.4. We write $x = t^{1/2}\xi$ in the left integral and $x = t\eta$ in the right, and hence we deduce that

$$a \approx \int_0^1 2 \left(\frac{1-\eta}{\eta} \right)^{1/2} d\eta = \pi. \quad (6.30)$$

6.1 Burgers' equation

Although the presence of a shock for (6.10) is entirely consistent with the derivation of the equation from an integral conservation law, nature appears generally to avoid discontinuities and singularities, and it is usually the case that in writing (6.10), we have neglected some term which acts to smooth the shock, so that the change of u is rapid but not abrupt.

A simple example of this arises in the theory of traffic flow on a road. On a one-lane carriageway, the density of cars is $\rho(x, t)$ (number per unit length, idealised as a continuum, which should be a reasonable assumption for road lengths of many

cars); x is distance along the carriageway, and t is time. If $v(x, t)$ is the local traffic vehicular speed, then a conservation law for cars is

$$\frac{\partial \rho}{\partial t} + \frac{\partial}{\partial x}(\rho v) = 0, \quad (6.31)$$

assuming no cars leave or join the carriageway. The car speed must be prescribed, and a simple and sensible prescription is to take $v = v(\rho)$: a driver drives at a speed which depends on density. More specifically, we might suppose that there is a maximum speed of v_0 when there is no traffic ($\rho = 0$), but the speed decreases as ρ increases, reaching zero when the distance between cars is zero, corresponding to a maximum density ρ_m say. A simple recipe which satisfies these constraints is

$$v = v_0 \left(\frac{\rho}{\rho_m} \right). \quad (6.32)$$

By scaling the variables suitably, we may take $v_0 = 1$, $\rho_m = 1$, and then we have

$$\rho_t + c(\rho)\rho_x = 0, \quad (6.33)$$

where

$$c(\rho) = 1 - 2\rho. \quad (6.34)$$

This is equivalent to (6.10), with $u = 1 - 2\rho$, and therefore we can in general expect shocks to form. Since $0 < \rho < 1$, a difference here is that we can have $c < 0$ for $\rho > \frac{1}{2}$.

Suppose first that $\rho < \frac{1}{2}$. A local reduction in ρ is like a bump for $u = 1 - 2\rho$, and will form a forward propagating shock where $\rho_+ > \rho_-$; cars driving through the low density precursor will suddenly hit a traffic jam at high density. Equivalently, a local rise in density leads to a forward-propagating shock with $\rho_+ > \rho_-$.

On the other hand, suppose that $\rho > \frac{1}{2}$. With $w = 2\rho - 1$, then $w_t - ww_x = 0$, and a similar discussion arises, with the direction of x reversed. Thus a local rise in ρ causes a shock to form in which, again, $\rho_+ > \rho_-$, and the shock now propagates backwards. In all cases, the individual driver experiences the shock as a sudden reduction of speed (the car speed is $1 - \rho$ and is larger than the wave speed $1 - 2\rho$: thus cars approach and travel through the shock).

The occurrence of shocks is a common experience to anyone who has driven on a motorway, and can be caused by lane closures, motorway junctions, or speed restrictions. In general, collisions do not occur, and one may ascribe this to a smoothing mechanism; the question arises, what could this be?

Drivers arguably adjust their speed not only according to the inter-car distance (the direct density effect), but also depending on how much traffic they see ahead. A common exhibition of this is the tailgater. Driving at the speed limit on a motorway in the outside lane will attract tailgaters if there is little traffic ahead, but not if the road is full. That is, at a constant v , ρ may increase above its ideal value if ρ in front is less, i.e. if $\partial\rho/\partial x < 0$. A simple modification for v which describes this is (in scaled units)

$$v = 1 - \rho - \kappa\rho_x, \quad (6.35)$$

where κ is constant. From this we can deduce the advection-diffusion equation

$$\frac{\partial \rho}{\partial t} + (1 - 2\rho) \frac{\partial \rho}{\partial x} = \kappa \frac{\partial}{\partial x} \left(\rho \frac{\partial \rho}{\partial x} \right), \quad (6.36)$$

and the non-local dependence of v on ρ_x is represented as a (nonlinear) diffusion term.

What is the effect of this on the structure of the solutions? If κ is small, we should suppose that it is not much, so that shocks would start to form. However, the neglect of the diffusion term becomes invalid when the derivatives of ρ become large. In fact, the diffusion term is trying to do the opposite of the advective term. The latter is trying to fold the initial profile together like an accordion, while the former is trying to spread everything apart. We might guess that a balanced position is possible, in which the nonlinear advective term keeps the profile steep, but the diffusion prevents it actually folding over (and hence causing a discontinuity), and this will turn out to be the case.

If we suppose instead of (6.35) that

$$v = 1 - \rho - \frac{\kappa}{\rho} \rho_x, \quad (6.37)$$

which might represent the fact that the strength of tailgating becomes more severe, the emptier the road ahead, then the diffusion term becomes linear, and we have Burgers' equation for $u = 1 - 2\rho$:

$$u_t + uu_x = \kappa u_{xx}. \quad (6.38)$$

Shock structure

We suppose $\kappa \ll 1$, and that $u_t + uu_x \approx 0$, and a shock forms at $x = x_S(t)$. Our aim is to show that (6.38) supports a *shock structure*, i.e. a region of rapid change near x_S for u_- to u_+ .

To focus on the shock, we need to rescale x near x_S , and we do this by writing

$$x = x_S(t) + \kappa X. \quad (6.39)$$

Burgers' equation becomes

$$\kappa u_t - \dot{x}_S u_X + uu_X = u_{XX}. \quad (6.40)$$

We expect the characteristic solution (with $\kappa = 0$) to be approximately valid far from x_s , and so appropriate conditions (technically, these are *matching conditions*) are

$$u \rightarrow u_{\pm} \text{ as } X \rightarrow \pm\infty, \quad (6.41)$$

and we take these values as prescribed from the *outer* solution (i.e., the solution of $u_t + uu_x = 0$).

Since $\kappa \ll 1$, (6.40) suggests that u relaxes rapidly (on a time scale $t \sim \kappa \ll 1$) to a quasi-steady state (quasi-steady, because u_+ and u_- will vary with t) in which

$$-\dot{x}_S u_X + uu_X \approx u_{XX}, \quad (6.42)$$

whence

$$K - \dot{x}_s u + \frac{1}{2} u^2 \approx u_X, \quad (6.43)$$

and prescription of the boundary conditions implies

$$K = \dot{x}_s u_+ - \frac{1}{2} u_+^2 = \dot{x}_s u_- - \frac{1}{2} u_-^2, \quad (6.44)$$

whence

$$\dot{x}_s = \frac{[\frac{1}{2} u^2]_-^+}{[u]_-^+}, \quad (6.45)$$

which is precisely the jump condition we obtained in (6.13). The solution for u is then

$$u = c - (u_- - c) \tanh \left[\frac{1}{2} (u_- - c) X \right], \quad (6.46)$$

where $c = \dot{x}_S$.

6.2 The Fisher equation

In Burgers' equation, a wave arises as a balance between nonlinear advection and diffusion. In Fisher's equation,

$$u_t = u(1 - u) + u_{xx}, \quad (6.47)$$

a wave arises as a mechanism of transferring a variable from an unstable steady state ($u = 0$) to a stable one ($u = 1$). Whereas Burgers' equation balances two transport terms, Fisher's equation balances diffusive transport with an algebraic source term. It originally arose as a model for the dispersal of an advantageous gene within a population, and has taken a plenary rôle as a pedagogical example in mathematical biology of how reaction (source terms) and diffusion can combine to produce travelling waves.

We pose (6.47) with boundary conditions

$$\begin{aligned} u &\rightarrow 1, \quad x \rightarrow -\infty, \\ u &\rightarrow 0, \quad x \rightarrow +\infty. \end{aligned} \quad (6.48)$$

It is found (and can be proved) that any initial condition leads to a solution which evolves into a travelling wave of the form

$$u = f(\xi), \quad \xi = x - ct, \quad (6.49)$$

where

$$f'' + cf' + f(1 - f) = 0, \quad (6.50)$$

and

$$f(\infty) = 0, \quad f(-\infty) = 1. \quad (6.51)$$

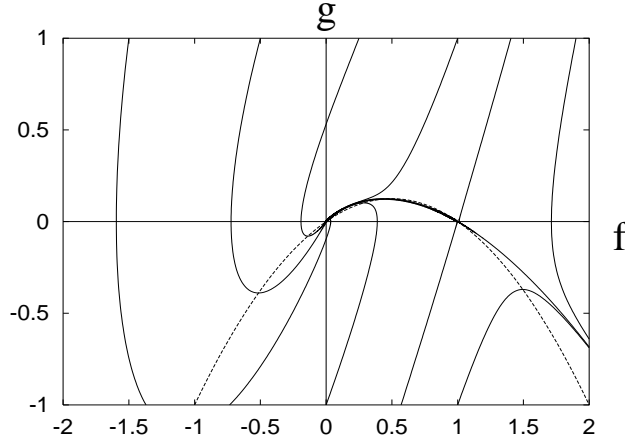


Figure 6.6: Phase portrait of Fisher equation, (6.52), for $c = 2$. Note how close the connecting trajectory (thick line) is to the g nullcline. This is why the large c approximation is accurate *for this trajectory*.

In the (f, g) phase plane, where $g = -f'$, we have

$$\begin{aligned} f' &= -g, \\ g' &= f(1-f) - cg, \end{aligned} \quad (6.52)$$

and a travelling wave corresponds to a trajectory which moves from $(1,0)$ to $(0,0)$.

Linearisation of (6.52) near the fixed point $(f^*, 0)$ via $f = f^* + F$ leads to

$$\begin{pmatrix} F \\ g \end{pmatrix}' = \begin{pmatrix} 0 & -1 \\ 1 - 2f^* & -c \end{pmatrix} \begin{pmatrix} F \\ g \end{pmatrix}, \quad (6.53)$$

with solutions $e^{\lambda\xi}$, where $\lambda^2 + c\lambda + (1 - 2f^*) = 0$. We anticipate $c > 0$; then $(1,0)$ is a saddle point, while $(0,0)$ is a stable node if $c \geq 2$ (and a spiral if $c < 2$). For $c \geq 2$, a connecting trajectory exists as shown in figure 6.6: in practice the minimum wave speed $c = 2$ is selected. (Connecting trajectories also exist if $c < 2$, but because $(0,0)$ is a spiral, these have oscillating tails as $u \rightarrow 0$, which are unstable and also (for example, if u is a population) unphysical.)

Explicit solutions for (6.50) are not available, but an excellent approximation is easily available. We put

$$\xi = c\Xi, \quad (6.54)$$

so

$$\nu f'' + f' + f(1-f) = 0, \quad (6.55)$$

with $\nu = 1/c^2 = 1/4$ for $c = 2$. Taking $\nu \ll 1$ and writing $f = f_0 + \nu f_1 + \dots$, we have

$$\begin{aligned} f_0' + f_0(1-f_0) &= 0, \\ f_1' + (1-2f_0)f_1 &= -f_0'', \end{aligned} \quad (6.56)$$

and thus

$$f_0 = \frac{e^{-\Xi}}{1 + e^{-\Xi}}. \quad (6.57)$$

Also, noting that $1 - 2f_0 = -f_0''/f_0'$ (differentiate (6.56)₁),

$$f_1 = f_0(1 - f_0) \ln[f_0(1 - f_0)], \quad (6.58)$$

and so on. Even the first term gives a good approximation, and even for $c = 2$.

6.3 Solitons

The Fisher wave is an example of a solitary travelling wave. Another type of solitary wave is the soliton, as exemplified by solutions of the Korteweg-de Vries equation

$$u_t + uu_x + u_{xxx} = 0. \quad (6.59)$$

This has travelling wave solutions $u = f(\xi)$, $\xi = x - ct$, where

$$f''' + ff' - cf' = 0, \quad (6.60)$$

and solitary waves with $f \rightarrow 0$ at $\pm\infty$ satisfy the first integral

$$f'' + \frac{1}{2}f^2 - cf = 0, \quad (6.61)$$

and thus

$$\frac{1}{2}f'^2 + \frac{1}{6}f^3 - \frac{1}{2}cf^2 = 0, \quad (6.62)$$

with solution

$$f = \frac{3}{2}c \operatorname{sech}^2 \frac{\sqrt{c}}{2}\xi. \quad (6.63)$$

Thus there is a one parameter family of these solitary waves, and they are called solitons, because they have the remarkable particle-like ability to ‘pass through’ each other without damage, except for a change of relative phase. Despite the nonlinearity, they obey a kind of superposition principle. Soliton equations (of which there are many) have many other remarkable properties, beyond the scope of the present discussion.

Some understanding of the solitary wave arises through an understanding of the balance between nonlinearity (uu_x) and dispersion (u_{xxx}). The dispersive part of the equation, $u_t + u_{xxx} = 0$, is so called because waves $\exp[ik(x - ct)]$ have wave speed $c = -k^2$ which depends on wavenumber k ; waves of different wavelengths ($2\pi/k$) move at different speeds and thus disperse. On the other hand, the nonlinear advection equation $u_t + uu_x$ has a focussing effect, which (from a spectral point of view) concentrates high wave numbers near shocks (rapid change means large derivatives means high wavenumber). So the nonlinearity tries to move high wavenumber modes in from the left, while the dispersion tries to move them to the left: again a balance is struck, and a travelling wave is the result.

6.4 Snow melting

An example of some of the ideas presented so far occurs in the study of melting snow. In particular, it is found that pollutants which may be uniformly distributed in snow (e.g. SO_2 from sulphur emissions via acid rain) can be concentrated in melt water run-off, with a consequent enhanced detrimental effect on stream pollution. The question then arises, why this should be so.

The model we use is based on precepts of groundwater flow, and will be more fully explained in Chapter 7. Suppose we have a snow pack of depth h in $0 < z < h$, where z is a coordinate pointing downwards from the snow surface. Snow is a porous aggregate of ice crystals, and meltwater formed at the surface can percolate through the snow pack to the base, where run-off occurs. (We ignore effects of re-freezing of meltwater). The flux of water u downwards is given by Darcy's law

$$u = \frac{k}{\mu} \left[-\frac{\partial p}{\partial z} + \rho g \right], \quad (6.64)$$

where u is measured as a velocity, and represents volume per unit area per unit time; p is the (pore) water pressure, ρ is density, g is gravity, μ is viscosity, k is permeability. The permeability k is related to the saturation S , and we will assume

$$k = k_0 S^3, \quad (6.65)$$

where the saturation S is the volume fraction of the pore space which is occupied by water. For $S = 1$, the snow is fully saturated (no air), for $S = 0$ it is fully dry (no water).

Conservation of the liquid water implies

$$\phi \frac{\partial S}{\partial t} + \frac{\partial u}{\partial z} = 0, \quad (6.66)$$

where ϕ is the porosity (volume of pore space per unit volume of snow). Finally, the water pressure is related to the air pressure (p_a , taken as constant) by the capillary pressure

$$p_c = p_a - p, \quad (6.67)$$

and this is a function of S : we take

$$p_c(S) = p_0 \left(\frac{1}{S} - S \right), \quad (6.68)$$

based on typical experimental results.

Suitable boundary conditions in a melting event might be to prescribe the melt flux at the surface:

$$u = u_0 \quad \text{at} \quad z = 0. \quad (6.69)$$

If the base is impermeable, then

$$u = 0 \quad \text{at} \quad z = h. \quad (6.70)$$

This is certainly not realistic if S reaches 1 at the base, since then ponding must occur and presumably melt drainage via a channelised flow, but we examine the initial stages of the flow using (6.70). Finally, we suppose $S = 0$ at $t = 0$. Again, this is not realistic in the model (it implies $p_c = \infty$) but it is a feasible approximation to make.

Simplification of this model now leads to the Darcy-Richards equation in the form

$$\phi \frac{\partial S}{\partial t} + \frac{3k_0 \rho g}{\mu} S^2 \frac{\partial S}{\partial z} = \frac{k_0 p_0}{\mu} \frac{\partial}{\partial z} \left[S(1 + S^2) \frac{\partial S}{\partial z} \right], \quad (6.71)$$

which, as we see, is a convective-diffusion equation of Burgers type. The quantity $K = k_0 \rho g / \mu$ is known as the saturated hydraulic conductivity; it is a velocity, and represents the highest rate at which water can flow through the snow steadily under gravity.

To scale the equation, we note that S is dimensionless and of $O(1)$ by definition. We choose scales for z and t :

$$z \sim h, \quad t \sim \frac{\phi h}{K}; \quad (6.72)$$

the model then becomes

$$\frac{\partial S}{\partial t} + 3S^2 \frac{\partial S}{\partial z} = \kappa \frac{\partial}{\partial z} \left[S(1 + S^2) \frac{\partial S}{\partial z} \right], \quad (6.73)$$

where

$$\kappa = \frac{p_0}{\rho g h}. \quad (6.74)$$

if we choose $p_0 = 1 \text{ kPa}$, $\rho = 10^3 \text{ kg m}^{-3}$, $g = 10 \text{ m s}^{-2}$, $h = 1 \text{ m}$, then $\kappa = 0.1$. it follows that (6.73) has a propensity to form shocks, these being diffused by the term in κ over a distance $O(\kappa)$ (by analogy with the shock structure for the Burgers equation).

We want to solve (6.73) with the initial condition

$$S = 0 \quad \text{at} \quad t = 0, \quad (6.75)$$

and the boundary conditions

$$S^3 - \kappa S(1 + S^2) \frac{\partial S}{\partial z} = \frac{u_0}{K} \quad \text{on} \quad z = 0, \quad (6.76)$$

and

$$S^3 - \kappa S(1 + S^2) \frac{\partial S}{\partial z} = 0 \quad \text{at} \quad z = 1. \quad (6.77)$$

Roughly, for $\kappa \ll 1$, these are

$$\begin{aligned} S &= S_0 \quad \text{at} \quad z = 0, \\ S &= 0 \quad \text{at} \quad z = 1, \end{aligned} \quad (6.78)$$

where $S_0 = (u_0/K)^{1/3}$, which we initially take to be $O(1)$ (and < 1 , so that surface ponding does not occur).

Neglecting κ , the solution is the step function

$$\begin{aligned} S &= S_0, \quad z < z_f, \\ S &= 0, \quad z > z_f, \end{aligned} \tag{6.79}$$

and the shock front at z_f advances at a rate \dot{z}_f , given from the jump condition

$$\dot{z}_f = \frac{[S^3]_+}{[S]_+} = S_0^2. \tag{6.80}$$

In dimensional terms, the shock front moves at speed $u_0/\phi S_0$, which is in fact obvious (given that it has constant S behind it).

The shock structure is similar to that of Burgers' equation. We put

$$z = z_f + \kappa Z, \tag{6.81}$$

and S rapidly approaches the quasi-steady solution $S(Z)$ of

$$-VS' + 3S^2S' = [S(1 + S^2)S']', \tag{6.82}$$

where $V = \dot{z}_f$; hence

$$S(1 + S^2)S' = -S(S_0^2 - S^2), \tag{6.83}$$

in order that $S \rightarrow S_0$ as $Z \rightarrow -\infty$, and where we have chosen

$$V = S_0^2, \tag{6.84}$$

(as $S_+ = 0$), thus reproducing (6.80). The solution is a quadrature,

$$\int^S \frac{(1 + S^2)dS}{(S_0^2 - S^2)} = -Z, \tag{6.85}$$

with an arbitrary added constant (amounting to an origin shift for Z). Hence

$$S - \frac{(1 + S_0^2)}{2S_0} \ln \left[\frac{S_0 + S}{S_0 - S} \right] = Z. \tag{6.86}$$

The shock structure is shown in figure 6.7, and one particular feature is noteworthy; the profile terminates where $S = 0$ at $Z = 0$. In fact, (6.83) implies that $S = 0$ or (6.86) applies. Thus when S given by (6.86) reaches zero, the solution switches to $S = 0$. The fact that $\partial S/\partial Z$ is discontinuous is not a problem because the diffusivity $S(1 + S^2)$ goes to zero when $S = 0$. In fact, this *degeneracy* of the equation is a signpost for fronts with discontinuous derivatives, and we shall encounter this situation again when we study non-linear diffusion. Essentially, the profile can maintain discontinuous gradients at $S = 0$ because the diffusivity is zero there, and there is no mechanism to smooth the jump away.

Suppose now that $k_0 = 10^{-9} \text{ m}^2$ (a plausible value) and $\mu/\rho = 10^{-6} \text{ m}^2 \text{ s}^{-1}$, then the saturated hydraulic conductivity $K = k_0 \rho g / \mu = 10^{-2} \text{ m s}^{-1}$. On the other hand,

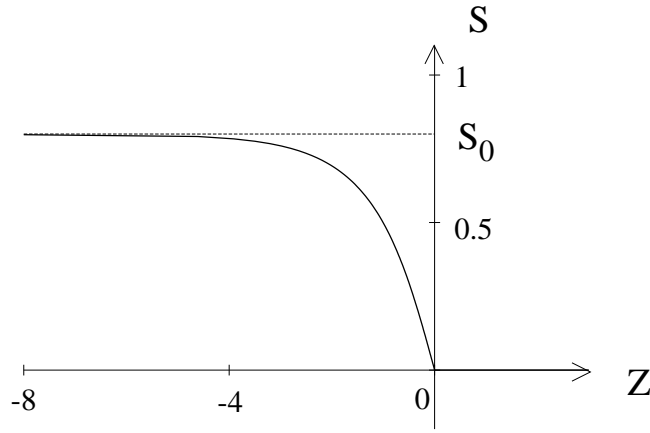


Figure 6.7: $S(Z)$ given by (6.86); the shock front terminates at the origin.

if a metre thick snow pack melts in ten days, this implies $u_0 \sim 10^{-6} \text{ m s}^{-1}$. Thus $S_0^2 = u_0/K \sim 10^{-4}$, and the approximation $S \approx S_0$ looks less realistic. With

$$S^3 - \kappa S(1 + S^2) \frac{\partial S}{\partial z} = S_0^3, \quad (6.87)$$

and $S_0 \sim 10^{-2}$ and $\kappa \sim 10^{-1}$, it seems that one should assume $S \ll 1$. We define

$$S = \left(\frac{S_0^3}{\kappa} \right)^{1/2} s, \quad (6.88)$$

note that $(S_0^3/\kappa)^{1/2} \sim 0.03$, so that (6.87) becomes

$$\beta s^3 - s \left[1 + \frac{S_0^3}{\kappa} s^2 \right] \frac{\partial s}{\partial z} = 1 \quad \text{on } z = 0, \quad (6.89)$$

and we have $S_0^3/\kappa \sim 10^{-3}$, $\beta = (S_0/\kappa)^{3/2} \sim 0.3$.

We neglect the term in S_0^3/κ , so that

$$\beta s^3 - s \frac{\partial s}{\partial z} \approx 1 \quad \text{on } z = 0, \quad (6.90)$$

and substituting (6.88) into (6.73) leads to

$$\frac{\partial s}{\partial \tau} + 3\beta s^2 \frac{\partial s}{\partial z} \approx \frac{\partial}{\partial z} \left[s \frac{\partial s}{\partial z} \right]. \quad (6.91)$$

A simpler analytic solution is no longer possible, but the development of the solution will be similar. The flux condition (6.90) at $z = 0$ allows the surface saturation to build up gradually, and a shock will only form if $\beta \gg 1$ (when the preceding solution becomes valid).

6.5 Similarity solutions

If, on the other hand, $\beta \ll 1$, then the saturation profile approximately satisfies

$$\begin{aligned} \frac{\partial s}{\partial \tau} &= \frac{\partial}{\partial z} \left[s \frac{\partial s}{\partial z} \right], \\ -s \frac{\partial s}{\partial z} &= \begin{cases} 1 & \text{on } z = 0, \\ 0 & \text{on } z = 1. \end{cases} \end{aligned} \quad (6.92)$$

At least for small times, the model admits a *similarity solution* of the form

$$s = \tau^\alpha f(\eta), \quad \eta = z/\tau^\beta, \quad (6.93)$$

where satisfaction of the equations and boundary conditions requires $2\alpha = \beta$ and $2\beta = 1 = \alpha$, whence $\alpha = 1/3$, $\beta = 2/3$, and f satisfies

$$(ff')' - \frac{1}{3}(f - 2\eta f') = 0, \quad (6.94)$$

and the condition at $z = 0$ becomes

$$-ff' = 1 \quad \text{at } \eta = 0. \quad (6.95)$$

The condition at $z = 1$ can be satisfied for small enough τ , as we shall see, because the equation (6.94) is degenerate, and f reaches zero in a finite distance, η_0 , say, and $f = 0$ for $\eta > \eta_0$. As $\eta = 1/\tau^{2/3}$ at $z = 1$, then this solution will satisfy the no flux condition at $z = 1$ as long as $\tau < \eta_0^{-3/2}$, when the advancing front will reach $z = 1$.

To see why f behaves in this way, integrate once to find

$$f(f' + \frac{2}{3}\eta) = -1 + \int_0^\eta f d\eta. \quad (6.96)$$

For small η , the right hand side is negative, and f is positive (to make physical sense), so f decreases (and in fact $f' < -\frac{2}{3}\eta$). For sufficiently small $f(0) = f_0$, f will reach zero at a finite distance $\eta = \eta_0$, and the solution must terminate. On the other hand, for sufficiently large f_0 , $\int_0^\eta f d\eta$ reaches 1 at $\eta = \eta_1$ while f is still positive (and $f' = -\frac{2}{3}\eta_1$ there). For $\eta > \eta_1$, then f remains positive and $f' > -\frac{2}{3}\eta$ (f cannot reach zero for $\eta > \eta_1$ since $\int_0^\eta f d\eta > 1$ for $\eta > \eta_1$). Eventually f must have a minimum and thereafter increase with η . This is also unphysical, so we require f to reach zero at $\eta = \eta_0$. This will occur for a range of f_0 , and we have to select f_0 in order that

$$\int_0^{\eta_0} f d\eta = 1, \quad (6.97)$$

which in fact represents global conservation of mass. Figure 6.8 shows the schematic form of solution both for $\beta \gg 1$ and $\beta \ll 1$. Evidently $\beta \sim 1$ will have a travelling front solution between these two end cases.

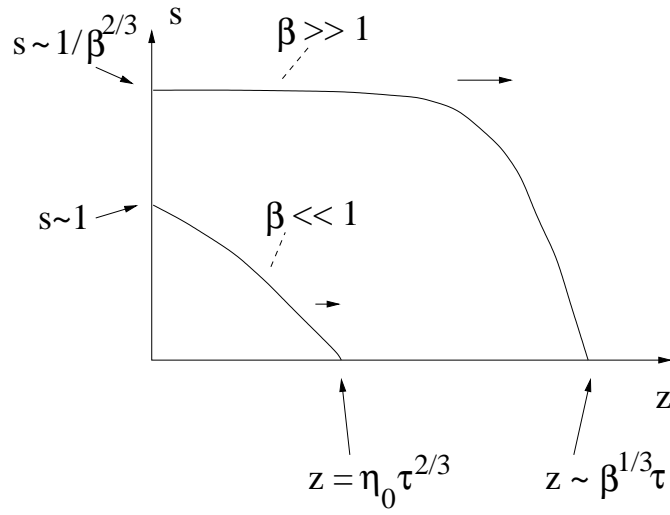


Figure 6.8: Schematic representation of the evolution of s in (6.91) for both large and small β .

Exercises

- 6.1 A simple model for the flow of a mixture of two fluids along a tube (e.g., air and water) is

$$\alpha_t + (\alpha v)_z = 0$$

$$-\alpha_t + [(1 - \alpha)u]_z = 0$$

$$\rho_g[(\alpha v)_t + (\alpha v^2)_z] = -\alpha p_z,$$

$$\rho_l[\{(1 - \alpha)u\}_t + \{D_l(1 - \alpha)u^2\}_z] = -(1 - \alpha)p_z,$$

where p is pressure, u and v are the two fluid velocities, α is the volume fraction of the fluid with speed v , ρ_g is its density, and ρ_l is the density of the other fluid. Show that there are two characteristic speeds $dz/dt = \lambda$, satisfying

$$(\lambda - u)^2 = (D_l - 1)[u^2 + 2u(\lambda - u)] - s^2(\lambda - v)^2,$$

where

$$s = \left[\frac{\rho_g(1 - \alpha)}{\rho_l \alpha} \right]^{1/2}.$$

Deduce that the characteristic speeds are real if, when $D_l - 1 \ll 1$, $s \ll 1$,

$$D_l \gtrsim 1 + \left\{ \frac{s(u - v)}{u} \right\}^2.$$

In particular, show that the roots are complex if $D_l = 1$ and $u \neq v$. What does this suggest concerning the well-posedness of the model?

6.2 The function $u(x, t)$ satisfies

$$u_t + uu_x = \alpha(1 - u^2)$$

for $-\infty < x < \infty$, where $\alpha > 0$, and with $u = u_0(x)$ at $t = 0$, and $0 < u_0 < 1$ everywhere. Show that the characteristic solution can be written parametrically in the form

$$u = \frac{u_0(s) + \tanh \alpha t}{1 + u_0(s) \tanh \alpha t}, \quad \exp[\alpha(x - s)] = \cosh \alpha t + u_0(s) \sinh \alpha t.$$

Sketch the form of the characteristics for an initial function such as $u_0(s) = a/(1 + s^2)$. Show that, in terms of s and t , u_x is given by

$$u_x = \frac{[\alpha \operatorname{sech}^2 \alpha t] u'_0(s)}{[1 + u_0(s) \tanh \alpha t][\alpha + \{u'_0(s) + \alpha u_0(s)\} \tanh \alpha t]},$$

and deduce that a shock will form if $u'_0 + \alpha(1 + u_0)$ becomes negative for some s . Show that if $u_0 = a/(1 + s^2)$ and a is small, this occurs if

$$\alpha \lesssim \frac{3a\sqrt{3}}{8}.$$

6.3 Discuss the formation of shocks and the resulting shock structure for the equation

$$u_t + u^\alpha u_x = \varepsilon [u^\beta u_x]_x,$$

where $\alpha, \beta > 0$, and $\varepsilon \ll 1$. (Assume $u > 0$, and $u \rightarrow 0$ at $\pm\infty$.)

Show that the equation

$$u_t + uu_x = \varepsilon uu_{xx}$$

admits a shock structure joining u_- to a lower value u_+ , but not one in which the wave speed $c = [\frac{1}{2}u^2]_-^+ / [u]_-^+$. Why should this be so?

6.4 Use phase plane methods to study the existence of travelling wave solutions to the equation

$$u_t = u^p(1 - u^q) + [u^r u_x]_x,$$

when (i) $p = 1, q = 2, r = 0$; (ii) $p = 1, q = 1, r = 1$.

6.5 Two examples of integrable partial differential equations which admit soliton solutions are the nonlinear Schrödinger (NLS) equation

$$iu_t = |u|^2 u + u_{xx},$$

and the sine-Gordon equation

$$u_{tt} - u_{xx} = \sin u.$$

Show that these equations admit solitary wave solutions (which are in fact solitons).

- 6.6 In a model of snow melting, it is assumed that the permeability is $k = k_0 S^\alpha$, and the capillary suction is $p_c(S) = p_0(S^{-\beta} - S)$, where $\alpha, \beta > 0$, and S is the saturation. How does the choice of different values of α and β affect the formation and propagation of shock waves, and their internal structure?

Chapter 7

Nonlinear diffusion

Like travelling wave solutions, similarity solutions are important indicators of solution behaviour. For example, in the example we have just seen, the existence of a propagating front solution is a hallmark of the degeneracy of the diffusion coefficient where the saturation goes to zero.

A particularly good illustration of this behaviour is in the general nonlinear diffusion equation

$$u_t = (u^m u_x)_x, \quad (7.1)$$

which arises in many contexts. We shall illustrate the derivation of this equation for a fluid droplet below. Typically, (7.1) represents the speed of the density of some quantity u with a diffusive flux $-u^m u_x$. A standard kind of problem to consider is then the release of a concentrated amount at $x = 0$ at $t = 0$. We can idealise this by supposing that at $t = 0$ (in suitable units),

$$u = 0, \quad x \neq 0, \quad \int_{-\infty}^{\infty} u(x) dx = 1. \quad (7.2)$$

This apparently contradictory prescription idealises the concept of a very concentrated local injection of u . For example, (7.1) with (7.2) could represent the diffusion of sugar in hot (one-dimensional) tea from an initially emplaced sugar grain. (7.2) defines the delta function $\delta(x)$, an example of a generalised function. One can think of generalised functions as being (defined by) the equivalence classes of well-behaved functions u_n with appropriate limiting behaviour. For example, the delta function is defined by the class of well-behaved functions u_n for which

$$\int_{-\infty}^{\infty} u_n(x) f(x) dx \rightarrow f(0) \quad (7.3)$$

for all well-behaved $f(x)$. As a shorthand, then,

$$\int_{-\infty}^{\infty} \delta(x) f(x) dx = f(0) \quad (7.4)$$

for any f , but the ulterior definition is really in (7.3). In practice, however, we think of a delta function as a ‘function’ of x , zero everywhere except for a (very) sharp spike at $x = 0$.

In solving (7.1), we also apply boundary conditions

$$u \rightarrow 0 \quad \text{as } x \rightarrow \pm\infty, \quad (7.5)$$

and these, together with the equation, imply that

$$\int_{-\infty}^{\infty} u \, dx = 1 \quad (7.6)$$

for all time.

A similarity solution is appropriate because there are no intrinsic space or time scales for the problem. It is in this context that one can expect the solution to look the same at different times on different scales. In general, as t varies, then the length scale might vary as $\xi(t)$ and the amplitude of the solution u might vary as $U(t)$. That is, if we look at u/U as a function of x/ξ , it will look the same for all t . This in turn implies that the solution takes the form

$$u = U(t)f \left[\frac{x}{\xi(t)} \right], \quad (7.7)$$

and this is one of the forms of a similarity solution.

It is often the case that U and ξ are powers of t , and the exponents are to be chosen so that the problem has such a solution. This is best seen by example. If we denote $\eta = x/\xi(t)$, and substitute the form (7.7) into (7.1), (7.5) and (7.6), we find

$$\frac{U'}{U}f - \frac{\xi'}{\xi}\eta f' = \frac{U^m}{\xi^2}[f^m f']', \quad (7.8)$$

where $U' = dU/dt$, $\xi' = d\xi/dt$, but $f' = df/d\eta$. The initial/boundary conditions become

$$f(\pm\infty) = 0, \quad (7.9)$$

and the normalisation condition (7.6) is

$$U\xi \int_{-\infty}^{\infty} f \, d\eta = 1. \quad (7.10)$$

A solution can be found provided the t dependence vanishes from the model, and this requires $U\xi = 1$ (the constant can be taken as one without loss of generality), whence (7.8) becomes

$$[f^m f']' + \xi^{m+1}\xi'(\eta f)' = 0, \quad (7.11)$$

and $\xi^{m+1}\xi'$ must be constant. It is algebraically convenient to choose $\xi^{m+1}\xi' = 2/m$, thus

$$\eta = x \left[\frac{m}{2(m+2)t} \right]^{\frac{1}{m+2}}, \quad (7.12)$$

and a first integral of (7.11) is

$$f^m f' + \frac{2}{m}\eta f = 0, \quad (7.13)$$

with the constant of integration being zero (because $f \rightarrow 0$ as $\eta \rightarrow \pm\infty$). Thus either $f = 0$, or

$$f = [\eta_0^2 - \eta^2]^{1/m}, \quad (7.14)$$

so that the solution has the form of a cap of finite extent, given by (7.14) (for $|\eta| < \eta_0$, and $f = 0$ for $|\eta| > \eta_0$). The value of η_0 is determined from $\int_{-\infty}^{\infty} f d\eta = 1$, and is

$$\eta_0 = \frac{1}{\left[2 \int_0^{\pi/2} \cos^{\frac{m+2}{m}} \theta d\theta\right]^{\frac{m}{m+2}}}. \quad (7.15)$$

The finite extent of the profile is due to the degeneracy of the equation when $m > 0$. (The limit $m \rightarrow 0$ regains the Gaussian solution of the heat equation by first putting $\eta = \sqrt{m}\eta_0\zeta$, $f = F/\sqrt{m}$, and noting that $\eta_0 \approx (\pi m)^{-m/2}$ as $m \rightarrow 0$ (this last following by application of Laplace's method to (7.15)).) The graph of $f(\eta)$ is shown in figure 7.1.

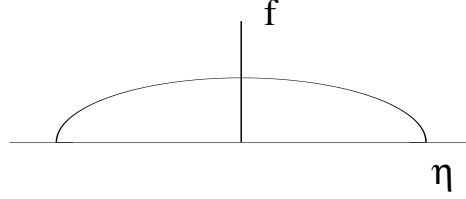


Figure 7.1: $f(\eta)$ given by (7.14).

7.1 The viscous droplet

An example of where the nonlinear diffusion equation can arise is in the dynamics of a drop of viscous fluid on a level surface. If the fluid occupies $0 < z < h(x, y, t)$ and is shallow, then lubrication theory gives the approximation

$$\begin{aligned} \nabla p &= \mu \frac{\partial^2 \mathbf{u}}{\partial z^2}, \\ p_z &= -\rho g, \end{aligned} \quad (7.16)$$

in which $\mathbf{u} = (u, v, 0)$ is the horizontal component of velocity, and ∇ is the horizontal gradient $(\partial/\partial x, \partial/\partial y, 0)$. With $p = 0$ at $z = h$, we have the hydrostatic pressure $p = \rho g(h - z)$, so that $\nabla p = \rho g \nabla h$, and three vertical integrations of (7.16)₁ (with zero shear stress $\partial \mathbf{u}/\partial z = 0$ at $z = h$ and no slip $\mathbf{u} = 0$ at $z = 0$) yield the horizontal fluid flux

$$\mathbf{q} = \int_0^h \mathbf{u} dz = -\frac{\rho g}{3\mu} h^2 \nabla h. \quad (7.17)$$

Conservation of fluid volume for an incompressible fluid is $h_t + \nabla \cdot \mathbf{q} = 0$, and thus

$$h_t = \frac{\rho g}{3\mu} \nabla \cdot [h^3 \nabla h], \quad (7.18)$$

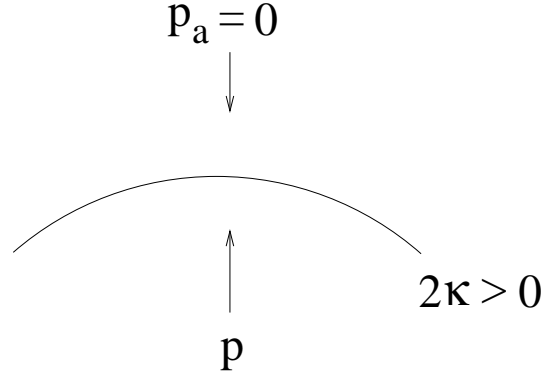


Figure 7.2: The surface shown has positive curvature when the radius of curvature is measured from below the surface; in this case equilibrium requires $p > p_a$.

corresponding to (7.1) (in two space dimensions) with $m = 3$. A drop of fluid placed on a table will spread out at a finite rate.

That this does not continue indefinitely is due to surface tension. Rather than having $p = 0$ at $z = h$ (where the atmospheric pressure above is taken as zero), the effect of surface tension is to prescribe

$$p = 2\gamma\kappa, \quad (7.19)$$

where γ is the surface tension, and κ is the mean curvature relative to the fluid droplet (i.e. $\kappa > 0$ if the interface is concave, as illustrated in figure 7.2). The curvature is defined as $2\kappa = \nabla \cdot \mathbf{n}$, where \mathbf{n} is the unit normal pointing away from the fluid (i.e., upwards). At least this shorthand definition works if we define

$$\mathbf{n} = \frac{(-h_x, -h_y, 1)}{[1 + |\nabla h|^2]^{1/2}}, \quad (7.20)$$

thus

$$2\kappa = -\nabla \cdot \left[\frac{\nabla h}{\{1 + |\nabla h|^2\}^{1/2}} \right]. \quad (7.21)$$

It is less obvious that it will work more generally, since there are many ways of defining the interface as $\phi(x, y, z) = 0$ and thus $\mathbf{n} = \nabla \phi / |\nabla \phi|$ (that is (7.20) uses $\phi = z - h$); but in fact it does not matter, since we may generally take $\phi = (z - h)P$, so that $\nabla \phi = (-h_x, -h_y, 1)$ on $z = h$, and $\nabla \phi / |\nabla \phi|$ is the same expression as in (7.21).

For shallow flows, we replace $p = 0$ on $z = h$ by $p = -\gamma \nabla^2 h$ there, and thus

$$p \approx \rho g(h - z) - \gamma \nabla^2 h, \quad (7.22)$$

and (via (7.17)), (7.18) is modified to

$$h_t = \nabla \cdot \left[\frac{h^3}{3\mu} \nabla \{ \rho g h - \gamma \nabla^2 h \} \right]. \quad (7.23)$$

The fourth order term is also ‘diffusive’, insofar as it is a smoothing term: this is most easily seen by considering the fate of modes $e^{\sigma t + i k x}$ for the linear equation $h_t = -h_{xxxx}$: $\sigma = -k^4$: high wave number (high gradient) modes are rapidly damped. Surface tension can thus also act to smooth out shocks. The effect of surface tension relative to the diffusional gravity term is given by the Bond number

$$Bo = \frac{\rho g l^2}{\gamma}, \quad (7.24)$$

where l is the lateral length scale of the drop. This is the (only) dimensionless parameter which occurs when (7.23) is written dimensionlessly.

For a drop released on a table, (7.23) still predicts unending dispersal, but if the full nonlinear curvature term (7.21) is kept, then a steady state will exist, and surface tension keeps the drop of finite extent.

7.2 Advance and retreat: waiting times

The similarity solution (7.14) predicts an infinite slope at the margin (where $f = 0$) if $m > 1$ (and a zero slope if $m < 1$). If one releases a finite quantity at $t = 0$, then one expects the long time solution to be this similarity solution. The question then arises as to how this similarity solution is approached, in particular if the initial drop has finite slope at the margin.

This question can be addressed in a more general way by studying the behaviour near the margin $x = x_S(t)$ of a solution $h(x, t)$ of (7.1),

$$h_t = (h^m h_x)_x. \quad (7.25)$$

Suppose that $h \sim c(x_S - x)^\nu$ for x near x_S . Then satisfaction of (7.25) requires

$$\dot{x}_S \approx c^m [\nu(m+1) - 1] (x_S - x)^{\nu m - 1}. \quad (7.26)$$

Note that the similarity solution (7.14) has \dot{x}_S finite when $\nu = 1/m$, consistent with (7.26), and more generally we see that the margin will advance at a rate $\dot{x}_S \approx c^m/m$ if $h \sim c(x_S - x)^{1/m}$.

Suppose now that $m > 1$, and we emplace a drop with finite slope, $\nu = 1$. Then the right hand side of (7.26) is zero at $x = x_S$, and thus $\dot{x}_S = 0$: the front does not move. What happens in this case is that the drop flattens out: there is transport of h towards the margin, which steepens the slope at x_S until it becomes infinite, at which point it will move. This pause while the solution fattens itself prior to margin movement is called a *waiting time*.

Conversely, if $m < 1$, then the front moves (forward) if the slope is zero, $\nu = 1/m$. If the slope is finite, $\nu = 1$, then (7.25) would imply infinite speed. An initial drop of finite margin slope will instantly develop zero front slope as the margin advances.

(7.26) does not allow the possibility of retreat, because it describes a purely diffusive process. The possibility of both advance and retreat is afforded by a model of a viscous drop with accretion, one example of which is the mathematical model of an

ice sheet. Essentially, an ice sheet, such as that covering Antarctica or Greenland, can be thought of as a (large) viscous drop which is nourished by an accumulation rate (of ice formed from snow). A general model for such a nourished drop is

$$h_t = (h^m h_x)_x + a, \quad (7.27)$$

where a represents the accumulation rate. Unlike the pure diffusion process, (7.27) has a steady state

$$h = \left[\frac{(m+1)a}{2} \right]^{\frac{1}{m+1}} (x_0^2 - x^2)^{\frac{1}{m+1}}, \quad (7.28)$$

where x_0 must be prescribed. (In the case of an ice sheet, we might take x_0 to be at the continental margin.) (7.28) is slightly artificial, as it requires $a = 0$ for $x > x_0$, and allows a finite flux $-h^m h_x = ax_0$ where $h = 0$. More generally, we might allow accumulation and ablation (snowfall and melting), and thus $a = a(x)$, with $a < 0$ for large $|x|$. In that case the steady state is

$$h = \left[(m+1) \int_x^{x_0} s \, dx \right]^{\frac{1}{m+1}}, \quad (7.29)$$

where the balance is

$$s = \int_0^x a \, dx, \quad (7.30)$$

and x_0 is defined to be where accumulation balances ablation,

$$\int_0^{x_0} a \, dx = 0. \quad (7.31)$$

This steady state is actually stable, and both advance and retreat can occur. Suppose the margin is at x_S , where $a = a_S = -|a_S|$ ($a_S < 0$, representing ablation). If we put $h \approx c(x_S - x)^\nu$, then (7.27) implies

$$\nu c \dot{x}_S (x_S - x)^{\nu-1} \approx \nu c^{m+1} [\nu(m+1) - 1] (x_S - x)^{[\nu(m+1)-2]} - |a_S|, \quad (7.32)$$

and there are three possible balances of leading order terms.

The first is as before,

$$\dot{x}_S \approx c^m [\nu(m+1) - 1] (x_S - x)^{\nu m - 1}, \quad (7.33)$$

and applies generally if $\nu < 1$. Supposing $m > 1$, then we have advance, $\dot{x}_S \approx c^m/m$ if $\nu = 1/m$, but if $\nu > 1/m$, this cannot occur, and the margin is stationary if $1/m < \nu < 1$. If $\nu = 1$, then $\nu(m+1) - 2 = m - 1 > 0$, so that

$$\dot{x}_S \approx -|a_S|/c, \quad (7.34)$$

and the margin retreats; if $\nu > 1$, then instantaneous adjustment to finite slope and retreat occurs.

The ice sheet exhibits the same sort of waiting time behaviour as the viscous drop without accretion. For $1/m < \nu < 1$, the margin is stationary, and if $x_S < x_0$ then the margin slope will steepen until $\nu = 1/m$, and advance occurs. On the other hand, if $x_S > x_0$, then the slope will decrease until $\nu = 1$, and retreat occurs. In the steady state, a balance is achieved (from (7.29)) when $\nu = 2/(m+1)$.

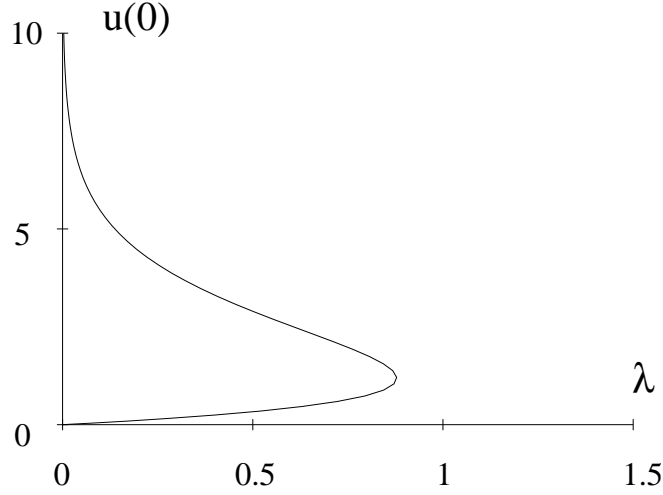


Figure 7.3: Maximum values of u , $u(0)$, as a function of the parameter λ . Blow-up occurs if $\lambda \gtrsim 0.878$.

7.3 Blow-up

Further intriguing possibilities arise when the source term is nonlinear. An example is afforded by the nonlinear (diffusion) equation

$$u_t = u_{xx} + \lambda e^u, \quad (7.35)$$

which arises in the theory of combustion. Indeed, as we saw earlier, combustion occurs through the fact that multiple steady states can exist for a model such as (6.70), and the same is true for (7.35), which can have two steady solutions. In fact, if we solve $u'' + \lambda e^u = 0$ with boundary conditions $u = 0$ on $x = \pm 1$, then the solutions are

$$u = 2 \ln \left[A \operatorname{sech} \left\{ \sqrt{\frac{\lambda}{2}} Ax \right\} \right], \quad (7.36)$$

where $A = \exp[u(0)/2]$, and A satisfies

$$A = \cosh \left[\sqrt{\frac{\lambda}{2}} A \right], \quad (7.37)$$

which has two solutions if $\lambda < 0.878$, and none if $\lambda > 0.878$: the situation is depicted in figure 7.3. If we replace e^u by $\exp[u/(1 + \varepsilon u)]$, $\varepsilon > 0$, we regain the top (hot) branch also, as in figure 5.2.

One wonders what the absence of a steady state for (7.35) if $\lambda > \lambda_c$ implies. The time-dependent problem certainly has a solution, and an idea of its behaviour can be deduced from the spatially independent problem, $u_t = \lambda e^u$, with solution $u = \ln[1/\{\lambda(t_0 - t)\}]$: u reaches infinity in a finite time. This phenomenon is known

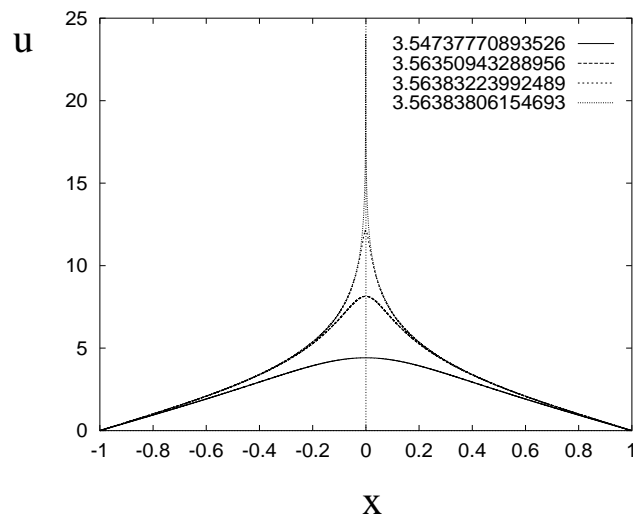


Figure 7.4: Solution of $u_t = u_{xx} + e^u$ on $[-1, 1]$, with $u = 0$ at $x = -1, 1$ and $t = 0$. The solution is shown for four times close to the blow-up time $t_c = 3.56384027594971$. The many decimal places should not be treated too seriously, but they do indicate the logarithmic suddenness of the runaway.

as *thermal runaway*, and more generally the creation of a singularity of the solution in finite time is called *blow-up*. Numerical solutions of the equation (7.35) including the diffusion term show that blow-up still occurs, but at an isolated point; figure 7.4 shows the approach to blow-up as t approaches a critical blow-up time t_c .

In fact, one can prove generally that no steady solutions exist for λ greater than some critical value, and also that in that case, blow-up will occur in finite time. To do this, we use some pretty ideas of higher grade mathematics.

Suppose we want to solve the more general problem

$$u_t = \nabla^2 u + \lambda e^u \quad \text{in } \Omega, \quad (7.38)$$

with $u = 0$ in the boundary $\partial\Omega$, and $u = 0$ at $t = 0$ (these conditions are for convenience rather than necessity). We will be able to prove results for (7.38) which are comparable to those for the ordinary differential equation version (cf. (6.77))

$$\dot{w} = -\mu_1 w + \lambda e^w, \quad (7.39)$$

because, in some loose sense, the Laplacian operator ∇^2 resembles a loss term.

More specifically, we recall some pertinent facts about the (Helmholtz) eigenvalue problem

$$\nabla^2 \phi + \mu \phi = 0 \quad \text{in } \Omega, \quad (7.40)$$

with $\phi = 0$ on $\partial\Omega$. There exists a denumerable sequence of real eigenvalues $0 < \mu_1 \leq \mu_2 \leq \dots$, with $\mu_n \rightarrow \infty$ as $n \rightarrow \infty$, and corresponding eigenfunctions ϕ_1, ϕ_2, \dots which form an orthonormal set (using the L^2 norm), thus

$$(\phi_i, \phi_j) \equiv \int_{\Omega} \phi_i \phi_j dV = \delta_{ij}, \quad (7.41)$$

where δ_{ij} is the Kronecker delta ($= 1$ if $i = j$, 0 if $i \neq j$). These eigenvalues satisfy a variational principle of the form

$$\mu_i = \min \int_{\Omega} |\nabla \phi|^2 dV, \quad (7.42)$$

where ϕ ranges over functions of unit norm, $\|\phi\|_2 = \{\int \phi^2 dV\}^{1/2} = 1$, which are orthogonal to ϕ_j for $j < i$; (more generally $\mu_i = \min \{\int |\nabla \phi|^2 / \int \phi^2\}$ if ϕ is not normalised on to the unit sphere $\|\phi\|_2 = 1$). In particular

$$\mu_1 = \min_{\|\phi\|_2=1} \int_{\Omega} |\nabla \phi|^2 dV, \quad (7.43)$$

and the corresponding ϕ_1 is of one sign, let us say positive.

We take the inner product of the equation (7.38) with ϕ_1 and divide by $\int \phi_1 dV$; defining

$$v(t) = \frac{\int_{\Omega} u \phi_1 dV}{\int_{\Omega} \phi_1 dV} = \int_{\Omega} u d\omega, \quad (7.44)$$

where $d\omega = \phi_1 dV / \int_{\Omega} \phi_1 dV$ is a measure on Ω (with $\int_{\Omega} d\omega = 1$), and using Green's theorem, we find

$$\dot{v} = \lambda \int_{\Omega} e^u d\omega - \mu_1 v, \quad (7.45)$$

and the equation for v is close to the ordinary differential equation (7.39).

Now we use Jensen's inequality. This says that if we have an integrable function g on Ω and a convex function $f(x)$ (i.e. one that bends upwards, $f'' > 0$), then

$$f \left[\int_{\Omega} g d\omega \right] \leq \int_{\Omega} f[g] d\omega \quad (7.46)$$

for any measure ω on Ω such that $\int_{\Omega} d\omega = 1$. We have chosen ω to be so normalised, and e^u is convex: thus

$$\int_{\Omega} \exp(u) d\omega \geq \exp \left[\int_{\Omega} u d\omega \right] = e^v, \quad (7.47)$$

so that

$$\dot{v} \geq \lambda e^v - \mu_1 v. \quad (7.48)$$

It is now easy to prove non-existence and blow-up for λ greater than some critical value λ_c . Firstly, u must be positive, and hence also v . (For suppose $u < 0$: since $u = 0$ at $t = 0$ and on $\partial\Omega$, then u attains its minimum in Ω at some $t > 0$, at which point $u_t \leq 0$, $u_{xx} \geq 0$, which is impossible, since then $u_t - u_{xx} = \lambda e^u \leq 0$.) For any v , $e^v \geq ev$, thus $\dot{v} \geq (\lambda e - \mu_1)v$. In a steady state, $\dot{v} = 0$, and $v > 0$ (clearly $u = 0$ is not a solution), so this is impossible if

$$\lambda > \mu_1/e. \quad (7.49)$$

This implies non-existence of a solution for $\lambda > \lambda_c$, where $\lambda_c \leq \mu_1/e$.

In a similar vein, if $\lambda > \mu_1/e$, then

$$\dot{v} > \mu_1[e^{v-1} - v], \quad (7.50)$$

and $v > w$, where

$$\dot{w} = \mu_1(e^{w-1} - w), \quad w(0) = 0. \quad (7.51)$$

(This is a standard comparison argument: $v = w$ at $t = 0$, and $\dot{v} > \dot{w}$ there, so $v - w$ is initially positive. It remains so unless at some future time $v - w$ reaches zero again, when necessarily $\dot{v} - \dot{w} \leq 0$ — which is impossible, since $\dot{v} > \dot{w}$ whenever $v = w$.) But $w \rightarrow \infty$ in finite time ($\dot{w} > 0$ so that $w \rightarrow \infty$ as t increases, and as $w \rightarrow \infty$, $e^{-w}\dot{w} \approx \mu e^{-1}$, so e^{-w} reaches zero in finite time); therefore also v reaches infinity in finite time. Finally

$$v = \int_{\Omega} u \, d\omega \leq \sup_{\Omega} u, \quad (7.52)$$

since $\int_{\Omega} d\omega = 1$: hence $u \rightarrow \infty$ in finite time.

In fact $u \rightarrow \infty$ at isolated points, and usually at one isolated point. As blow-up is approached, one might suppose that the nature of the solution in the vicinity of the blow-up point would become independent of the initial (or boundary) conditions, and thus that some form of similarity solution might be appropriate.

This is indeed the case, although the precise structure is rather complicated. We examine blow-up in one spatial dimension, x . As a first guess, the logarithmic nature of blow-up in the spatially independent case, together with the usual square-root behaviour of the space variable in similarity solutions for the diffusion equation, suggests that we define

$$\tau = -\ln(t_0 - t), \quad \eta = \frac{x - x_0}{(t_0 - t)^{1/2}}, \quad u = -\ln[\lambda(t_0 - t)] + g(\eta, \tau), \quad (7.53)$$

where blow-up occurs at $x = x_0$ at $t = t_0$; hence g satisfies

$$g_{\tau} = g_{\eta\eta} - \frac{1}{2}\eta g_{\eta} + e^g - 1. \quad (7.54)$$

The natural candidate for a similarity solution is then a steady solution $g(\eta)$ of (7.54), satisfying

$$g'' - \frac{1}{2}\eta g' + (e^g - 1) = 0, \quad (7.55)$$

and matching to a far field solution $u(x, t_0)$ would suggest

$$g \sim -2 \ln |\eta| \quad \text{as } \eta \rightarrow \pm\infty, \quad (7.56)$$

and solutions of (7.55) with this asymptotic structure do exist — but not at each end. (7.55) admits even solutions, and if we restrict ourselves to these, then we may take

$$g'(0) = 0, \quad g(0) \neq 0. \quad (7.57)$$

(If $g(0) = 0$, then $g \equiv 0$ is the solution.) However, it is found that such solutions have a different asymptotic behaviour as $\eta \rightarrow \infty$, namely

$$g \sim -\frac{A}{|\eta|} \exp\left[\frac{1}{4}\eta^2\right], \quad (7.58)$$

and $A = A[g(0)] > 0$ for $g(0) \neq 0$ (and $A(0) = 0$), and these cannot match to the outer solution. If one alternately prescribes (7.56) as $\eta \rightarrow +\infty$, for example, then the solution is asymmetric, and has the exponential behaviour (7.58) as $\eta \rightarrow -\infty$. thus the appealingly simple similarity structure implied by steady solutions of (7.54) is wrong (and actually, the solution of the initial value problem (7.54) satisfying (7.56) tends to zero as $\tau \rightarrow \infty$).

However, (7.54) itself develops a local similarity structure as $\tau \rightarrow \infty$, using a further similarity variable

$$z = \frac{\eta}{\tau^{1/2}} = \frac{x - x_0}{(t_0 - t)^{1/2}[-\ln(t_0 - t)]^{1/2}}. \quad (7.59)$$

Rewriting (7.54) in terms of z and τ yields

$$g_\tau + \frac{1}{2}zg_z + 1 - e^g = \frac{1}{\tau}[g_{zz} + \frac{1}{2}zg_z]. \quad (7.60)$$

At leading order in τ^{-1} this has a solution

$$g = -\ln[1 + \frac{1}{4}cz^2], \quad (7.61)$$

where c is indeterminate, and this forms the basis for a formal expansion. It is algebraically convenient to use (7.61) to define c as a new variable, and also to write

$$s = \ln \tau; \quad (7.62)$$

Then (7.60) becomes

$$c_z = \frac{2}{\tau z^3} \left[2c + 4zc_z + z^2c_{zz} + z^2 \left\{ -\frac{[c + \frac{1}{2}zc_z]^2}{1 + \frac{1}{4}cz^2} + c + \frac{1}{2}zc_z - c_s \right\} \right]. \quad (7.63)$$

We seek a solution for (7.63) in the form

$$c \sim c_0(z, s) + \frac{1}{\tau}c_1(z, s) + \frac{1}{\tau^2}c_2(z, s) + \dots, \quad (7.64)$$

and then, since $\tau d/d\tau = d/ds$, we have

$$c_s \sim \dot{c}_0 + \frac{1}{\tau}(\dot{c}_1 - c_1) + \frac{1}{\tau^2}(\dot{c}_2 - 2c_2) + \dots, \quad (7.65)$$

where $\dot{c}_2 \equiv \partial c_2 / \partial s$. Substituting this into (7.63) and equating powers of τ , we find

$$c_0 = C_0(s), \quad (7.66)$$

where C_0 is arbitrary, and

$$c_{1z} = \frac{2}{z^3} \left[2C_0 + z^2 \left\{ -\frac{C_0^2}{1 + \frac{1}{4}C_0 z^2} + C_0 - \dot{C}_0 \right\} \right]. \quad (7.67)$$

The arbitrary function C_0 arises because the order of the approximate equation is reduced. In order to specify it, and other arbitrary functions of s which arise at each

order, we require that the solutions c_i be smooth, and this requires that there be no term on the right hand side of (7.67) proportional to $1/z$ as $z \rightarrow 0$, in order that logarithmic singularities not be introduced. Specifically, we require at each stage of the approximation that

$$\frac{\partial c_i}{\partial z} = \frac{2}{z^3} [a_{0i} + a_{1i}z + a_{3i}z^3 + \dots]; \quad (7.68)$$

so that $z^2 c_i$ is smooth. Applying this to (7.67) requires that

$$\dot{C}_0 = C_0(1 - C_0), \quad (7.69)$$

so that $C_0 \rightarrow 1$ as $s \rightarrow \infty$, and then

$$c_1 = -\frac{2C_0}{z^2} + C_1(s) + C_0^2 \ln[1 + \frac{1}{4}C_0 z^2]. \quad (7.70)$$

At $O(1/\tau^2)$, we then have

$$c_{2z} = \frac{2}{z^3} \left[2c_1 + 4zc_{1z} + z^2 c_{1zz} + z^2 \left\{ -(\dot{c}_1 - c_1) + (c_1 + \frac{1}{2}zc_{1z}) - \frac{2c_0(c_1 + \frac{1}{2}zc_{1z})}{1 + \frac{1}{4}c_0 z^2} + \frac{1}{4}c_0^2 c_1 z^2 (1 + \frac{1}{4}c_0 z^2)^2 \right\} \right], \quad (7.71)$$

and applying the regularity condition (7.68), we find, after some algebra,

$$\dot{C}_1 = 2(1 - C_0)C_1 + \frac{5}{2}C_0^3, \quad (7.72)$$

so that $C_1 \rightarrow C_{10} + \frac{5}{2}s$ as $s \rightarrow \infty$. Thus finally we obtain the local similarity solution

$$u \approx -\ln \left[\lambda \left\{ t_0 - t + \frac{c(x - x_0)^2}{4[-\ln(t_0 - t)]} \right\} \right], \quad (7.73)$$

where $c \approx C_0(s)$, $s = \ln \tau = \ln[-\ln(t_0 - t)]$.

Exercises

- 7.1 Write down the equation satisfied by a similarity solution of the form $u = t^\beta f(\eta)$, $\eta = x/t^\alpha$, for the equation

$$u_t = (u^m u_x)_x \quad \text{in } 0 < x < \infty,$$

where $m > 0$, with $u^m u_x = -1$ at $x = 0$, $u \rightarrow 0$ as $x \rightarrow \infty$, $u = 0$ at $t = 0$. Show that $\int_0^\infty f d\eta = 1$, and show that in fact f reaches zero at a finite value η_0 . Is the requirement that $m > 0$ necessary?

7.2 u satisfies the equation

$$u_t = [D(u)u_x]_x \quad \text{in } 0 < x < \infty,$$

with $u = 0$ at $x \rightarrow \infty$ and $t = 0$. For a general function D (not a power of u), for what kind of boundary condition at $x = 0$ does a similarity solution exist? What if, instead, $D = D(u_x)$? Write down suitable equations and boundary conditions for the similarity function in each case.

7.3 A small droplet satisfies the surface-tension controlled equation

$$h_t = -\frac{\gamma}{3\mu} \nabla \cdot [h^3 \nabla \nabla^2 h].$$

A small quantity $\int h dV = Q$ is released at time zero at the origin. Find a suitable similarity solution in one and two spatial dimensions.

7.4 A gravity-driven drop of fluid spreads out on a flat surface. Its viscosity μ is a function of shear rate, so that in (7.16),

$$\rho g \nabla h = \frac{\partial \tau}{\partial z},$$

$$\frac{\partial \mathbf{u}}{\partial z} = A|\tau|^{n-1} \boldsymbol{\tau}.$$

(A constant viscosity fluid has $n = 1$.) Show that the horizontal fluid flux is

$$\mathbf{q} = -\frac{A(\rho g)^n}{n+2} |\nabla h|^{n-1} h^{n+2} \nabla h,$$

and deduce that

$$\frac{\partial h}{\partial t} = \frac{A(\rho g)^n}{n+2} \nabla \cdot [h^{n+2} |\nabla h|^{n-1} \nabla h].$$

Find similarity solutions in one and two dimensions for the initial emplacement of a finite volume at the origin. What happens as $n \rightarrow \infty$ or $n \rightarrow 0$?

7.5 Suppose a two-dimensional drop as in question 7.4 is subjected to a spatially varying accumulation $a(x)$, with $xa' < 0$ for $x \neq 0$. Find appropriate local behaviour near the right hand margin $x = x_s > 0$, where $h = 0$, if $\dot{x}_s > 0$, $\dot{x}_s < 0$, $\dot{x}_s = 0$.

7.6 Let u satisfy

$$u_t = \lambda u^p + u_{xx},$$

with $u = 1$ on $x = \pm 1$ and $t = 0$. Prove that if λ is large enough, u must blow up in finite time if $p > 1$. Supposing this happens at time t_0 at $x = 0$, show that a possible local similarity structure is of the form

$$u = \frac{1}{(t_0 - t)^\beta} f(\xi), \quad \xi = \frac{x}{(t_0 - t)^{1/2}},$$

and prove that $\beta = 1/(p-1)$. Show that in this case, f would satisfy

$$f'' - \frac{1}{2}\xi f' + \lambda f^p - \beta f = 0,$$

and explain why appropriate boundary conditions would be

$$f \sim |\xi|^{-2\beta} \quad \text{as } \xi \rightarrow \pm\infty,$$

and show that such solutions might be possible. Are any other limiting behaviours possible?

7.7 By direct integration, show that the solution of

$$u'' + \lambda e^u = 0$$

satisfying $u = 0$ on $x = \pm 1$ is

$$u = 2 \ln \left[A \operatorname{sech} \left\{ \sqrt{\frac{\lambda}{2}} Ax \right\} \right],$$

and find a transcendental equation for A . Hence show that no solution exists for $\lambda > \lambda_c$, and derive and solve (numerically) an algebraic equation for λ_c .

If the equation is to be solved in $[0, 1]$, with $u' = 0$ on $x = 0$ and $u' = -1$ on $x = 1$, find the solution, and plot $u(0)$ as a function of λ . Is there a critical value λ_c ? If so, find it; if not, why not?

7.8 (i) Find an exact solution of the Gel'fand equation

$$\nabla^2 \theta + \lambda e^\theta = 0 \quad \text{in } 0 < r < 1,$$

where r is the cylindrical polar radius, and $\theta = 0$ on $r = 1$. [*Assume cylindrical symmetry, and a suitable condition of regularity at $r = 0$.*] Show that there is a critical parameter λ_c such that no solution exists for $\lambda > \lambda_c$, and find its value.

(ii) Write down the ordinary differential equation satisfied by a spherically symmetric solution of the Gel'fand equation in part (i). Suppose that $\theta = 0$ on $r = 1$ and $\theta_r = 0$ on $r = 0$ (why?). By putting

$$p = \lambda r^2 e^\theta, \quad q = 2 + r\theta_r, \quad r = e^{-t},$$

show that $p(t)$ and $q(t)$ satisfy the ordinary differential equations

$$\begin{aligned} \dot{p} &= -pq, \\ \dot{q} &= p + q - 2. \end{aligned}$$

By consideration of trajectories for p and q in the phase plane, show that multiple solutions exist for $\lambda \approx 2$, and infinitely many at $\lambda = 2$. Sketch the corresponding response diagram of $\theta(0)$ versus λ .

Chapter 8

Reaction-diffusion equations

The development of mathematical biology in the last thirty years has led to one particular pedagogical example of wave and pattern formation, and that is in the coupled sets of equations known as reaction-diffusion equations. The general type is

$$\frac{\partial u_i}{\partial t} + f_i(\mathbf{u}) + \nabla \cdot [D_{ij} \nabla u_j], \quad (8.1)$$

for n reactants u_1, \dots, u_n , where the summation convention (sum over repeated suffixes, here j) is implied, but much of what is known about the behaviour of such systems can be illustrated with the two species equations

$$\begin{aligned} u_t &= f(u, v) + D_1 \nabla^2 u, \\ v_t &= g(u, v) + D_2 \nabla^2 v. \end{aligned} \quad (8.2)$$

The phenomena which we find are closely allied to the behaviour of the underlying dynamical system

$$\begin{aligned} \dot{u} &= f(u, v), \\ \dot{v} &= g(u, v), \end{aligned} \quad (8.3)$$

and we will discuss three types of behaviour: wave trains, solitary waves, and stationary patterns, first in generality and then by example.

8.1 Wave trains

One way in which periodic travelling waves, or wave trains, can arise is when the underlying kinetics (8.3) is oscillatory. In a spatially distributed medium, the phase of the oscillatory kinetics will generally vary in space, but diffusion allows neighbouring phase oscillators to be coupled, in a kind of nearest neighbour resonance. The effect of diffusion is to cause the oscillations to propagate in space, and a periodic travelling wave results.

8.1.1 λ - ω systems

A particularly simple example where this can be seen explicitly is in so-called lambda-omega systems, which are two-dimensional reaction diffusion systems of the form

$$\begin{aligned} u_t &= \lambda u - \omega v + D \nabla^2 u, \\ v_t &= \omega u + \lambda v + D \nabla^2 v, \end{aligned} \quad (8.4)$$

in which λ and ω are functions of $(u^2 + v^2)^{1/2}$; thus the system is nonlinear. It can conveniently be written in the form

$$c_t = f(|c|)c + D \nabla^2 c, \quad (8.5)$$

where $c = u + iv$ and $f = \lambda + i\omega$.

8.1.2 Slowly varying waves

It suffices to consider components which diffuse equally rapidly, so that we may consider the suitably scaled equation

$$\mathbf{w}_t = \mathbf{f}(\mathbf{w}) + \nabla^2 \mathbf{w}, \quad (8.6)$$

where $\mathbf{w} \in \mathbf{R}^n$.

Suppose that the reaction kinetics admit an attractive limit cycle for the underlying system $\mathbf{w}_t = \mathbf{f}(\mathbf{w})$, and denote this as $\mathbf{W}_0(t)$, i.e.

$$\mathbf{W}_0' = \mathbf{f}(\mathbf{W}_0). \quad (8.7)$$

Suppose further that we look for solutions which are slowly varying in space. We define slow time and space scales τ and \mathbf{X} as

$$\tau = \varepsilon t, \quad \mathbf{X} = \sqrt{\varepsilon} \mathbf{x} \quad (8.8)$$

and seek formal solutions in the form $\mathbf{w}(\mathbf{X}, t, \tau)$, where

$$\mathbf{w}_t + \varepsilon \mathbf{w}_\tau = \mathbf{f}(\mathbf{w}) + \varepsilon \nabla^2 \mathbf{w}, \quad (8.9)$$

and $\nabla = \nabla_{\mathbf{X}}$ now. Expanding \mathbf{w} as

$$\mathbf{w} \sim \mathbf{w}_0 + \varepsilon \mathbf{w}_1 + \dots \quad (8.10)$$

leads to

$$\begin{aligned} \mathbf{w}_{0t} &= \mathbf{f}(\mathbf{w}_0), \\ \mathbf{w}_{1t} - J \mathbf{w}_1 &= -\mathbf{w}_{0\tau} + \nabla^2 \mathbf{w}_0, \end{aligned} \quad (8.11)$$

and so on, here $J = Df(\mathbf{w}_0)$ is the Jacobian of \mathbf{f} at \mathbf{w}_0 . After an initial transient, we may take

$$\mathbf{w}_0 = \mathbf{W}_0(t + \psi), \quad (8.12)$$

where $\psi(\tau, \mathbf{X})$ is the slowly-varying phase, and $J = Df(\mathbf{W}_0)$ is a periodic matrix. Thus we find that \mathbf{w}_1 satisfies

$$\mathbf{w}_{1t} - J\mathbf{w}_1 = -(\psi_\tau - \nabla^2\psi)\mathbf{W}'_0 + |\nabla\psi|^2\mathbf{W}''_0. \quad (8.13)$$

Note that $\mathbf{s} = \mathbf{W}'_0$ satisfies the homogeneous equation $\mathbf{s}_t - J\mathbf{s} = \mathbf{0}$. It follows that the solution of (8.13) is

$$\mathbf{w}_1 = -t(\psi_\tau - \nabla^2\psi)\mathbf{s} + |\nabla\psi|^2\mathbf{u}, \quad (8.14)$$

where

$$\mathbf{u} = M(t) \int_0^t M^{-1}(\tau) J(\tau) \mathbf{s}(\tau) d\tau + M(t) \mathbf{c}, \quad (8.15)$$

and M is a fundamental matrix for the homogeneous equation, i.e., $M' = JM$. Floquet's theorem implies that

$$M = Pe^{t\Lambda}, \quad (8.16)$$

where P is periodic of period T (the same as that of the limit cycle \mathbf{W}_0). We can take Λ to be diagonal if the characteristic multipliers are distinct, and since we assume \mathbf{W}_0 is attracting, the eigenvalues of Λ will all have negative real part, except one of zero corresponding to \mathbf{s} . With a suitable choice of basis, we then have

$$(e^{t\Lambda})_{ij} \rightarrow \delta_{i1}\delta_{j1} \quad \text{as } t \rightarrow \infty, \quad (8.17)$$

i.e., a matrix with the single non-zero element being unity in the first element. In this case the first column of P is \mathbf{s} , i.e., $P_{i1} = s_i$.

From (8.15), we have

$$\mathbf{u} = P(t) \int_0^t e^{\eta\Lambda} P^{-1}(t-\eta) J(t-\eta) \mathbf{s}(t-\eta) d\eta + M\mathbf{c}. \quad (8.18)$$

The effect of the transient dies away as $t \rightarrow \infty$, and if we ignore it, then we can take $M_{ij} = s_i\delta_{j1}$, and thus $M\mathbf{c} = c_1\mathbf{s}$, and

$$\mathbf{u} = \mathbf{s} \left[\int_0^t \alpha(\eta) d\eta + c_1 \right], \quad (8.19)$$

where the periodic function α is given by

$$\alpha = (P^{-1})_{1m} J_{mj} s_j. \quad (8.20)$$

We define the mean of α to be

$$\bar{\alpha} = \frac{1}{T} \int_0^T \alpha(\eta) d\eta, \quad (8.21)$$

so that

$$\beta = \int_0^t (\alpha - \bar{\alpha}) d\eta \quad (8.22)$$

is periodic with period T . Then (8.14) is

$$\mathbf{w}_1 = [t\{-\psi_\tau + \nabla^2\psi + \bar{\alpha}|\nabla\psi|^2\} + c_1 + \beta]\mathbf{s}, \quad (8.23)$$

and in order to suppress secular terms (those which grow in t), we require the phase ψ to satisfy the evolution equation

$$\psi_\tau = \nabla^2\psi + \bar{\alpha}|\nabla\psi|^2. \quad (8.24)$$

This is an integrated form of Burgers' equation; in one dimension, $u = -\psi_X/2\bar{\alpha}$ satisfies $u_\tau + uu_X = u_{XX}$. Disturbances will form shocks, which are jumps of phase gradient. More generally, if $\mathbf{u} = -\nabla\psi/2\bar{\alpha}$, then (bearing in mind that $\text{curl } \mathbf{u} = \mathbf{0}$) we find

$$\mathbf{u}_\tau + (\mathbf{u} \cdot \nabla)\mathbf{u} = \nabla^2\mathbf{u}, \quad (8.25)$$

which is the Navier-Stokes equation with no pressure term. Phase gradients move down phase gradients, and form defects where the (sub-)characteristics intersect.

Solutions of (8.24) which vary with X correspond to travelling wave trains. For example, in one dimension, waves travel locally at speed $dX/dt \approx -(\partial\psi/\partial X)^{-1}$. In general, however, the phase of the oscillation becomes constant at long times if zero flux boundary conditions $\partial\psi/\partial n = 0$ are prescribed at container boundaries, and wave trains die away. However, this takes a long time (if ε is small), and while spatial gradients are present, the solutions have the form of waves. For example, *target patterns* are created when an impurity creates a local inhomogeneity in the medium. Suppose the effect of such an impurity is to decrease the natural oscillation period by a small amount (of $O(\varepsilon)$) at a point, which we take to be the origin; then it is appropriate to specify

$$\psi = \tau \quad \text{at} \quad R = 0, \quad (8.26)$$

where R is the polar radius, and ψ tends towards the solution $\psi = \tau - f(R)$ as $t \rightarrow \infty$, where f satisfies

$$f'' + \frac{1}{R}f' - \bar{\alpha}f'^2 - 1 = 0, \quad (8.27)$$

together with $f(0) = 0$ and an appropriate no flux condition at large R ; such a condition can always be implemented by consideration of a small boundary layer near the boundary. The relevant solution if $\bar{\alpha} > 0$ is

$$f(R) = \frac{1}{\bar{\alpha}} \ln I_0(\sqrt{\bar{\alpha}}R), \quad (8.28)$$

where I_0 is the modified Bessel function of order zero. At large R , $\psi \sim R/\sqrt{\bar{\alpha}}$, which represents a travelling wave of speed $dR/dt \approx \sqrt{\bar{\alpha}}$. If, on the other hand, $\bar{\alpha} < 0$, then $f(R) = \frac{1}{\bar{\alpha}} \ln J_0(\sqrt{|\bar{\alpha}|}R)$, which blows up at finite R , and travelling wave solutions of this type do not exist. At large R , f' is constant, and the wave speed is approximately constant, $dR/dt \approx \sqrt{\bar{\alpha}}$, corresponding to an outward travelling planar wave train.

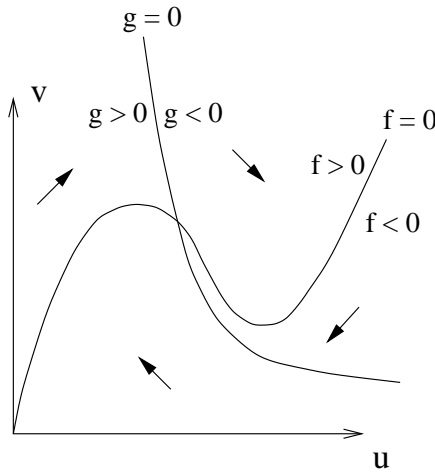


Figure 8.1: Phase diagram for kinetics of (8.29).

8.2 Activator-inhibitor system

An example of a system supporting travelling wave solutions is the activator-inhibitor system

$$\begin{aligned} u_t &= f(u, v) + \nabla^2 u, \\ v_t &= g(u, v) + \nabla^2 v, \end{aligned} \quad (8.29)$$

where the nullclines of the kinetics are as shown in figure 8.1 (cf. figure 4.7). This system is called an activator-inhibitor system because $\partial f / \partial v > 0$, thus increased v activates u , while $\partial g / \partial u < 0$, so increased u inhibits v . When the intersection is on the decreasing part of $f = 0$, as shown, then $\partial f / \partial u > 0$, $\partial g / \partial v < 0$, and $-f_u / f_v > -g_u / g_v$, whence the determinant D of the Jacobian of $(u, v)^T$ at the fixed point is positive. Hence the fixed point is unstable if $f_u + g_v > 0$, and a limit cycle exists in this case if trajectories are bounded. For example, if $f = F/\varepsilon$, $\varepsilon \ll 1$, this is the case, and the limit cycle takes the relaxational form shown in figure 4.7. The addition of diffusion allows travelling wave trains to exist, as described above.

8.3 Solitary waves in excitable media

Suppose now the intersection point of the nullclines $f = 0$ and $g = 0$ is as shown in figure 8.2. The fixed point of the underlying dynamical system is now stable, but relatively small perturbations to v can cause large excursions in u , as shown. When diffusion is included, these large excursions can travel as solitary waves. The simplest way to understand how this comes about is if we allow u to have fast reaction kinetics and take v as having zero diffusion coefficient.

In one dimension, a suitably scaled model is then

$$\varepsilon u_t = f(u, v) + \varepsilon^2 u_{xx},$$

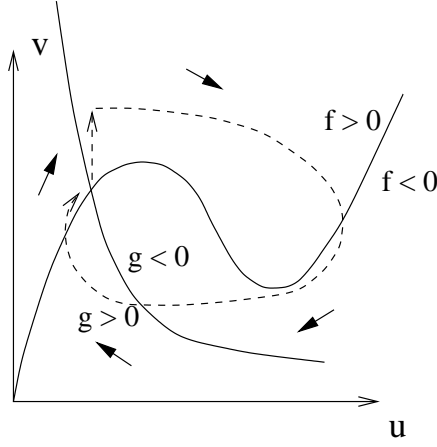


Figure 8.2: Phase plane for excitable kinetics.

$$v_t = g(u, v), \quad (8.30)$$

and we look for a travelling wave solution of the form

$$u = u(\xi), \quad v = v(\xi), \quad \xi = ct - x, \quad (8.31)$$

where c is to be found. Then

$$\begin{aligned} \varepsilon c u' &= f + \varepsilon^2 u'', \\ c v' &= g, \end{aligned} \quad (8.32)$$

and the idea is to seek a trajectory for which $(u, v) \rightarrow (u^*, v^*)$ as $\xi \rightarrow \pm\infty$ (here (u^*, v^*) is the fixed point of the system). The form of this trajectory is shown in figure 8.3. On the slow parts of the wave, $f \approx 0$ and $c v' \approx g$ (and we anticipate $c > 0$). On the fast parts, we put $\xi = \varepsilon \Xi$; then $v \approx \text{constant}$, and we denote v_+ ($= v^*$) and v_- as the corresponding values of v ; v_- is unknown (as is c).

On the fast parts of the wave, we define $u' = w$ (where now $u' = du/d\Xi$), so that

$$\begin{aligned} u' &= w, \\ w' &= cw - f_{\pm}(u), \end{aligned} \quad (8.33)$$

where $f_{\pm}(u) = f(u, v_{\pm})$. The graphs of f_+ and f_- are similar, and are shown in figure 8.4, where we see that construction of the connecting branches PQ and RS requires that the fixed points P and Q , or R and S , of (8.33) have a connecting trajectory. In general, this will not be the case, but we can choose c to connect P to Q (since v_+ is known), and then we choose v_- to connect R to S (with this same value of c). The form of the resulting travelling wave is shown in figure (8.5).

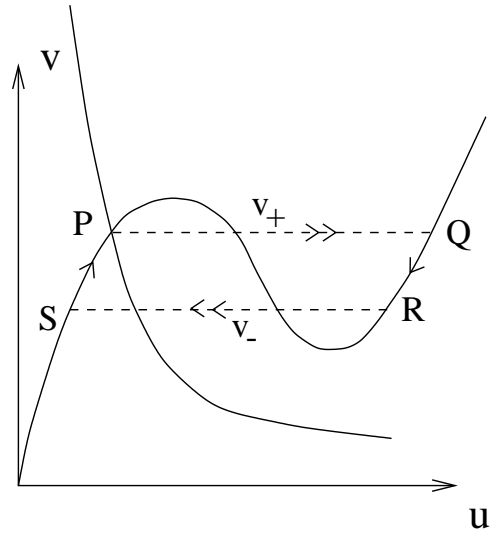


Figure 8.3: Phase plane for solitary wave trajectory.

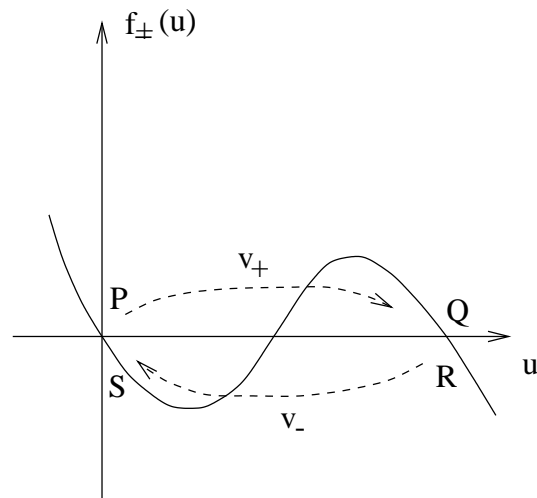


Figure 8.4: Phase plane connection for the fast parts of the travelling wave.

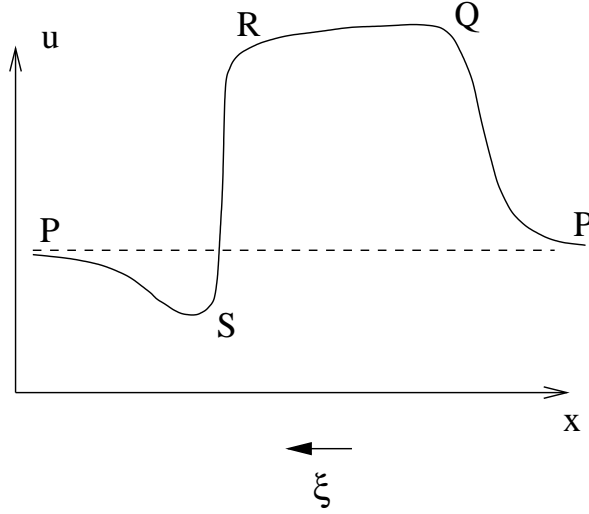


Figure 8.5: Spatial form of the travelling wave.

8.4 Pattern formation

We have seen that an activator (v)-inhibitor (u) system

$$\begin{aligned}\dot{u} &= f(u, v), \\ \dot{v} &= g(u, v),\end{aligned}\tag{8.34}$$

admits periodic travelling waves when the uniform state is unstable, and solitary waves when it is stable (and the activator diffuses slowly). Stationary patterns can occur when a stable steady state of (8.34) is rendered spatially unstable by different component diffusivities. Suppose then that

$$\begin{aligned}u_t &= f(u, v) + u_{xx}, \\ v_t &= g(u, v) + dv_{xx},\end{aligned}\tag{8.35}$$

is an activator-inhibitor system with $f_v > 0$, $g_u > 0$; the restriction to one spatial dimension is inconsequential. The parameter d here represents the ratio of activator to inhibitor diffusivities. Note that when $d \rightarrow 0$, we expect solitary wave propagation, at least for the phase diagram of figure 8.2, where also $f_u < 0$, $g_v < 0$ at the fixed point.

With the stationary state denoted as (u^*, v^*) , we assume it is stable in the absence of diffusion; thus assume

$$\begin{aligned}T &= f_u + g_v < 0, \\ \Delta &= f_u g_v - f_v g_u > 0,\end{aligned}\tag{8.36}$$

both evaluated at (u^*, v^*) . We put

$$\begin{pmatrix} u \\ v \end{pmatrix} = \begin{pmatrix} u^* \\ v^* \end{pmatrix} + \mathbf{w} e^{\sigma t + i k x},\tag{8.37}$$

linearisation of (8.35) then yields

$$(M - k^2 D - \sigma) \mathbf{w} = \mathbf{0}, \quad (8.38)$$

where

$$M = \begin{pmatrix} f_u & f_v \\ g_u & g_v \end{pmatrix}, \quad D = \begin{pmatrix} 1 & 0 \\ 0 & d \end{pmatrix}. \quad (8.39)$$

The eigenvalues σ are the roots of

$$\sigma^2 - T_d \sigma + \Delta_d = 0, \quad (8.40)$$

where

$$\begin{aligned} T_d &= T - (1 + d)k^2, \\ \Delta_d &= \Delta - k^2(df_u + g_v) + dk^4. \end{aligned} \quad (8.41)$$

The steady state is stable if and only if $T_d < 0$ and $\Delta_d > 0$ (cf. figure 4.4). Now $T < 0$ and $\Delta > 0$ by assumption: hence $T_d < 0$, and thus instability occurs if and only if $\Delta_d < 0$. Since $\Delta > 0$, we see from (8.39) that this can only occur if $df_u + g_v > 0$. Thus either $f_u > 0$ or $g_v > 0$, and the system cannot be excitable. Since $f_u + g_v < 0$, we see that a necessary condition for instability is that $d \neq 1$. Because d is the ratio of two diffusivities, this instability is known as *diffusion-driven instability* (DDI), or *Turing instability*, after the originator of the theory.

To be specific, let us suppose the situation to be that of figure 8.1, i.e. $f_u > 0$, $g_v < 0$: then we require $d > 1$ for DDI. The precise criterion for instability is that $\min \Delta_d < 0$, and, from (8.41), this is

$$df_u + g_v > 2[\Delta d]^{1/2}, \quad (8.42)$$

and this can be reduced to

$$d > \left[\frac{\Delta^{1/2} + \{f_v |g_u|\}^{1/2}}{f_u} \right]^2. \quad (8.43)$$

The resulting instability is direct and not oscillatory (in time), though it is oscillatory in space. We can therefore expect stationary finite amplitude patterns to emerge as the stable solutions, and this is indeed what often occurs.

The form of these putative steady solutions as d becomes large can be studied by seeking periodic (in space) solutions of

$$\begin{aligned} u_{xx} + f(u, v) &= 0, \\ v_{xx} + \varepsilon^2 g(u, v) &= 0, \end{aligned} \quad (8.44)$$

where we define $\varepsilon^2 = 1/d \ll 1$. As u varies, v is approximately constant, and thus the equation for u can be integrated to give the first integral

$$\frac{1}{2}u_x^2 + \int_{u_-}^u f \, du = 0, \quad (8.45)$$

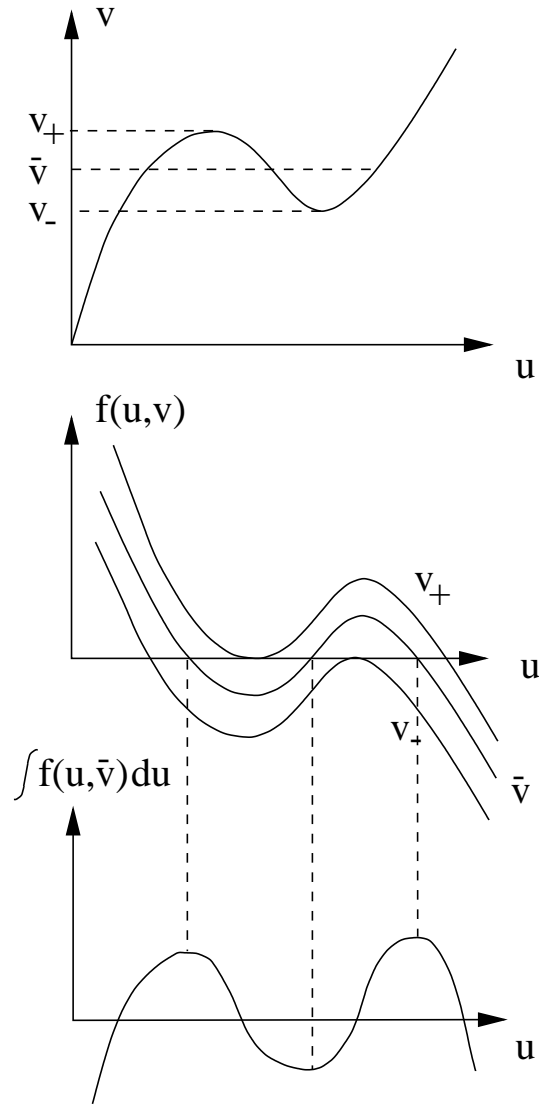


Figure 8.6: Definition of the values v_{\pm} defined by the function $f(u, v)$. The middle graph shows the function $f(u, v)$ as a function of u for various v , and the lowest graph is the potential $\int^u f(u) du$ for the value of $v = \bar{v}$ corresponding to the middle of these three curves.

where we suppose $u = u_-$ is the minimum during the oscillation. If $u = u_+$ at the maximum, then

$$\int_{u_-}^{u_+} f(u, \bar{v}) du = 0, \quad (8.46)$$

and this is only possible if $v = \bar{v} \in (v_-, v_+)$, as defined in figure 8.6. For each such \bar{v} , there is a family of periodic solutions parameterised by u_- . The choice of \bar{v} and u_- must then be made so that v is periodic, and this requires

$$\int_0^P g[u(x; \bar{v}, u_-), \bar{v}] dx = \int_0^P xg[u(x; \bar{v}, u_-), \bar{v}] dx = 0, \quad (8.47)$$

where P is the period of the pattern.

One particular case of interest is when u_- and u_+ lie on the $f = 0$ nullcline, for then $u \rightarrow u_{\pm}$ as $x \rightarrow \pm\infty$, and the u solution represents a rapid transition layer between two slowly varying regions where $f \approx 0$. A periodic sequence of such rapid transitions between slowly varying regions can be found if there are two values of \bar{v} where u_{\pm} lie on $f = 0$. For the present case where $f_v > 0$, this is not, however, possible.

Exercises

8.1 (i) The complex reactant concentration c satisfies the reaction diffusion system

$$c_t = f(|c|)c + D\nabla^2 c,$$

where $f(|c|) = \lambda(|c|) + i\omega(|c|)$, and λ and ω are real-valued. Show that if $D = 0$, $|c| = |c|\lambda(|c|)$, and deduce that as $t \rightarrow \infty$, $|c| \rightarrow c^*$, where $\lambda(c^*) = 0$ and $\lambda'(c^*) < 0$. Hence show that the eventual solution is the limit cycle $c = c^* \exp[i\omega(c^*)t]$.

(ii) Now suppose $D \neq 0$ and $\lambda' < 0$. Show that travelling waves exist provided $k\sqrt{D} < \{\lambda(0)\}^{1/2}$. What happens if $\lambda(0) < 0$?

(iii) Suppose, finally, that $\lambda(0) > 0$, but that also $\lambda' > 0$. What do you think might happen in this case?

8.2 When an oscillatory reaction-diffusion system has an imperfection of size comparable to, or larger than, the wave length, then spiral waves can occur. This is because the wave trains need not be in phase round the boundary of the obstacles. For example, consider a slowly varying system (8.6) with solutions $\mathbf{w} \approx \mathbf{W}_0(t + \psi)$, where ψ satisfies the diffusion equation $\psi_{\tau} = \nabla^2 \psi$. The effect of the surface $r = a$, say, is to alter the period, and we can suppose $\psi = -\tau + m\theta$ on $r = a$, where m is an integer (so that \mathbf{w} is single valued, if we suppose the period of \mathbf{W}_0 is normalised to be 2π).

Put $\psi = -\tau + m\theta + \phi(r)$, and show that if we require $\phi' = 0$ on $r = a$ (so that $\partial \mathbf{w} / \partial n = 0$ there), then a steady solution is

$$\psi = -\tau + m\theta + \frac{1}{2}a^2[\ln(r/a) - \frac{1}{4}(r^2/a^2)],$$

which represents a spiral. Note that the integer m is unconstrained.

8.3 The Fitzhugh-Nagumo equations are

$$\begin{aligned}\varepsilon u_t &= u(a - u)(u - 1) - v + \varepsilon^2 u_{xx}, \\ v_t &= bu - v,\end{aligned}$$

where $0 < a < 1$, $\varepsilon \ll 1$, and b is positive and large enough that $u = v = 0$ is the only steady state. Show that the system is excitable, and show, by means of a phase plane analysis, that solitary travelling waves of the form $u(\xi), v(\xi)$, $\xi = ct - x$, are possible with $c > 0$ and $u, v \rightarrow 0$ as $\xi \rightarrow \pm\infty$.

8.4 u and v satisfy the equations

$$\begin{aligned}\delta u_t &= \varepsilon^2 u_{xx} + f(u, v), \\ v_t &= v_{xx} + g(u, v),\end{aligned}$$

where

$$f(u, v) = u[F(u) - v], \quad g(u, v) = v[u - G(v)],$$

and $F(u)$ is a unimodal function ($F'' < 0$) with $F(0) = 0$, while $G(v)$ is monotone increasing ($G' > 0$) and $G(0) > 0$, and there is a unique point (u_0, v_0) in the positive quadrant where $f(u_0, v_0) = g(u_0, v_0) = 0$, and $F'(u_0) < 0$. (For example $F = u(1 - u)$, $GH = 0.5 + v$.)

Examine the conditions on δ and ε^2 which ensure that diffusive-driven instability of (u_0, v_0) occurs.

If the upper and lower branches of F^{-1} are denoted as $u_+(v) > u_-(v)$, explain why u_- is unstable when $\varepsilon \ll 1$. By constructing phase portraits for v when $u = 0$ and when $u = u_+(v)$, and ‘gluing’ them together at a fixed value $v = v^*$, show that spatially periodic solutions exist which are ‘patchy’, in the sense that u alternates rapidly between $u_+(v)$ and 0.

8.5 An activator–inhibitor reaction–diffusion model takes the non-dimensional form

$$\begin{aligned}\frac{\partial u}{\partial t} &= \frac{u^2}{v} - bu + \frac{\partial^2 u}{\partial x^2}, \\ \frac{\partial v}{\partial t} &= u^2 - v + d \frac{\partial^2 v}{\partial x^2},\end{aligned}$$

where $u(x, t), v(x, t)$ are the concentrations of the chemicals at spatial coordinate x and time t , and b, d are positive parameters.

Which is the activator and which is the inhibitor? Find the non-zero spatially uniform steady state and, from first principles, determine the conditions for it to be driven unstable by diffusion. Show that the parameter domain for which diffusion-driven instability is given by $0 < b < 1$, $db > 3 + 2\sqrt{2}$, and sketch the instability region in (b, d) parameter space. Show that the critical wave number k_c at the onset of instability is

$$k_c^2 = \frac{1 + \sqrt{2}}{d}.$$

References

Fowler, A. C. 1997 Mathematical models in the applied sciences. C.U.P., Cambridge.